



Brine grades in Andean salars: When basin size matters A review of the Lithium Triangle

Romina Lucrecia López Steinmetz, Stefano Salvi

► To cite this version:

Romina Lucrecia López Steinmetz, Stefano Salvi. Brine grades in Andean salars: When basin size matters A review of the Lithium Triangle. *Earth-Science Reviews*, 2021, 217, pp.103615. 10.1016/j.earscirev.2021.103615 . hal-03204125

HAL Id: hal-03204125

<https://hal.science/hal-03204125>

Submitted on 21 Apr 2021

HAL is a multi-disciplinary open access archive for the deposit and dissemination of scientific research documents, whether they are published or not. The documents may come from teaching and research institutions in France or abroad, or from public or private research centers.

L'archive ouverte pluridisciplinaire **HAL**, est destinée au dépôt et à la diffusion de documents scientifiques de niveau recherche, publiés ou non, émanant des établissements d'enseignement et de recherche français ou étrangers, des laboratoires publics ou privés.

Journal Pre-proof

Brine grades in Andean salars: When basin size matters A review
of the Lithium Triangle



Romina Lucrecia López Steinmetz, Stefano Salvi

PII: S0012-8252(21)00115-X

DOI: <https://doi.org/10.1016/j.earscirev.2021.103615>

Reference: EARTH 103615

To appear in: *Earth-Science Reviews*

Received date: 16 May 2020

Revised date: 9 February 2021

Accepted date: 27 March 2021

Please cite this article as: R.L.L. Steinmetz and S. Salvi, Brine grades in Andean salars: When basin size matters A review of the Lithium Triangle, *Earth-Science Reviews* (2021), <https://doi.org/10.1016/j.earscirev.2021.103615>

This is a PDF file of an article that has undergone enhancements after acceptance, such as the addition of a cover page and metadata, and formatting for readability, but it is not yet the definitive version of record. This version will undergo additional copyediting, typesetting and review before it is published in its final form, but we are providing this version to give early visibility of the article. Please note that, during the production process, errors may be discovered which could affect the content, and all legal disclaimers that apply to the journal pertain.

Brine grades in Andean salars: when basin size matters A review of the Lithium Triangle

Romina Lucrecia López Steinmetz^{1,*} lucrecialopezsteinmetz@hotmail.com, Stefano Salvi²

stefano.salvi@get.omp.eu

¹IDEVEA (CONICET - UTN), Av. GRAL. J.J. Urquiza 314, 5600 San Rafael, Mendoza, Argentina

²University of Toulouse, CNRS, GET, IRD, OMP, 14 Av. Edouard Belin, Toulouse 31400, France

*Corresponding author

Abstract

The Lithium Triangle, a zone of the Central Andes characterized by the presence of lithium (Li)-rich salt pans within endorheic basins, has gained a worldwide reputation chiefly due to its exceptional Li brine-type deposits. We summarize scientific hydrochemical reports, totaling a data set composed of 477 brine samples across the Lithium Triangle. Brine compositions are predominantly of the $\text{Cl}^- - \text{SO}_4^{2-}$ / $\text{Na}^+ - \text{Mg}^{2+}$ type, however, major brine chemistry and Li^+ grades vary across the Andean plateau. Brine compositions show some degree of geographic organization but no clear pattern was observed in the Li^+ distribution across the plateau. We highlight an interdependency between the areal surfaces of salt pans and endorheic basins, which, related to Li concentrations, show the following linear proportions: 1) a 1:5 to 1:10 proportionality between the surfaces of basin catchments and those of salt pans; 2) a 2:1 proportionality between maximum and mean Li values; the latter implies that the equation $\text{mean Li} \approx \frac{1}{2} \text{ max Li}$ can be employed to predict indicative mean

grades during Li surveys in the Central Andes. In addition, the concentrations of Li can be addressed with respect to the area of salt pans and/or its basin catchments: it would be not only the largest, but also the oldest salars that are expected to hold the greatest Li concentrations. Finally, the area involving all salt pans in the Andean plateau is more than three times the size of what is known as the Lithium Triangle and has a curved crescent shape; we thus propose referring to it in the future as the Lithium Crescent.

Keywords: salt pan; endorheic basin; hydrochemistry; Andes

1. Introduction and historical background

The demand for lithium (Li) has recently known a great increase worldwide due to its application in the fabrication of rechargeable batteries (for mobile phones, personal computers, electric vehicles, etc.). Known global lithium resources involve about 31 Mt, which would represent ~1.50 times the global estimated demand up to the year 2100 (Kesler et al., 2012). Nowadays, lithium is mostly obtained from pegmatite- and brine-type deposits. The former consist of conventional Li mining and represent ~4 Mt (~13%) of estimated resources. Apart from an additional 5 to 6 Mt potential production from hydrothermal solutions and oilfields (Kesler et al., 2012), the remaining ~2/3 (~68%) of global lithium resources are contained in brine-type deposits. This makes them indispensable to meet the growing demand and has caused Li-rich salars to attain the status of an economically, technologically and geopolitically strategic resource (Garrett, 2004; Gruber and Medina, 2010; Mohr et al., 2010; Houston et al., 2011; Kesler et al., 2012; López Steinmetz and Fong, 2019).

Li is a relatively abundant element on Earth with a concentration in the upper continental crust of about 35 ± 11 ppm (Teng et al., 2004). As Li is a very reactive and

geochemical incompatible element, it is commonly present in natural waters as a solute, in its ionic form, Li⁺. The mean Li concentration in sea water is 0.18 mg L⁻¹ (Riley and Tongudai, 1964), whereas continental waters are characterized by highly variable Li values. Salt pans (salars or salt flats, desert areas where salts accumulate) in arid regions of the globe store brines that contain Li concentrations often averaging two to three orders of magnitude above those in sea water. Most brine-type deposits involve concentrations of more than 400 mg L⁻¹ of Li.

The Andean plateau in South America, one of the most peculiar geological features on Earth, has gained a worldwide reputation due to its exceptional Li brine-type deposits (Kesler et al., 2012). The constraints imposed by environmental challenges and the need for strong technological developments to replace fossil fuels are global factors that have driven the Andean Li rush during now more than a decade. Under the effect of the lithium rush, the plateau region became known as “The Lithium Triangle”. This was an informal appellation originally designating the area comprised between the Salar de Atacama in Chile (#12 in Fig. 1), the principal Li mine in the world (Moraga et al., 1974; Ide and Kunasz, 1989; Kunasz, 2006), the Salar de Uyuni (#3) in Bolivia to the north (Ericksen and Salas, 1987; Risacher and Fritz, 1991), and the Salar de Hombre Muerto (#43) in Argentina to the south (Godfrey et al., 2013) (Fig. 1). This delimitation of the Andean Lithium Triangle then became established based on the relevance of these three salars, which have been the most important Li spots during the last years. However, there are several more Li-bearing salt pans in this Andean region, many of which located outside of this triangle (Fig. 1). In addition, the nonscientific literature (i.e., diverse press articles, NI reports of mining prospects, etc.) commonly considers all the Andean salt flats as containing significant amounts of Li, although data on brine hydrochemistry, including Li grades, are still quite limited, to this date. Therefore, we consider it is important to delimit the area containing all known salt pans. As shown in Figure

1b, such region (in green) corresponds to a curved crescent shape of more than three times the size of the Triangle (in pink), to which we propose referring to as the Lithium Crescent.

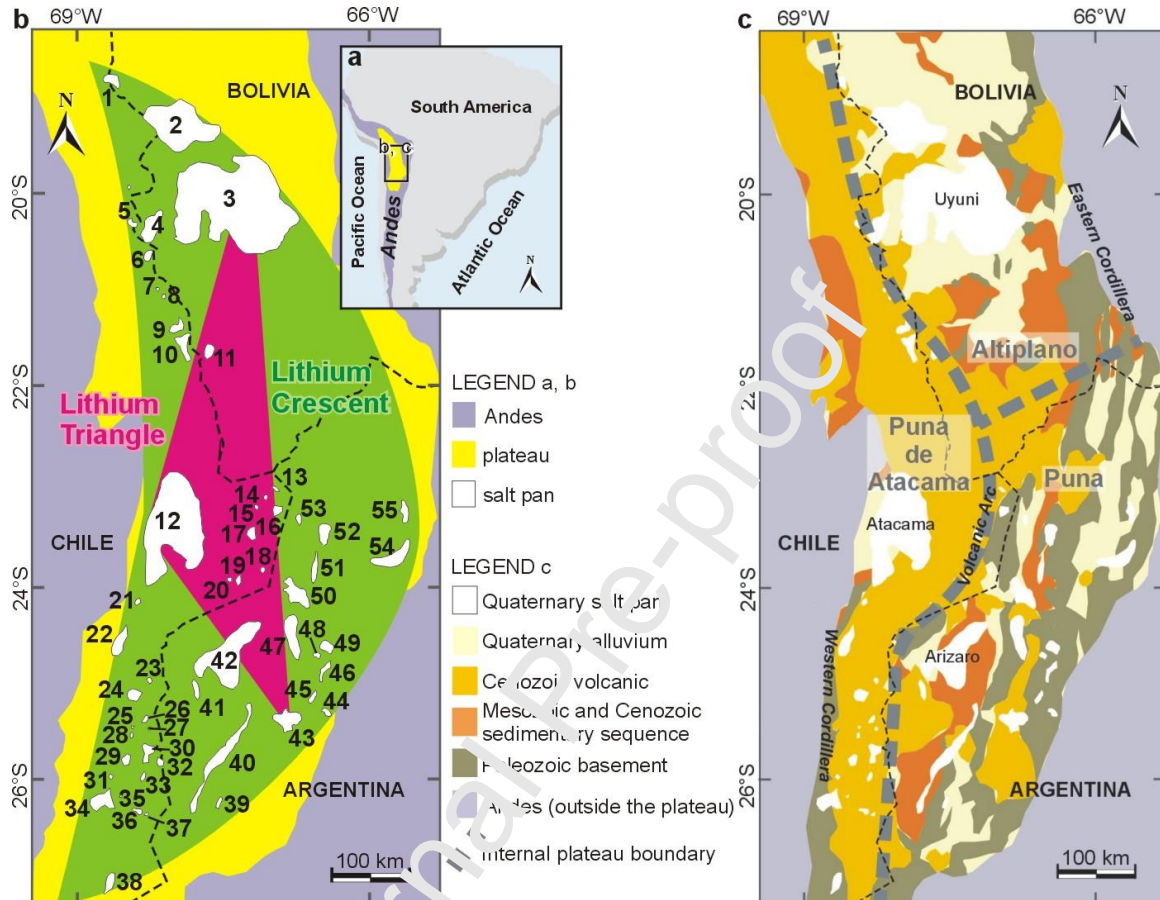


Figure 1. Simplified maps showing the location of a) the Andean plateau and b) salt pans, the Lithium Triangle (pink), and proposed Lithium Crescent (green) corresponding to the area involving all salt pans on the plateau. c) Simplified lithological map of the Andean plateau (modified from Allmendinger et al., 1997), showing the location of the Puna, Puna de Atacama and Altiplano. Dashed black lines represent national borders. Salt pans are numbered in panel b as in Table 1.

The interest for Andean salt pans and their resources began almost a century ago. The first studies were conducted across the Puna de Atacama in northern Chile by geoscientists of the USGS (United States Geological Survey). To this early period of hydrological and geochemical surveys correspond the reports made by Clark (1924), Erickson (1961, 1963), and Dingman (1967). A few years later, during the 70's, lithium was already perceived as an important resource, as reveals the book "Lithium Resources and Requirement by the year

2000” edited in 1976 by James Vine (also of the USGS). Some of the chapters in this book have become milestone contributions on the topic (e.g., Erickson et al., 1976b; Kunasz, 1976). During this period, the Chilean State started having an active role on the geological surveying of the Puna de Atacama (the Chilean and western part of the Andean plateau), and on the study of the hydrochemistry of the Salar de Atacama (Moraga et al., 1974; Vila, 1975). Exploration of Andean salars and their Li resources formally began in 1975, when the Chilean State, in association with private companies, conducted the first formal survey of the Salar de Atacama (Kunasz, 1976). Simultaneously, the USGS announced the first results of analyses on two brines samples from the Salar de Uyuni, revealing Li⁺ concentrations as high as 490 and 1,510 mg L⁻¹ (Erickson et al., 1976a, 1976b). Since those times, Atacama and Uyuni founded the biggest expectations on the emerging interest in Li-brine type deposits (Mardones, 1986).

The role of the USGS in generating the fundamental knowledge on the hydrochemistry of Andean salt pans, especially in the Puna de Atacama but also in the Bolivian Altiplano (see Erickson et al., 1977), remained predominant for more than half a century and continued up to the end of the 80’s (see Stoertz and Erickson, 1974; Erickson and Salas, 1977; Erickson et al., 1978; Erickson and Salas 1987; Ide and Kunasz, 1989). The two following decades were characterized by the acquisition of vast hydrochemical data sets of many Chilean salars (Alonso and Risacher, 1996; Risacher and Alonso, 1996; Risacher et al., 2003) and Uyuni (Risacher and Fritz, 1991; Risacher and Fritz, 2000; Risacher and Frits, 2009; Lowenstein and Risacher, 2009). These new major contributions, which included for example the hydrochemical characterization of more than 170 brine samples across the entire Uyuni (Risacher and Fritz, 1991), were in charge of a French-Chilean council headed by Professors François Risacher of the IRD (Institut de Recherche pour le Développement, France) and Hugo Alonso of the UCN (Universidad Católica del Norte, Chile). From this French-Chilean

collaboration emerged the hydrochemical data available today on the Puna de Atacama and Altiplano salt pans, and which remain currently used by COCHILCO (Corporación Chilena del Cobre, the Chilean public society owning mining properties for Cu, Li and other metals in Chile). Additional hydrological and hydrochemical studies, including isotopic assessments in salars and hydrothermal springs in the Puna de Atacama and Altiplano, have been conducted during the last years (e.g., Carmona et al., 2000; Boschetti et al., 2007; Vasquez et al., 2013; Boutt et al., 2016; among others). It was only concurrently to these recent studies that the lithium prospection started along the southeastern side of the Central Andes.

Salars in the Puna (i.e., the Argentine portion of the Andean plateau) have received much less attention than those in the Puna de Atacama and Altiplano. It was probably due to the major attraction caused by the enormous Li resources that stores Atacama (with exceptional Li mean concentrations of $1,400 \text{ mg L}^{-1}$; Moraga et al., 1974; Ide and Kunasz, 1989; Kunasz, 2006), and perhaps also due to the blinding expectations triggered by a salt pan having such a giant dimension as Uyuni ($10,580 \text{ km}^2$). It remains that the Puna salt pans stayed almost unexplored up to only a decade ago, despite the recent context of the Andean lithium rush. The first hydrochemical studies were conducted locally on a few salars: the Salar del Rincón (#50; Ovejero Toledo et al., 2009), Salar de Hombre Muerto (Godfrey et al., 2013), Olaroz (#52; Lora et al., 2016; Franco et al., 2016), Guayatayoc (#55; López Steinmetz, 2017), and the first isotopic data on the Salar de Ratones (#45), Centenario (#46), and Olaroz (Orberger et al., 2015; García et al., 2019; Franco et al., 2020). A broad survey of the Li-bearing salars in the Puna plateau was only recently accomplished, by geoscientist of the Argentine State, who investigated the brine hydrochemistry for the 17 major salars of this part of the Central Andes (López Steinmetz et al., 2018; López Steinmetz et al., 2020a). Because of this long-lasting lack of information, so far it has not been possible to address the hydrochemistry of Andean salt pans in a regional perspective, i.e., in a spatial-geographical

sense, which implies having an overview of all of these salt pans together. Almost a century after the first USGS surveys, the last surveying achievements in the Puna salars finally give us the opportunity of compiling the existing data set and globally assess the hydrochemistry of the Lithium Crescent.

Li-bearing Andean salt pans are exclusively hosted in endorheic basins (isolated hydrological units corresponding to internally drained areas). The onset of endorheism in the Andean plateau established in the Neogene, associated with the creation of orographic deserts within intermontane settings in response to plateau uplift, as well as widespread volcanism (Alonso et al., 1991; Vandervoort et al., 1995; Alonso et al., 2006; López Steinmetz et al. 2020b). The formation of endorheic basins and salt pans is a function of the spatial and temporal distribution of the topographic configuration, sedimentation and erosional processes, as well as climate (Sobel et al., 2003; Hilley and Strecker, 2005; García-Castellanos, 2006; Garreaud, 2009; Tremblay et al., 2015; López Steinmetz et al., 2020b). One might suspect that, under analogous climatic and geological conditions, whichever they may have been, the larger a basin catchment, the larger the size (and volume; i.e. depth) of the salt pan. But because Earth and its processes are typically multi-dimensionally (4D, space - time), heterogeneous and complex (Becker and Braun, 1999; Paola et al., 2009), this relationship cannot be taken for granted. One of the objectives of the present contribution is to address the interdependency between the areal surfaces (size) of salt pans and of their endorheic basins and relate them to Li grades within an Andean perspective. Remarkably, our findings indicate that this size function follows in fact a proportional ratio across the Andean plateau.

No clear geographical pattern in Li distribution (nor concentration) has been found across the Lithium Crescent (López Steinmetz et al., 2020a), except that maximum Li concentrations have been reported from salt pans located in the center of the plateau (Fig. 1). Similarly, consistently with the latest studies on this area (Egenhoff and Lucassen, 2003;

Peralta Arnold et al. 2017; García et al., 2019; Meixner et al., 2019), our observations rule out a geographical control on the primary source of Li (and its concentration), and suggest that a combination of basin-scale processes and endorheic surface sizes control, at least in part, Li grades. It is likely that the lithological characteristics of each salar will have contributed to its geochemical composition. However, to our knowledge, no such study has been carried out yet. Figure 1c shows a synthetic view of lithologies underlying salt pans in the Andean plateau. Any given salar sits on several units, which influence the specific input of the lithology on a salar's chemical signature that are in also probably controlled by more large basin-scale processes like hydrothermalism.

In addition to the salar/basin size function, further objectives of the present contribution are: - to summarize the hydrochemical data sets of brines from salt pans at the Andean scale; - to identify regional patterns (i.e., spatial-geographical) for Li distribution and brine concentrations; - to recognize useful criteria (e.g., hydrochemical, geographical, geomorphological, etc.) for surveying of Li-brine type deposits; - to discuss in absolute and comparative terms the relevance and potential of Andean prospects. A better knowledge of the salars in this region of the Andes and of their Li endowment will necessarily prove beneficial for a better governance of natural resources, whether it be administrative exercise, private sector investment strategies, or simply contributing to the public knowledge.

2. Geology of the Andean Plateau

The Andes display along the western South America (Fig. 1). The Orogenic processes that conducted to the Andes mountain building started in the early Cenozoic after major reorganization of tectonic plates in the eastern Pacific, driving the convergence of the Nazca and South American plates (Tassara, 2005, and references therein).

The Andean plateau (Fig. 1 B) is a tectonic elevation area settled in the Central Andean zone. It occupies parts of northern Chile and Argentina, western Bolivia and southernmost Peru. The plateau involves the internally drained basins of the Central Andes (Allmendinger et al., 1997), which largely correspond to the areas settled above the 3 km elevation contour (Isacks, 1988).

The plateau involves a >60-70 km-thick crust and thin lithosphere (without or with very thin lithospheric mantle, see Allmendinger et al., 1983; Coira et al., 1993; Allmendinger and Gubbels, 1996; Whitman et al., 1996). The plateau is flanked to east and west by morphotectonic units of the continental plate, the Eastern and Western Cordilleras (Fig. 1 C), whereas in the N-S direction the plateau extent coincides with abrupt dip changes along the subduction zone, from flat ($<10^\circ$) to normal ($\sim 30^\circ$) subduction, and with the intersection of the Nazca and Juan Fernández oceanic ridge (Casara, 2005, and references therein). The Eastern Cordillera reaches 5-6 km elevation and it is a doubly-vergent deformation belt active until the middle-late Miocene (Heran et al., 1996; McQuarrie, 2002). South of 27°S , the tectonic style of the Eastern Cordillera transitions to uplifted basement blocks made of crystalline Palaeozoic rocks and the Sierras Pampeanas (Ramos et al., 2002). The Western Cordillera is an Eocene magmatic and tectonic belt (Mpodozis and Ramos, 1989) that is related to a west-vergent thrust system (WTS, Muñoz and Charrier, 1996). The Western Cordillera has peaks that rise to ~ 6 Km-in-high and involves stratovolcanoes of Miocene and younger age at the margin of the plateau (Jordan et al., 2010).

The geological characteristics of the Andean plateau vary along-strike. Internal plateau changes on topography, volcanism, tectonic style and subduction conditions, among others relevant aspects, have led to identify major internal plateau subdivisions: the Altiplano (15° - 22°S), the Puna (22° - 27°S) and the Puna de Atacama (east of the volcanic arc) (Jordan et al. 1983, Mpodozis and Ramos, 1989; Fig. 1 C). The Puna - Altiplano transition occurs at $\sim 22^\circ\text{S}$.

The Altiplano is characterized by a broad, low-relief, with a mean elevation of ~3.8 km. The Puna lies at an average elevation nearly a kilometer higher than the Altiplano, holds younger mafic magmatism (Maro et al., 2017), and its physiography involves several endorheic depressions bounded by basement-cored ranges (Whitman et al., 1996, Allmendinger et al., 1997, Jordan et al., 2010). The volcanic arc displays nearby N-S and separates the Altiplano-Puna on the eastern side of the plateau from the Puna de Atacama in the west. The volcanic arc (also known as the CVZ, the acronym for Central Volcanic Zone, 15°-28°S) is a chain of Miocene to Quaternary stratovolcanic complexes and andesitic/rhyodacitic domes of high-K calcalkaline affinities (Allmendinger et al., 1997; Kay et al., 1999, Jordan et al., 2010). The Puna de Atacama sets west of this volcanic arc and involves the Atacama basin, a major topographic and geologic anomaly that is one of several anomalous features occurring across the plateau margin at this latitude (Schurr et al., 1999; Götze and Krause, 2002; Belmonte, 2002).

From a stratigraphic point of view, the plateau is filled with synorogenic deposits that record clastic, volcanic, and evaporative Cenozoic episodes (Allmendinger et al., 1997; Baby et al., 1997; McQuarrie, 2002, Alonso et al., 2006). Most of compressive deformation and plateau uplift occurred in the Miocene and Pliocene all together with major felsic magmatism in the region. Large volumes of dacitic ignimbrites (over 104 km³ erupted volume) erupted from caldera complexes located in and to the east of the arc conducted to Altiplano-Puna plateau to be the largest Neogene ignimbrite province in the world (Babeyko et al., 2002, and references therein).

The plateau basement largely consist of Ordovician, and, locally, older metasedimentary marine, plutonic and volcanic rocks. Basement rocks dominate the outcrop along uplifted ranges. The basement is unconformable overlain by sparse exposures of marine calcareous sequences that record the Cretaceous - Paleocene rift basins. These deposits

correspond to the Salta Group (Brackebusch, 1883, 1891; nom. transl. Turner, 1959) in the Puna and its northwards equivalent Supersequences Puca and Coro-Coro (Sempere et al., 1997) in the Plateau and Western Cordillera of the Bolivian Andes.

Diachronic deformation (Hongn et al., 2007) drove Andean deposition in emergent continental basins. Cenozoic basin fill typically involves red beds, conglomerates and playa deposits containing interlayered evaporites and tuffs. Andean sequences resulted from sedimentation in interconnected and isolated basins during the evolving Andean foreland system (Lopez Steinmetz and Montero-Lopez, 2019, Montero-Lopez et al., 2020, Adad et al., 2020, and references therein). Regional isolation has strengthened once the plateau raised in the Mio-Pliocene. This period was characterized by a flare-up magmatism, regional uplift and the establishment of generalized endorheism (Isacks 1988; Kay et al., 1994, Allmendinger et al., 1997; Garzione et al., 2008, 2017, Gianni et al., 2020). The plateau rise and the Andean basin formation remain subjects of ongoing debate, as some data seems indicate that the formation of the high plateau, endorheism and intermontane basins could have started together and as early as the Paleogene (Canavan et al., 2014; Scott et al., 2018, López Steinmetz et al., 2020c). Quaternary alluvium covers the low-lying planes between mountain ranges and volcanoes. Halite dominated pans, locally known as *salares* and *salinas*, formed because of the extremely arid climatic conditions that prevail in these high-altitude endorheic basins since at least the Miocene (Alonso et al., 2006).

3. Material and Methods

The dataset in this article comprises two types of information: 1) major hydrochemistry including Li concentrations in brines from Andean salt pans, and 2) the areal surface (size) of these salt pans and of their basin catchments. The hydrochemical and Li data were obtained by compiling available information for 49 Andean salt pans published in the

scientific literature. All the areal surfaces of salt pan and respective basin catchments were obtained from satellite imagery. These values consist of geomorphological considerations of areal surfaces for 55 salt pans and their basin catchments, which include the 49 salt pans for which Li data were obtained, plus 6 additional salt pans from which there is no available hydrochemical information (i.e., Salar Grande, Capur, Los Infieles, Salar de la Laguna, La Piedra Parada, and Wheelwright). Surface sizes are summarized in Table 1. Salt pan locations are shown in Figure 1 and detailed in Table A1 of the Electronic Supplementary Data.

As detailed in the historical context outlined in Section 1, it is important to realize that the survey of Andean Li has involved a long period of data acquisition and that the available brine chemistry dataset emerged from diachronic sampling campaigns conducted by various scientists during different periods: 1) in most cases, the brine dataset from a particular salt pan results from a unique sampling campaign (i.e., no longitudinal sampling variation data are available), and 2) from a regional point of view (i.e., Andean plateau scale), when comparing the brine chemistry of different salt pan datasets are composed by diachronic sampling from one salt pan to the other. These aspects imply disparate frameworks for time-dependent conditions that can influence the sampling and analytical methodology. Examples include climate (which controls salinity saturation of brines regulating Li concentrations), sampling techniques (which determine the quality and representativeness of sampled brines), advances in analytical methodologies (which define hydrochemical data quality), etc. Therefore, we made sure to be particularly careful when assessing the validity of each dataset included in our regional brine hydrochemistry compilation: we only considered peer-reviewed scientific articles to construct our dataset.

The hydrochemical data compiled in this review (Table 2) correspond exclusively to residual brines from salt pans. Care was taken to exclude values from springs, rivers or streams from the dataset. In most cases, samples correspond to shallow and sub-surface brines

that were collected from hand-dug pits in the salt pans, i.e., at depths less than 1 m. In a few cases, samples were taken directly from brine pools (i.e., ponding brines) that had formed naturally in the salars (Risacher et al., 199; Lopez Steinmetz et al., 2018; 2020). Data considered for the Uyuni and Coipasa salars, in addition to near-surface brines, consists also of a collection of samples obtained at depths of up to 10 m from 40 holes dug in the salt crust of these salars. In Table 2, the sampling depths (in centimeters) are indicated by numbers in names of the 176 samples from Uyuni and Coipasa (for more details see Risacher and Fritz, 1991). Due to the regional scale of this review and, as just mentioned, the fact that most considered brines come from sampling within the salt pan, the specific location and depth of each of the 477 brines constituting our dataset (Table 2) are not reported here. In Table 2 all samples are grouped by salt pans which are located in Figure 1 and whose coordinates are provided in Table A1 of the Electronic Supplementary Data. In the following lines of this section, all references are provided to the scientific literature considered, as well as details on criteria for building the dataset. For further information on the sampling and analytical techniques deployed for specific data or the specific location of each sample, the reader is referred to the original papers from where the datasets were taken.

In this review, salt pans are grouped into Altiplano, Puna de Atacama and Puna salars, which is roughly equivalent to say Bolivian, Chilean and Argentinian, respectively, given that national borders follow natural boundaries in the plateau (Fig. 1). Readers that are not familiar with Andean geography, can find more detailed discussion on Andean salt pans and brine chemistry in the references listed in the following paragraphs.

The hydrochemical data set (Table 2) involves 477 brines samples and is composed of:

- 178 brine samples from the Altiplano salt pans that majorly correspond to data published by Risacher and Fritz (1991), and to a minor extent by Erickson and Salas (1987),

- 126 brine samples from the Puna salt pans (Ericksen and Salas, 1987; López Steinmetz, 2017; López Steinmetz et al., 2018; García et al., 2019; López Steinmetz et al., 2020a), and
- 173 brine samples from the Puna de Atacama salt pans reported by Moraga et al. (1974), Vila (1975), Ericksen and Salas (1987), and Risacher et al. (1999; summarized by COCHILCO, 2013).

For the case of the Salar de Atacama, we used samples ATA₀ and ATA_{do}, ATA, and Do1 to Do5 reported for Moraga et al. (1974) and Ericksen and Salas (1987), and ATA-05 and ATA-22 reported by Risacher et al. (1999), which are - to the best of our knowledge - the only available published data on brine samples collected within this salt pan, and offering a complete spectrum of major ions, Li, and TDS. It is important to note that Li values that are either i) isolated, from incomplete ionic characterizations, or ii) from non-scientific reports, were not taken into consideration. According to these criteria, the considered Li values are the unique, scientific published data of brine samples available from samples collected in the Andean salt pans, and offer a complete hydrochemical spectrum. Data reported in other scientific works correspond to inflow waters and/or hydrothermal springs, and not to residual brines lying within these salt pans, and/or do not offer a complete spectrum including TDS, major ions, and Li (i.e., Erickson et al., 1976a, 1976 b; Crespo et al., 1987; Rettig et al., 1987; Scandiffio and Alvarez, 1990; Scandiffio and Rodriguez, 1990; Mardones and Chong, 1991; Bevacqua, 1992; Garcés et al., 1996; López et al., 1996; Carmona et al., 2000; López Julián et al., 2001; Risacher et al., 2002; Banks et al., 2004; Vinante and Alonso, 2006; Boschetti et al., 2007; Ovejero Toledo et al., 2009; Salas et al., 2009; Schmidt, 2010; An et al., 2012; Durán Iriza, 2012; Vásquez et al., 2013; Boutt et al., 2016; Corenthal et al., 2016; Munk et al., 2018; Godfrey and Alvarez-Amado, 2020).

Mean brine compositions were computed from the information available, summarized in Table 3. In the case of the Salar de Atacama, we also considered values of 1,400 and 6,400

mg L^{-1} as the representative mean and maximum Li concentrations of the Atacama brines, respectively, as listed in Moraga et al. (1974; see also Ide and Kunasz, 1989; Kunasz, 2006). Accordingly, the hydrochemical and Li^+ concentrations of the Atacama brines (i.e., mean and maximum of 562 and $1,570 \text{ mg L}^{-1}$, respectively) from Moraga et al. (1974), Erickson and Salas (1987), and Risacher et al. (1999) are used for general characterizations such as shown in Figures 2 to 6, however, we used the 1,400 and $6,400 \text{ mg L}^{-1}$ mean and maximum Li concentrations when assessing this major salar in its regional context (Figs. 9 and 10). Li maximum (*max*) and mean concentrations of Li^+ and Mg^{2+} in all salars (Table 4) are also considered and discussed. Saturation indexes (SI) at standard ambient temperature and pressure (SATP, 25°C , 1 atm) were computed using the *Eqreeqc* 3.6.2 software, to address the saturation state of brines with respect to main salts. The most representative ranges of SI values are reported in the Results section.

4. Brine hydrochemistry across the Lithium Crescent

4.1. Altiplano salars

A few salt pans occur in the southern Bolivian Altiplano. Amongst these salars, the most prominent are Uyuni and Coipasa (#2): with an area of $10,000 \text{ km}^2$, Uyuni is by far the largest salt pan on Earth, and with its $1,650 \text{ km}^2$ Coipasa is the fourth largest salar in the Andean plateau (Fig. 1, Table 1). Empexa (#4 in Fig. 1) and Pastos Grandes (#11) also are large salars with their 402 and 124 km^2 , respectively. These salt pans are located at altitudes $>3.60 \text{ km asl}$, and their catchments involve endorheic basins having disparate surfaces that range between 600 and $45,200 \text{ km}^2$ (Table 1). None of these salt pans is yet being mined for lithium.

The brine chemistry of Uyuni and Coipasa was thoroughly described by Risacher and Fritz (1991), whereas only two isolated samples are available from Empexa and Pastos Grandes (Ericksen and Salas, 1987; Table 2). The Altiplano salt pans contain highly saline brines with mean TDS (Total Dissolved Solids) values comprised between 123 and 321 g L⁻¹ (Table 3), although in most cases TDS are in a range from 100 to ~220 g L⁻¹ (Risacher and Fritz, 1991; Table 2). The maximum TDS values reported are of 351 g L⁻¹ and 368 g L⁻¹, respectively from Uyuni and Coipasa (Ericksen and Salas, 1987).

Based on their major chemical compositions, brines in Uyuni are of the Mg²⁺ - Na⁺ / Cl⁻ - SO₄²⁻ type, with Mg²⁺ ≥ Na⁺, whereas in Coipasa, Empexa and Pastos Grandes brines are of the Na⁺ - Mg²⁺ / Cl⁻ - SO₄²⁻ type, with Na⁺ > Mg²⁺ (Fig. 2 and 3 a). Main characteristics of brines from Altiplano salars are their high Mg²⁺ concentrations and their relatively low K⁺ and Ca²⁺. Stoichiometric ionic ratios between Na⁺ and Cl⁻ are consistent with the equilibrium solubility of halite for a certain number of the Uyuni brines (i.e., SI ≈ 0, e.g., samples RA130, RB180, RC120), however, a large number of them plot along an oblique line with respect to the 1:1 proportion (Fig. 3 b), suggesting that the brine reached saturation with respect to (and thus precipitated) halite (SI > 0 and up to 0.36, e.g., samples RX10, RZ1, CA150). Except for some samples from Coipasa (e.g., CB150 and CA250), the fact that the SO₄²⁻ : Mg²⁺ ratio forms a trend Mg^{2+>}SO₄²⁻ perpendicular to the 1:1 line, is in turn consistent with the saturation of the brines with respect to epsomite (MgSO₄ 7H₂O, SI > 0 and up to 0.73, e.g., samples RZ1, RT15, RX10), and/or other Mg-bearing sulfated salts (Fig. 3 c).

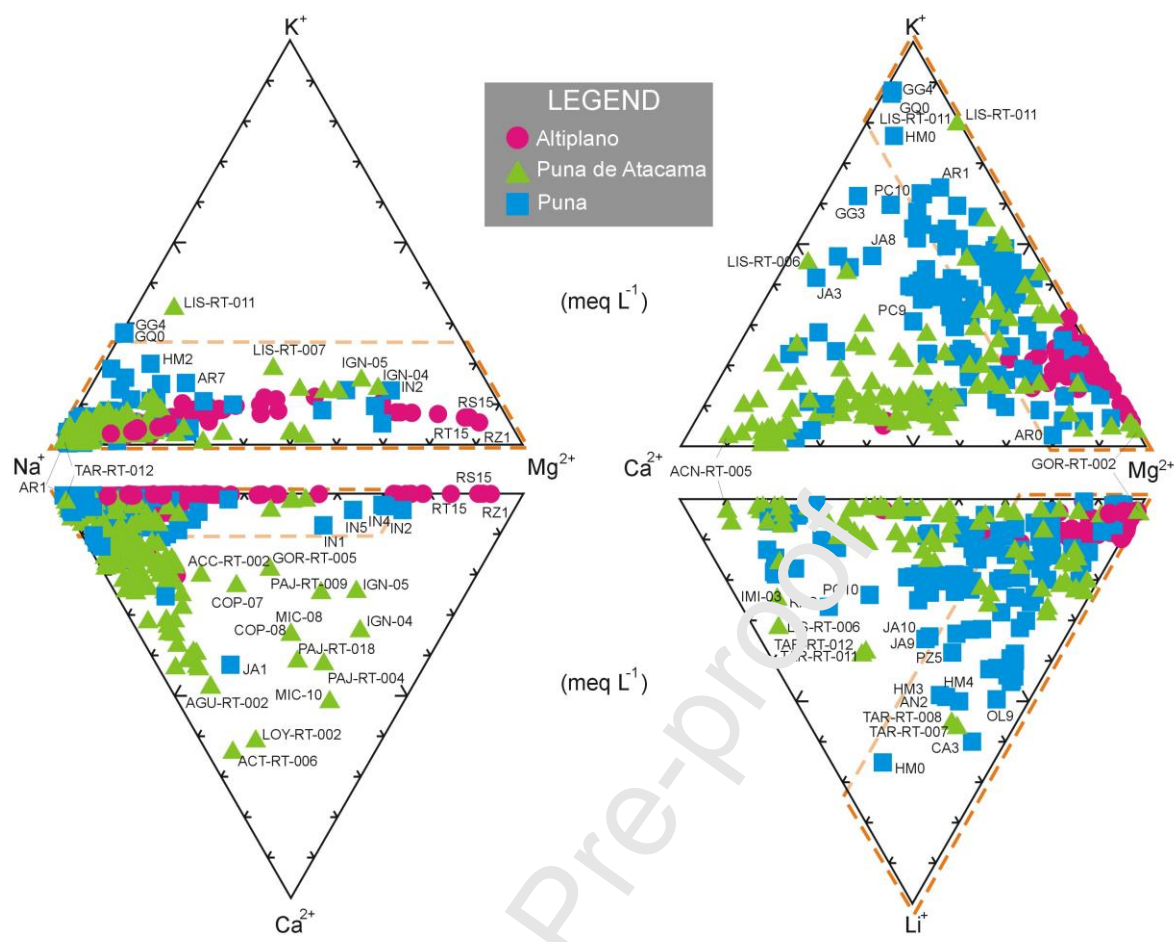


Figure 2. Ternary diagrams displaying relative cationic concentrations measured in brines from Andean salars. Plotted samples and concentrations correspond to those detailed in Table 2. Fields delimited by orange dashed line represent the hydrochemistry of brines from the Tibet Plateau (Li et al., 2019b).

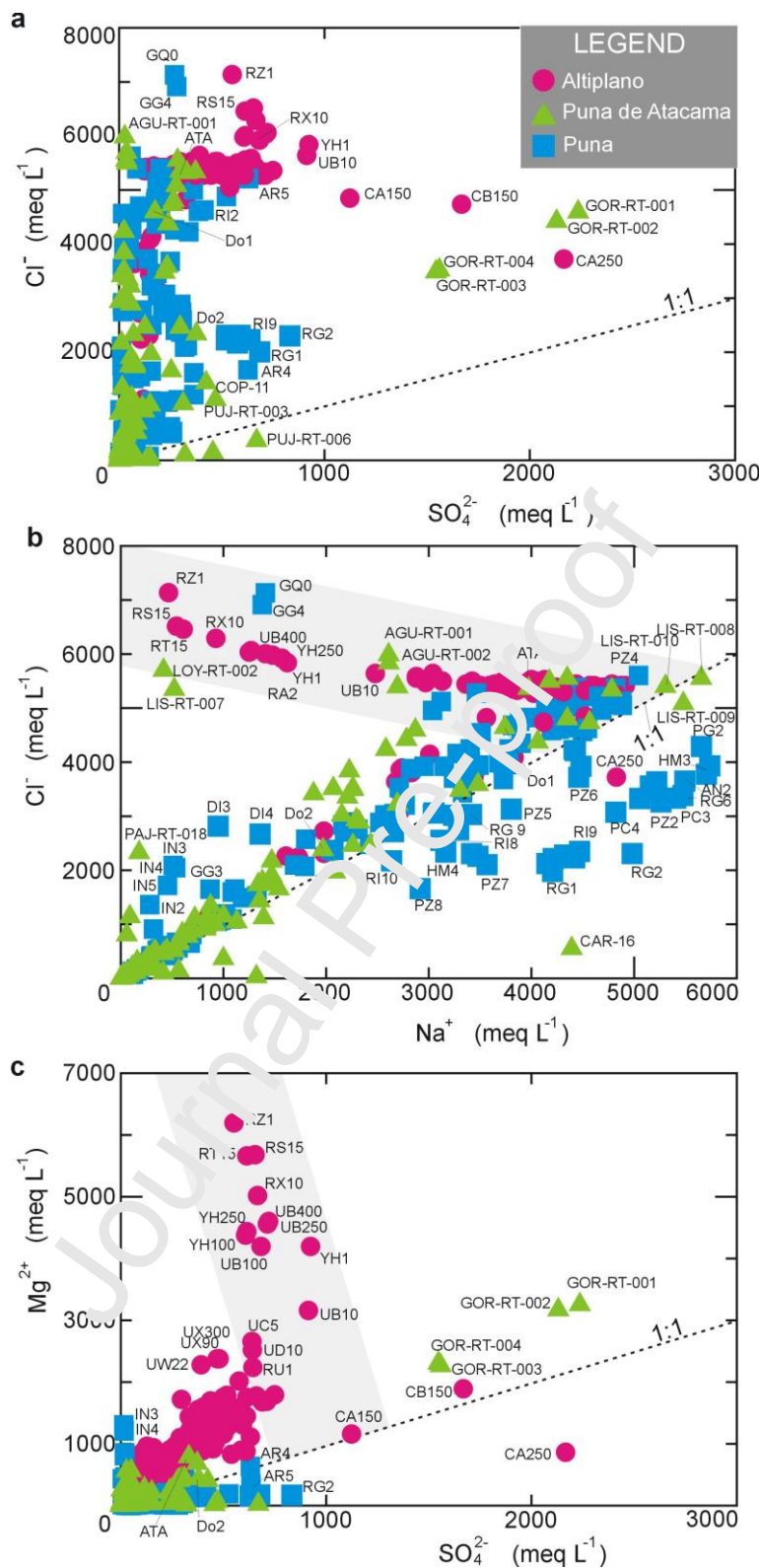


Figure 3. Scatter diagrams plotting the concentrations of a) SO_4^{2-} versus Cl^- , b) Na^+ versus Cl^- , and c) SO_4^{2-} versus Mg^{2+} in brines from Andean salars. Gray zones in panels a) and b) signal trends that are independent from the 1:1 ratio (dashed line) and that could correspond to brine saturation. Plotted values correspond to concentrations detailed in Table 2.

The mean Li^+ concentrations in Empexa and Coipasa are 213 and 258 mg L⁻¹, respectively, whereas the only available sample from Pastos Grandes indicates Li values as high as 1,640 mg L⁻¹ (Ericksen and Salas, 1987). In Uyuni the maximum reported Li value is of 4,720 mg L⁻¹ with a mean of 715 mg L⁻¹ (Risacher and Fritz, 1991; Tables 2 and 3). Two different tendencies are observed between the concentrations of Li^+ and Cl^- in the Altiplano brines: an oblique trend, which only includes a part of the Uyuni's brines, suggests a positive correlation between Li^+ and Cl^- , whereas a horizontal trend including samples at higher Li values, shows that the concentrations of Li^+ in most samples evolve independently from those of Cl^- (Fig. 4 a). Two different tendencies are also observed between Li^+ and Na^+ (Fig. 4 b). A certain amount of data from Uyuni form a roughly positive Li^+ versus Na^+ correlation. This trend is consistent with the correlation observed between Li^+ and Cl^- , and together suggest that the concentrations of Li^+ could be related to the equilibrium solubility of halite. Furthermore, the Pearson's correlation coefficient (R) corresponding to the mean concentrations of Li^+ , Cl^- and Na^+ across Andean salars ranges between 0.70 and 0.80 (Fig. 5). The second tendency depicted by the Li^+ versus Na^+ data trend includes most of the Altiplano brine samples, and forms an oblique line showing Li^+ increasing inversely to Na^+ , up to the concentrations of Uyuni samples RS15 and RZ1 (Figure 4 b). This pattern, which most likely corresponds to brine saturation with respect to halite, suggest that the Li^+ concentrations increase while halite precipitates.

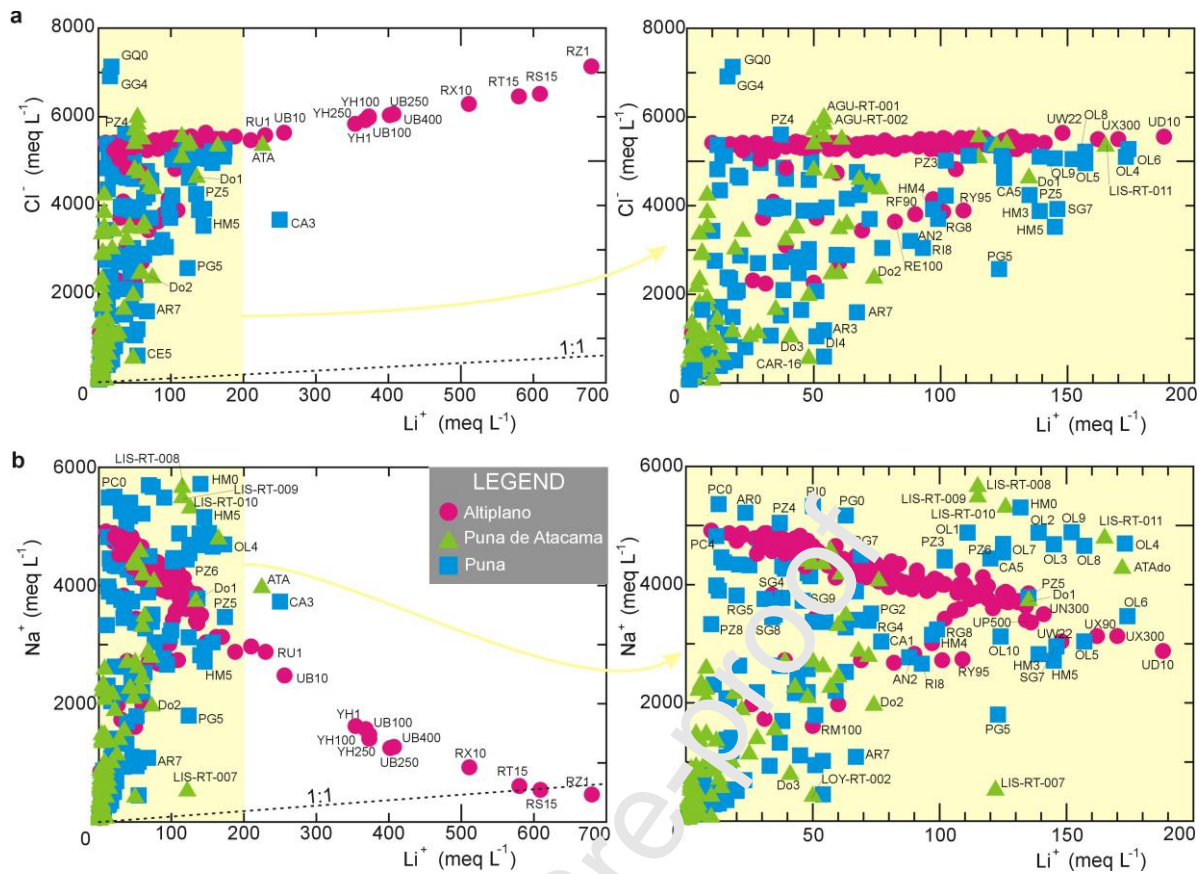


Figure 4. Scatter diagrams showing the variations of a) Li^+ versus Cl^- , and b) Li^+ versus Na^+ , in brines from Andean salars. Insets (yellow panels) offer a detailed view of the data displayed in the yellow boxes. Plotted values correspond to the concentrations detailed in Table 2.

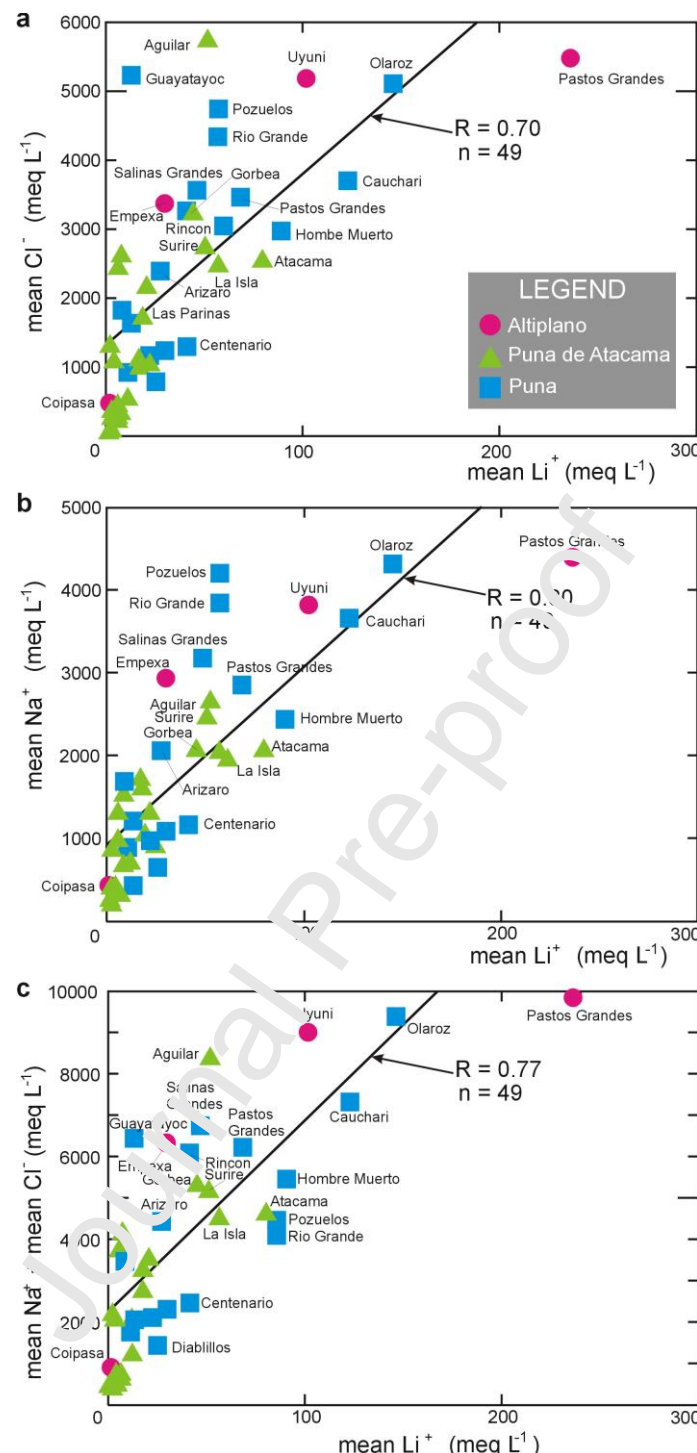


Figure 5. Scatter diagrams plotting the variations for the mean concentrations of a) Li^+ versus Cl^- , b) Li^+ versus Na^+ , and c) in Li^+ versus $\text{Na}^+ + \text{Cl}^-$, in the Andean salars according to values presented in Table 3. The plotted mean Li^+ concentration for Atacama results from considering values reported by Moraga et al. (1974), Erickson and Salas (1987), and Rischaeer et al. (1999). It is important to note that this value differ from the globally accepted mean Li concentration in Atacama that is 1,400 mg L⁻¹ (~202 meq L⁻¹; Moraga et al., 1974; Ide and Kunasz, 1989; Kunasz, 2006). R is the Pearson correlation coefficient, n is the total number of points in the data set (i.e., the number of salars).

An additional interesting feature of the Altiplano brines is that Li^+ also seems to correlate, in different proportions, with K^+ , B, and Mg^{2+} (Fig. 6). The $\text{K}^+:\text{Li}^+$ ratios in most Altiplano brines array along a 1:4 trending line, a pattern that could be consistent with the equilibrium solubility of 1:4 salts (complex K-, Li-, Na- Cl salts, yet undetermined). Samples plotting along an oblique trend to the 1:4 proportion suggest saturation of the brine with respect to these compound (Fig. 6 a). When comparing mean values, it can be observed that the correlation R between Li^+ and K^+ reaches 0.68, which confirms this pattern reflects a Li^+ - K^+ interdependency (Fig. 6 b).

The concentrations of Li^+ and B in the Altiplano brines plot along a line that defines a 3:1 proportion trend (Fig. 6 c), and mean values are highly correlated ($R = 0.78$; Fig. 6 d). The concentrations of Li^+ also increase consistently with those of Mg^{2+} (Fig. 6 e), with the $\text{Mg}^{2+}:\text{Li}^+$ ratios defining trends with correlations of about 1:50 in Coipasa, 1:13 in Empexa and Uyuni, and ~1:1 in Pastos Grandes (Fig. 6 e). The observed proportionalities between Li^+ , B and Mg^{2+} have not been yet explained and could correspond to the equilibrium solubility of complex borates and other salt or, alternatively, to the ionic influence of cations in exchangeable positions within clays. In any case, these proportionalities require further investigations. Interestingly, the Li^+ versus B pattern defined by the Altiplano brines is close to that displayed by brines from saline lakes in the Tibet Plateau (Fig. 6 c), which contains the second most important Li-brine type deposits on Earth (Zheng and Liu, 2009; Kesler et al., 2012; Li et al., 2019b, and references therein).

Mean Mg:Li ratios are 22 in Uyuni, 40 and 47 in the Empexa and Coipasa, respectively, and as low as 2 in Pastos Grandes (Fig. 6 C, Table 4). With Mg^{2+} means of >15,000 and >12,000 mg L⁻¹, the Uyuni and Coipasa brines contain amongst the highest magnesium concentrations in the Andean plateau (Figs. 2 and 5 e, Tables 3 and 4).

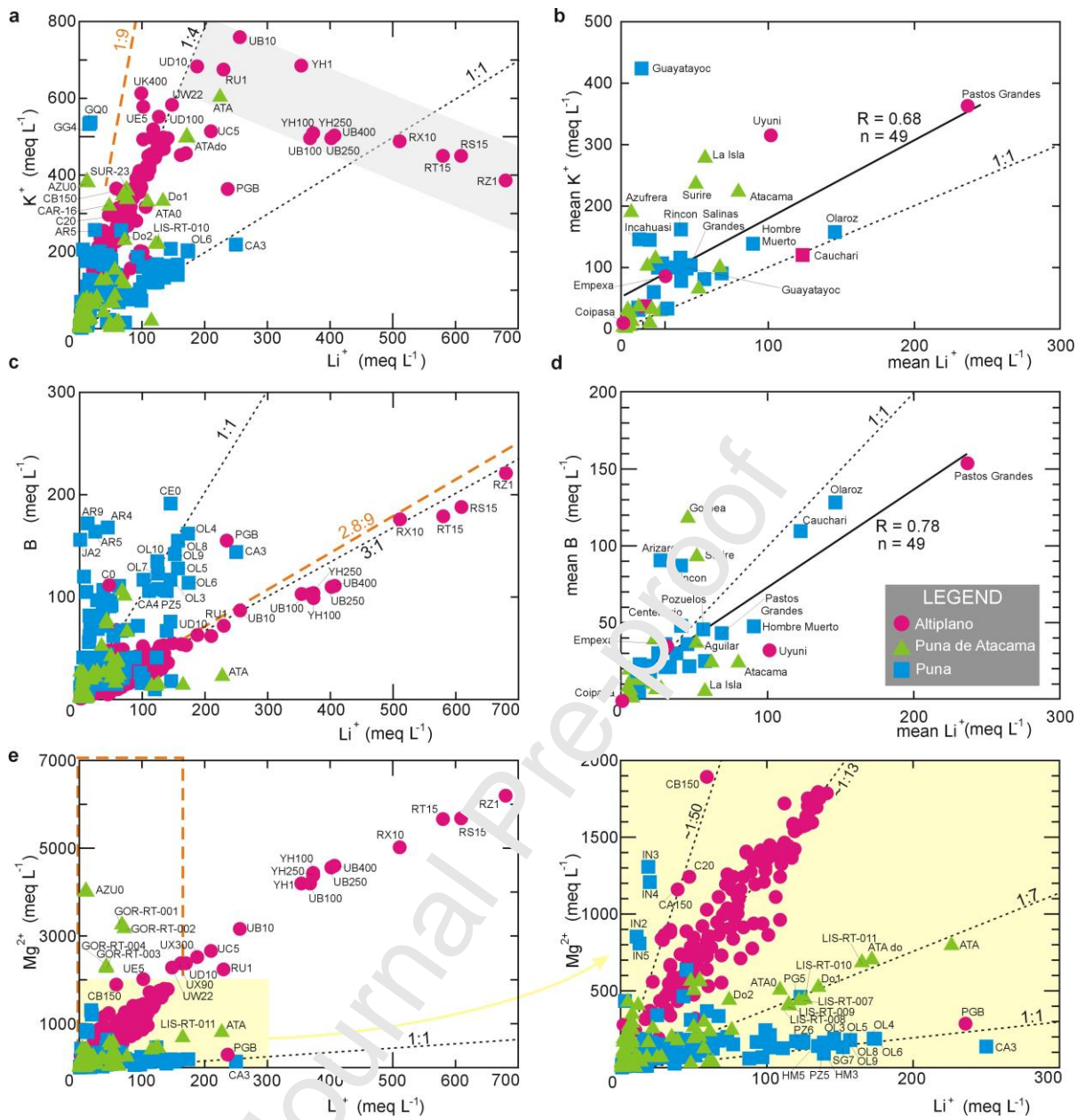


Figure 6. Scatter diagram showing the variation between the concentrations of a) Li^+ and K^+ , b) mean Li^+ and mean K^+ , c) Li^+ and B , d) mean Li^+ and mean B , and e) Li^+ and Mg^{2+} . Values plotted in a), c), and e) are for brine compositions presented in Table 2. Scatter diagrams b) and d) plot mean concentrations according to values summarized in Table 3. Continuous line: R correlation coefficient, with n = the total number of salars. Dashed line: stoichiometric ratio. Orange dashed line and rectangle: stoichiometric proportions (panels a and c) and field (panel e) characterizing brines from the Tibetan Plateau (data from Li et al., 2019b).

4.2. Puna de Atacama Salars

Salt pans in the Puna de Atacama are located at altitudes between 2,300 (Atacama) and 4,500 (Pujsa, #15) m asl (Table 1, Fig. 1). The surfaces of these salars and their endorheic

basins are highly variable. With its 3,000 km², Atacama is the largest Chilean salt pan and, with a catchment area of 18,100 km², also the largest endorheic basin in the Chilean portion of the plateau. The smallest salt pans, such as Salar de la Laguna (#35) and Ignorados (#27), are only of 1 km² (Table 1). In the Puna de Atacama, only the Salar de Atacama is presently being mined for Li.

The brine chemistry of salars in the Puna de Atacama was comprehensively addressed by Risacher et al. (1999). Brines have highly variable salinity, with TDS ranging up to 370 g L⁻¹. The highest salt concentrations are observed in brines from Sucre (#1), Atacama, and La Azufrera (#25), where mean values grade between 178 and 267 g L⁻¹ (Tables 2 and 3).

According to their major chemical compositions, the Puna de Atacama brines are of the Na⁺ - Mg²⁺ / Cl⁻ - SO₄²⁻ type (Figs. 2 and 3 a). A few brines contain Mg²⁺ ≥ Na⁺ (e.g., samples IGN-04 and 05, PAJ-RT-004 and 018, ACT-RT-006; Fig. 2), and/or Ca²⁺ ≥ Na⁺ and Mg²⁺ (e.g., samples ACT-RT-006, LOY-RT-002, MIC-10, and AGU-RT-002; Fig. 2). The concentrations of Cl⁻ are generally higher than those of SO₄²⁻, with few samples of low salinity having SO₄²⁻ > Cl⁻ (e.g., sample PUJ-RT-006 to 008, ACSS-RT-005 to 007, IGN-004 and 005; Fig 3 a). The main characteristics of salar brines in the Puna de Atacama are their high Ca²⁺ and their relatively low K⁺ when compared to brines from neighboring parts of the plateau (Fig. 2).

The Na⁺ versus Cl⁻ concentration patterns are quite similar to those observed in the Altiplano brines (Fig. 3 b). Stoichiometric ratios ~1:1 between Na⁺ and Cl⁻ are consistent with the equilibrium solubility of halite (SI ≈ 0, e.g., sample Do2; Fig. 3 b), and samples plotting oblique to the 1:1 proportion trend suggest brine halite saturation and precipitation (SI > 0 and up to 0.47, e.g., samples AGU-RT-001, LOY-RT-002, LIS-RT-007; Fig. 3 b). Similarly to the Altiplano brines, the SO₄²⁻ and Mg²⁺ concentrations plot along the 1:1 proportional line, which is consistent with the equilibrium solubility of epsomite (MgSO₄ 7H₂O), and/or other

Mg-bearing sulfates (Fig. 3 c). However, some brines do not match the $\text{SO}_4^{2-}:\text{Mg}^{2+}$ uniequivalent proportion trend, which implies the presence of other salts that are not in equilibrium with the brines (e.g., SI maxima for anhydrite and gypsum reach values of 1.07 and 1.10, respectively, in sample AGU-RT-001).

Li concentration in pan brines of the Puna de Atacama are very high. Indeed, the Puna de Atacama desert is known as having the richest Li brine-type deposits on Earth, and the salt pan of Atacama is the most important operating Li mine in world today, with mean Li grades of $1,400 \text{ mg L}^{-1}$ and maximum measured concentrations reaching $5,400 \text{ mg L}^{-1}$ (Moraga et al., 1974; Ide and Kunasz, 1989; Kunasz, 2006). Other than Atacama, high Li^+ concentrations were also measured, for instance, in La Isla (#30), Gorbea (#26), and Surire, where mean Li^+ grades are between 300 and 400 mg L^{-1} (Tables 2 and 3).

Despite that the Li^+ versus Cl^- and Na^+ concentrations distribute quite dispersedly, samples plot within the field defined by trends of the Altiplano brines (Fig. 4). Furthermore, mean Li^+ , Cl^- and Na^+ concentrations from the Puna de Atacama salars match the correlation lines characterizing other Andean brines (Fig. 5). Positive correlations could also exist between the concentrations of Li^+ and K^+ (Figs. 6 a and b). However, no evident correlation is observed between Li^+ and Ba^{2+} (Figs. 6 c and d), whereas some samples arrays along the 1:7 proportional line, which might imply the existence of complex Li, Mg bearing salts (Fig. 6 e).

Despite that nearly uniequivalent proportions of Mg and Li are found in El Tara (#13) and Imilac (#21), these ratios are most often $\neq 1$. $\text{Mg}^{2+}:\text{Li}^+$ ratios < 10 are observed in Pujsa, Loyoques (#16), La Isla, Las Parinas (#32), Surire, Maricunga (#38), and Atacama, whereas brines with Mg^{2+} concentrations about two orders of magnitude higher than those of Li^+ are found in Michincha (#7), Ignorados, and La Azufrera (Fig. 6 e, Table 4). This kind of brines, characterized by $\text{Mg}^{2+} \gg \text{Li}^+$, are also observed in brines from saline lakes in the Tibet Plateau (Fig. 6 e; Li et al., 2019b).

4.3. Puna Salars

The Puna plateau holds 17 major salars that are located at altitudes ranging between 3,269 (Incahuasi, #39) and 4,080 (Jama, #53) m asl (Table 1; Fig. 1). With the exception of giant Arizaro (1,708 km², #42) and the three smallest salars sizing less than 10 km² (Centenario, Diablillos, #44, and Ratones), salt pans surfaces range from 30 to 650 km² (Table 1). These salars are settled in endorheic basins with surfaces that mostly vary from 1,000 to 9,000 km². With 14,536 km², Rio Grande (#41) holds the largest basin catchment area, whereas the smallest basins correspond to the smallest salt pans (Table 1).

Amongst the Puna salt pans, only Hombre Muerto and Olaroz are being actively mined for Li. The brine chemistry in the Puna salars has been characterized by López Steinmetz et al. (2018) and López Steinmetz et al. (2020a). These brines contain highly variable saline content and ionic proportions. TDS as low as 6 g L⁻¹ have been found in some salars such as Jama, whereas TDS up to 381 g L⁻¹ were found at Olaroz, define the maximum measured values (García et al., 2019). Brines from the Puna salars are of the Na⁺ - K⁺ / Cl⁻ - SO₄²⁻ type in the north, of the Na⁺ - Mg²⁺ / Cl⁻ - SO₄²⁻ type in the south, and the SO₄²⁻ concentrations increase from south to north (Figs. 2 and 3 a).

Similar to the Altiplano and Puna de Atacama, most of the Puna brines have Na and Cl concentrations that correlate positively along a 1:1 stoichiometric ratio, which is consistent with equilibrium solubility of halite (SI ≈ 0, e.g., samples AR9, PC7; Fig. 3 b). Some degree of correlation could exist between SO₄²⁻ and Mg²⁺ in some samples such as AR4 and AR5. However, as depicted in Figure 3 c, the Mg²⁺:SO₄²⁻ ratios do not match the 1:1 trend, implying the existence of other Mg²⁺- and SO₄²⁻-bearing salts (e.g., maximum SI values for anhydrite and gypsum range from -3.19 to 0.54 and -2.95 to 0.63, respectively, in samples IN3 and RG2).

Amongst Puna salars, maximum Li⁺ values of 1,739 and 1,213 mg L⁻¹ were found in Cauchari and Olaroz, respectively (Tables 2 and 4). In addition to these salt pans, where mean Li concentrations reach 860 and 841 mg L⁻¹, respectively, high Li-graded brines are stored in Hombre Muerto, Pastos Grandes (#49), Pozuelos (#48), Rio Grande, Salinas Grandes, and Rincon (#50), where mean Li⁺ concentrations are between 280 and 570 mg L⁻¹ (Table 3).

According to its geochemical behavior, Li variations in brines are expected to be consistent with those of other conservative solutes such as Cl⁻ and Na⁺. Positive correlations can exist between the concentrations of Li⁺, Cl⁻ and Na⁺ in some cases (Figs. 4 and 5). Furthermore, Li also seems correlate positively with K⁺ and B, and to a minor extent also with Mg²⁺ (Fig. 6). Interestingly, the concentrations of Li⁺ and Y⁺ in the Olaroz and Cauchari (#51) brines display along the 1:1 ratio, whereas proportions in the remaining brines better fit the 1:4 dominant pattern defined by the Uyuni's brines (Figs. 6 a). Despite there is no clear pattern between Li⁺:B and Li⁺:Mg²⁺, nearly equivalent proportions are mainly observed in salt pans from the northern Puna (Figs. 6 c d and e). However, brines from the Southern Puna instead show ionic proportional patterns mainly displaying parallel to the vertical axis (i.e., parallel to the B and Mg²⁺ axes), such as for Incahuasi, which brines match the trend ~1:50 ratio of the Coipasa brines (Fig. 5 e).

With the exception of Incahuasi, which brines contain high Mg²⁺ concentrations that are in the range of those observed in Uyuni and Coipasa (Fig. 6 e), remaining Puna salt pans, especially in the northern Puna, show the lowest Mg²⁺ values amongst the entire Andean plateau (Fig. 2, Table 4). These salars are characterized by brines having mean Mg:Li ratios \leq 11, and some brines have exceptionally low ratios of 1 to 3, as the case of Ratones, Guayatayoc, Cauchari, and Olaroz (Table 4).

5. Discussion

5.1. Lack of Li geographical distribution

Andean Li-brine type deposits are found both in mature and in immature salars (Houston et al., 2011; Fig. 7 a and b). Andean mature salars, such as Atacama, correspond to halite dominated pans, whereas immature salars, like Uyuni and Olaroz, are mostly filled by clastic saline muds (Houston et al., 2011). Sometimes, mature and immature zones can be found in the same salt pan. For example, western Hombre Muerto corresponds to a mature pan, whereas its eastern side is an immature salar. An additional example is the Salar de Atacama. Here, the halite nucleus (i.e., mature salar) spreads for an area of 1,100 km² and ~1,000 m depth, in the southern part of the salar, whereas the northern part is clastic dominated and gypsum rich (Boutt et al. 2016; Corer'hal et al. 2016; and references therein).

However, the more often, Andean salt pans are complex combinations of crystalline salt layers, which are interbedded, in highly and variable proportions, with clastic fine -graded sequences (e.g., Salar del Rincon and Maricunga). In the practice, the predominant type tendency of a salt pan is revealed more clearly during the brine extraction. Pumping in mature and immature pans implicates different responses of the water (i.e., brine) table due to the contrasting porosity (and permeability) of the substrate (i.e., porous salt pan and impermeable clay and muddy -rich deposits, respectively). During operations, pumping in a mature salar conduces to the development of a shallow depression cone of the water table around the pumping well, whereas in immature salars the cone deepens faster than it extends horizontally (Houston et al., 2011).

Three major noteworthy observations need to be addressed concerning mature and immature salars. Firstly, there is no strict rule and the areal extent of mature salars does not necessarily exceed that of immature salars (see Table 1). Secondly, brines in halite-dominated pans does not always contain higher Li concentrations than immature salars (Houston et al.,

2011; see Table 3). Thirdly, high Li -graded brines are not necessarily related to saline nucleus. Furthermore, deeper brines are not systematically richer in lithium. For instance, in the salt pan of Atacama the Li concentration isopleths form a pattern consisting of concentric Li grade zones with maximum values located in the southern part – and not in middle – of the halite nucleus (Moraga et al. 1974; Stoertz and Erickson 1974; Ide and Kunasz 1989; Bevacqua 1992; Alonso and Risacher 1996; Carmona et al. 2000; Boschetti et al. 2007; Boutt et al. 2016; Corenthal et al. 2016). These concentric patterns are not the same at near surface levels as they are at depth. For example, if it is true that in the Uyuni salar Li concentrations increase concentrically and asymmetrically with depth, moving southward (Risacher and Fritz 1991; Fig. 7 c), in certain parts, Li concentrations do not change with depth, such as along the UI well where a constant Li concentration (300 mg L^{-1}) is reported from near surface down to 10 m depth (Fig. 7 c). An additional example of this is the Salar de Olaroz. The highest near surface concentrations of Li occur forming a pattern that can be followed along a NE-SW axis running through the middle of the salar (García et al., 2020; Fig. 7 d). Conversely, the pattern at ~200 m depth consists of two high Li level zones in the northern and southern parts of the salar, disrupted by an intermediate brine grade zone near the center of the pond (see García et al., 2020; Fig. 7 e).

Aridity is an important parameter controlling brine Li concentration along a vertical profile. By enhancing evaporation near the surface, it can cause shallower brines to have higher Li levels than those lying below. Clearly, a complex interplay of the above aspects to which add other factors such as the presence of hydrothermal springs and the role played by structures on Li-rich waters supply into the system, among many others listed by Godfrey et al. (2013; cf. also discussion below, sections 5.4 and 5.5), drive the singularity of each Andean salar. This notwithstanding, it is remarkable to observe that the major hydrochemical composition of brines is relatively similar across the Andean plateau (Fig. 8).

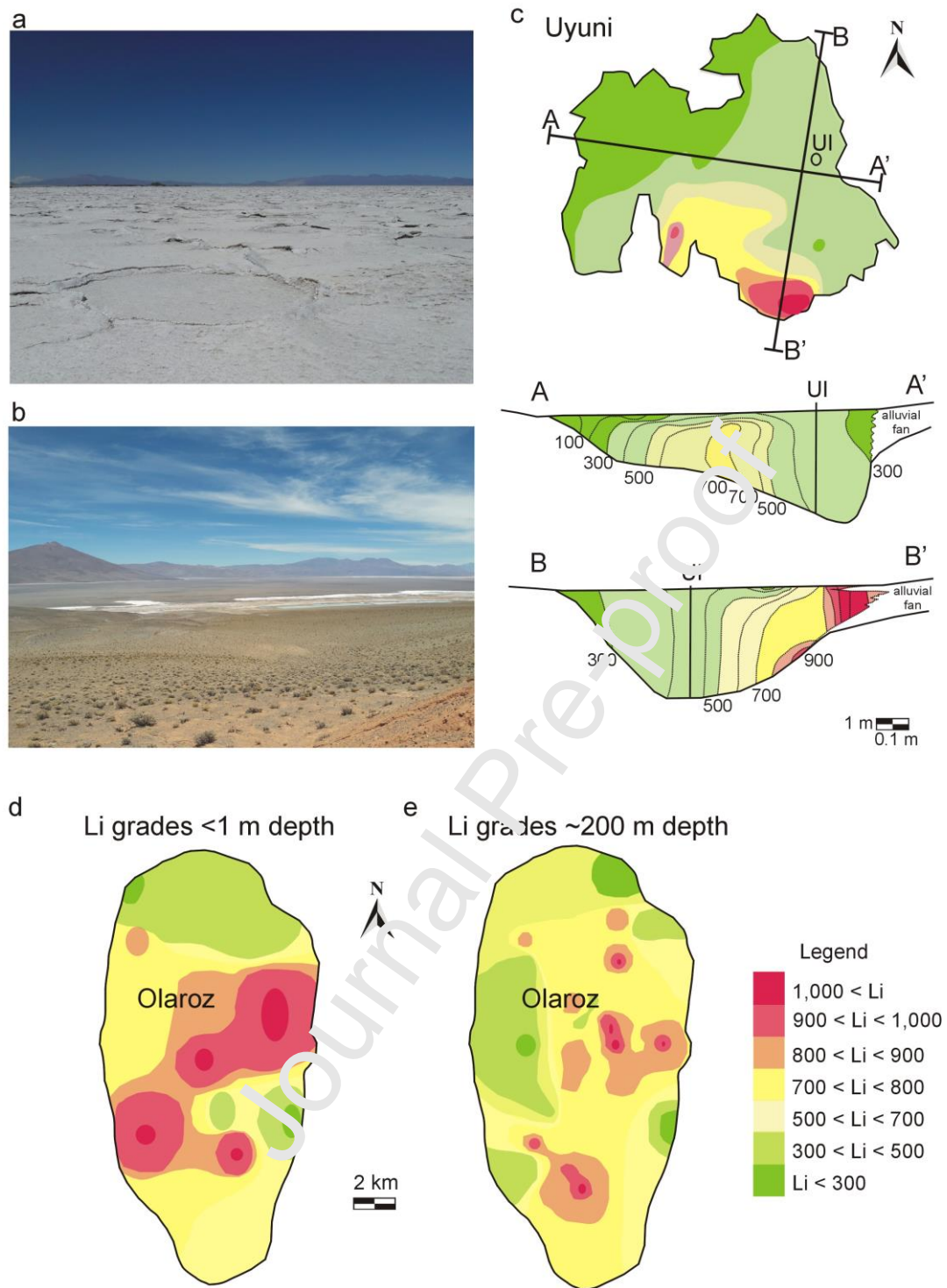


Figure 7. Pictures showing a) Salar de Pastos Grandes (Puna), and b) Salar del Rincón, respectively examples of mature and immature Andean salars. Notice the salt crust and the brown clastic surfaces. c) Map (upper panel) showing the Li isoconcentration curves in brines and the location of vertical profiles A-A' (middle panel) and B-B' (bottom panel) from Uyuni (modified from Risacher and Fritz, 1991). The location of well UI (referred in the text of section 5.1) is shown in panels. d and e) Map showing the concentration of Li in near surface (<1 m depth) and deep (~200 m depth) brines in Salar de Olaroz (modified from Garcia et al., 2020). Li concentrations are in mg L^{-1} .

A typical feature of evolved (evaporated) and highly saline waters is a composition marked by the presence of Cl^- and SO_4^{2-} , and a depletion in $\text{CO}_3^{2-}/\text{HCO}_3^-$ (Langbein, 1961; Hardie and Eugster, 1970; Eugster, 1980). Andean brines can be compared to those from Li-bearing saline lakes in the Tibetan Plateau (Li et al., 2019b, and references therein), despite obvious geological-environmental differences. In both cases, they commonly belong to the $\text{Cl}^- - \text{SO}_4^{2-}$ type, and the hydrochemical variability is generally marked by variations in the major cations (Figs. 2 and 3 a). Our data compilation indicates that composition with a $\text{Na}^+ - \text{Mg}^{2+}$ signature largely predominate in the whole Andean plateau (and in Tibet), with the exceptions of Uyuni ($\text{Mg}^{2+} - \text{Na}^+$ signature) and the Northern Puna salars ($\text{Na}^+ - \text{K}^+$ signature). Brines with high Mg^{2+} concentrations occur in the Altiplano, whereas they are generally depleted in this cation in the Northern Puna. Finally, Ca^{2+} shows the highest concentrations in the Puna de Atacama, west of the modern Andean volcanic arc (Fig. 8).

The association between Li and E evidenced by our data (Figs. 6 c and d) confirms the existence of a link between these two chemical elements in Andean evaporitic systems, as was indicated by Catalano (1964), Alonso et al. (1988), Alonso et al. (1991), Kistler and Helvaci (1994), and observed in other parts of the globe (e.g., Helvaci et al., 2004, and references therein). However, isotopic studies have shown that, in the Andes, Li and B share only a partial common origin (Kaseman et al., 2004). Two distinctive origins have been suggested as sources for boron: for the western plateau, isotopic values indicate a volcanic contribution, mostly Neogene meso-silicic pyroclastic rocks and related hydrothermal systems, whereas weathering of volcanoclastic sequences from the Paleozoic basement are the probable source of B in the eastern plateau (Kaseman et al., 2004). The Paleozoic basement is also considered to be the primary source of Li (Egenhoff and Lucassen, 2003; Peralta Arnold et al., 2017; García et al., 2019; Meixner et al., 2019). Such common origin is reflected by the strong association between Li and B ($R = 0.78$; Fig. 6 d). However, their concentration ratios grading

up to 3:1, and the fact that they are mostly characterized by Li>B south of ~22°S and B>Li to the north of it, point to the absence of unambiguous Li:B patterns, consistently with B and Li being sourced from different lithologies. While it appears clear that further studies on the Li-B geochemical relationships are necessary (e.g., Lopez Steinmetz et al., 2020a), it seems safe to suggest that B may not be an appropriate prospective tool for lithium, at least not in the Andean region.

Despite that major brine chemistry, as discussed above, shows some degree of geographical organization with respect to compositions (Fig. 8), there is no obvious Li⁺ distribution across the Andean plateau. Geographic patterns are also not observed for K, B, and Mg. The only common trend shown by those plots is that, as a whole, maximum Li⁺ values were reported from salt pans located in the central area of the plateau, between 66°30' – 68°30' W and 20° – 24° S (Figs. 9 a and b). This spatial distribution is consistent with that of other cations, such as Mg²⁺ (Figs. 9 c and d), confirming that the most saline brines and highest ionic concentrations occur in the middle of the Andean plateau desert. It would thus be expected that solute concentrations would decrease in salt pans located towards the desert borders. This pattern is intriguing and clearly worthy of further studies. In summary, Li concentrations across the Andean plateau lack a clear geographic distribution pattern, other than that depicted in Figure 9.

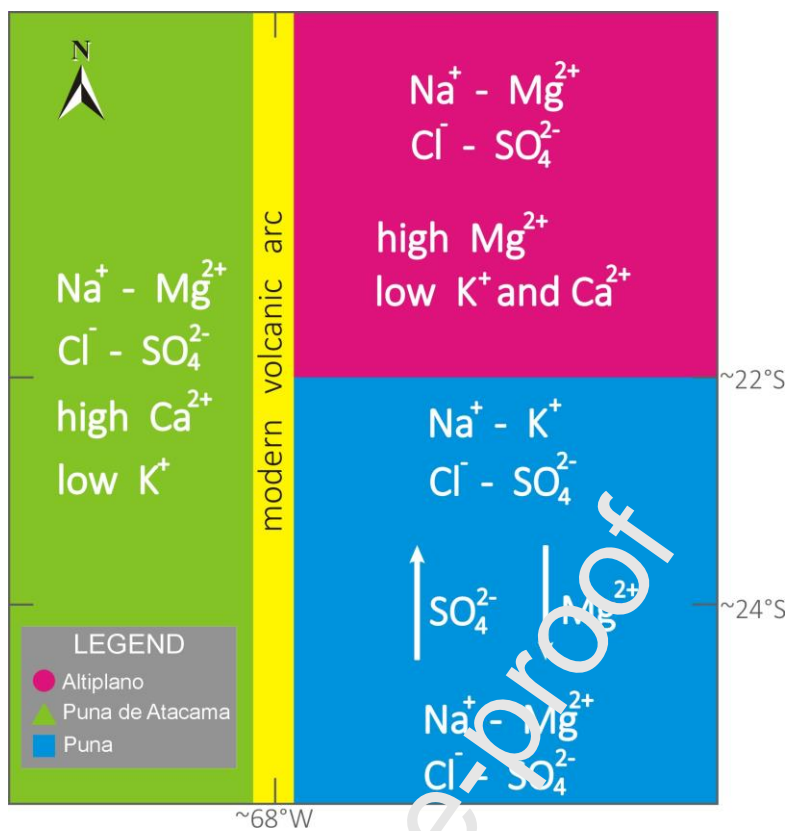


Figure 8. A schematic illustration of the internal subdivision of the Andean plateau (see legend), summarizing major brine chemistry in salt pans across the Lithium Crescent. “Modern volcanic arc” (yellow area) refers to the present-day situation; the past Cenozoic situation is not considered in this scheme.

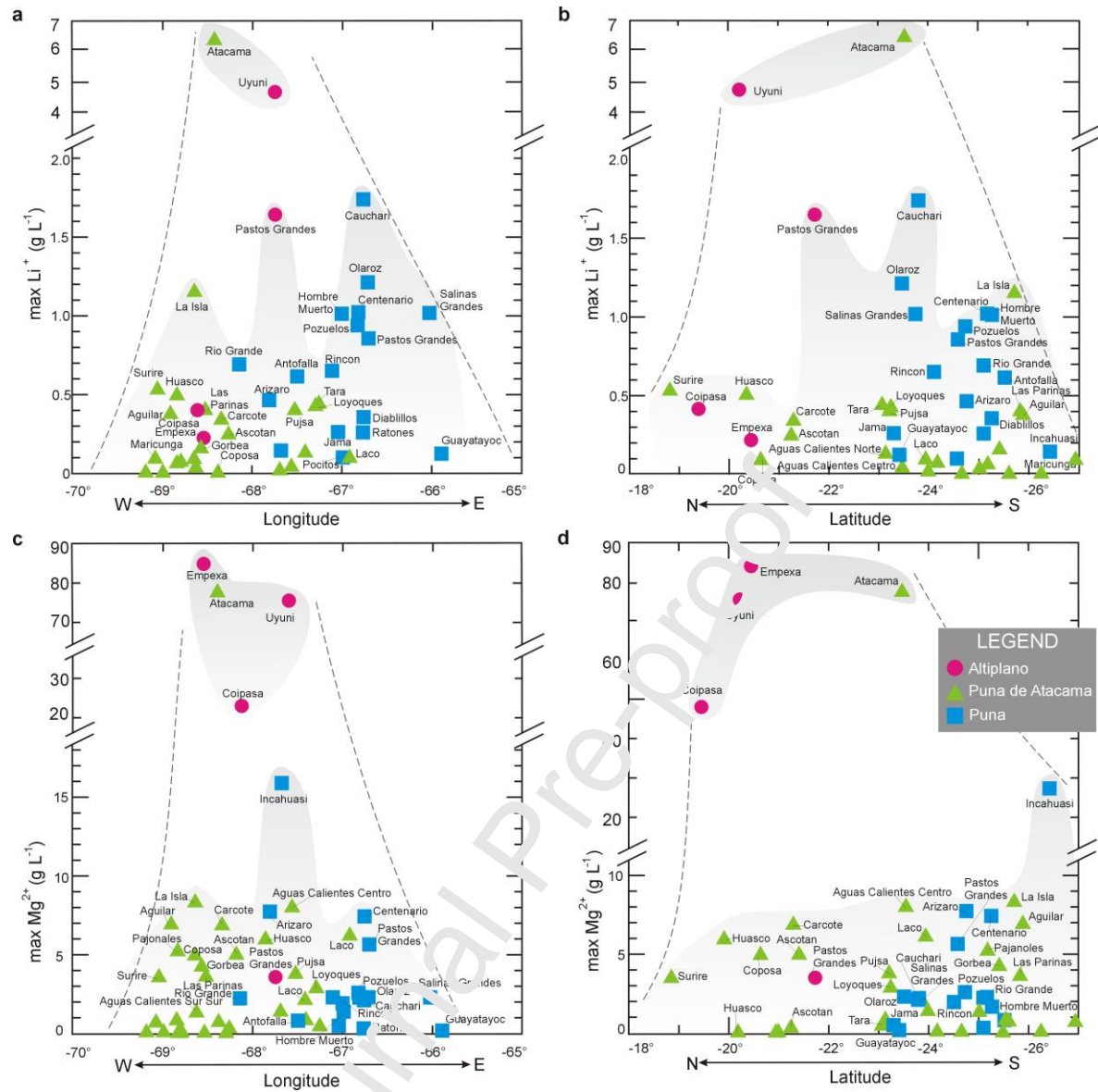


Figure 9. Scatter diagrams showing the maximum Li^+ (upper) and Mg^{2+} (bottom) concentrations according to longitude (a and c), and latitude (b and d) of salars across the Lithium Crescent. Notice that the considered maximum Li^+ and Mg^{2+} concentrations for Atacama are of 6,400 and 80,000 mg L^{-1} , respectively (Moraga et al., 1974; Ide and Kunasz, 1989; Kunasz, 2006). Plotted data correspond to values summarized in Table 4.

5.2. Link between salt pan and endorheic basin areas

The surfaces of the 55 salt pans studied across the Andean plateau (Fig. 1) appear to be related to those of their respective basin catchments, as revealed by the very good correlation obtained comparing their areas: $R = 0.89$ (Fig. 10 a). Two proportional size ranges are observed: basin catchments of Uyuni, Atacama and Arizaro are 5 times larger than their

salt pans, i.e., have a 1:5 size ratio (Fig. 10 a), whereas for the 52 remaining sites, salt pan to basin size proportions are close to the 1:10 ratio (Figs. 10 a and b). Coipasa and Guayatayoc are the two salt pans that least fit either of these relationships (these two cases are discussed further down).

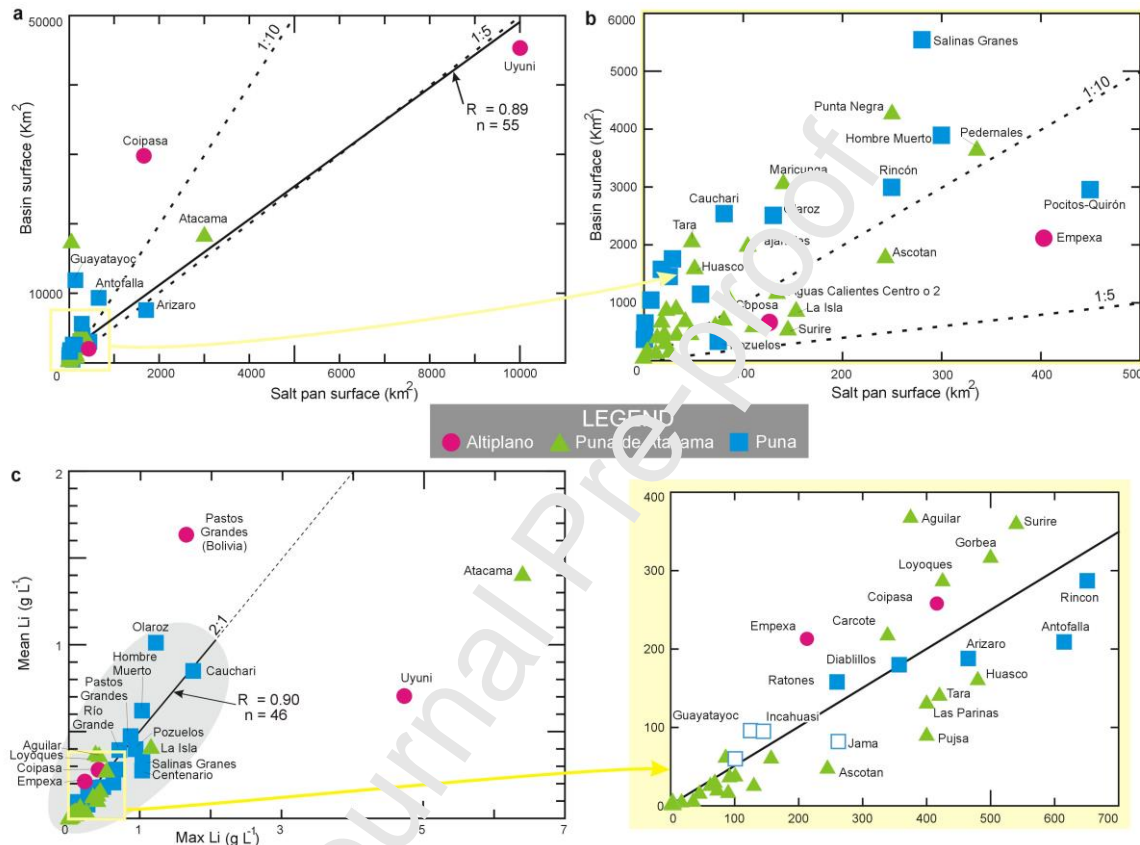


Figure 10. a and b) Scatter diagrams showing the relations between the surfaces of salt pans and their respective basin catchments. a) The correlation $R = 0.89$ was computed by considering all 55 Andean salt pans according to values summarized in Table 1. Note that the correlation line (continuous stroke) is close to the 1:5 proportion (dashed line). b) This panel expands the inset (in yellow) and plots data for the smallest salt pans. Note that most salt pans group close the 1:10 proportion. c) A scatter diagram plotting the relationship between the maximum (Max) and mean Li concentrations according to values summarized in Table 4. The regression R (continuous line) coincides with the stoichiometric proportion of 2:1 (dashed line) for 46 salt pans (n , gray area). Values for max/mean Li ratios are of 1 in Pastos Grandes (Bolivia), 7 in Uyuni, and 11 in Atacama. The inset offers an expanded view of the data displayed in the yellow box of panel c. R is the correlation coefficient (continuous lines), n is the number of salt pans.

The good correlation between salt pan and endorheic basin areas and the two proportional size ranges are very interesting patterns that undoubtedly deserve further specific investigation. Although this is beyond the purpose of this paper, it can be suggested that these relationships may arise from common trends in regional geological history, including lithology (i.e., substrate, tectonics, volcanism, etc.) and exogenous processes (e.g. climate-related such as regional aridity and its effect on rock weathering and erosion), across the Andean plateau.

Li-bearing Andean salt pans occur exclusively within endorheic basins. The onset of endorheism requires the convergence of the following parameters: suitable basin configuration (topographic barriers surrounding low lying areas), aridity (low precipitation – P – and high evaporation – E – rates, where P<E), hard substrate thus low erosion rates (in order for range-crossing rivers to fail incising deeply into the ranges and inhibit basin capture), and low aggradation rates (in order for sedimentation not to overfill the isolated area), amongst other variables (Sobel et al., 2003; Hilley and Strecker, 2005; García-Castellanos, 2006; Tremblay et al. 2015). Basement inherited heterogeneities (Hongn et al., 2007), Cenozoic Andean tectonics (actively uplifting ranges) and Neogene plateau rise were key factors for the formation of endorheic basins in the plateau, while the arid climate (Garreaud, 2009) has ensured their preservation (Vandervoort et al., 1995; López Steinmetz et al., 2020b). Within an endorheic basin, weathering and erosion of the catchments supply the suspended and dissolved load that is transported by rivers towards the low-lying area, where sediments and other products accumulate. Under arid conditions, salt pans form on these low-lying and hydrologically isolated areas (Melvin, 1991; Warren, 2010). Consequently, there is a clear link between the formation of internally drained areas and salt pans. However, as natural processes are typically heterogeneous and complex (Becker and Braun, 1999; Paola et al., 2009), this link clearly does not imply that we can estimate or model the size of endorheic

and saline units, let alone predict whether there might be proportionality between them. It could only be argued that if large catchments are more capable of generating a greater amount of suspended and dissolved load than smaller ones, then under similar conditions (i.e., geological history including lithology, deformation, volcanism and related hydrothermal processes, climate, etc.), large catchments would be required for the largest salt pans to form. For this reason, the fact that the size of salt pans adjusts proportionally to the size of endorheic basins, as revealed by our observations across the Andean plateau (Figs. 10 a and b), is a fascinating configuration for landscape studies. The salt pan/basin size proportionality could apply to other endorheic basins in arid regions. For instance, the Qaidam Basin (*ca.* 94°E - 38°N) in the northern Tibetan Plateau holds world-class Li-brine type deposits comprising 80% of the Li-brine resources found in China (Keslar et al., 2012). The basin's surface is 121,000 km², one-fourth of which covered by numerous saline lakes and playas (Yu et al., 2013). According to this, the ~1:1 salt pan/basin size ratio in Qaidam is close to the proportion found in Uyuni. The proportionality between the surfaces of salt pans and their endorheic basins should thus be checked in detail in other Tibetan Plateau basins and in other regions with internal drainage, in order to confirm the application of this relationship to other parts of the globe.

The poor salt pan-basin size association observed in the Guayatayoc and Coipasa salars appears to result from relatively late processes, i.e., younger than the basins. In the case of Guayatayoc, its basin is oversized with respect to the size of its salt pan (11,805 km² and 140 km², respectively). However, nearly half of the current extent of this basin formed in the Pleistocene, through the capture of the western watershed areas (López Steinmetz and Galli, 2015). This process resulted in the formation of a large (>500 km²) distributive fluvial system (*sensu* Weissman et al., 2015), which lead to the subdivision of the precursor flats and the formation of two individual salars and respective basins, Salinas Grandes and Guayatayoc.

This means that, before the Pleistocene, the unified surface area of the basins (Salinas Grandes + Guayatayoc; ~11,000 km²?) would correlate with the area of the precursor salt pans (Grandes + Guayatayoc + megafan, ~920 km²?). In the case of Coipasa and its oversized basin area, satellite imagery of geomorphological features suggests that the northern half of the basin's catchments (north of 18°50'S) is a remnant of an ancient independent drainage system that could have been incorporated into the Coipasa basin through the capture of the Lauca River.

5.3. Mean Li concentrations are half the maximum Li measured

Brines in Andean salt pans show a 2:1 proportionality between maximum Li values and mean concentrations (Fig. 10 c), with a correlation $R = 0.90$ for 46 salt pans. Atacama, Uyuni and the Bolivian Pastos Grandes do not fit this correlation, with maximum to mean Li proportions of 11:1, 7:1, and 1:1, respectively. The high degree of correlation together with the exceptional number of salt pans fitting the 2:1 proportion make this pattern a substantial feature across the Central Andes. It means that maximum and mean Li concentrations can be considered as mutual proxies in surveying Li brine-type deposits. Accordingly, an indicative value of the mean concentration of Li brines in a salt pan can be estimated as half the value of the maximum measured, and vice versa, a relationship that can be expressed as:

$$\text{mean Li} \approx \frac{1}{2} \text{ max Li} \quad (1)$$

In the case where only few grade data were collected in one salt pan, the mean Li grade would be hard to determine. The difficulty in obtaining representative mean (and *max*) Li values arises from the need to acquire a large dataset in order for the mean Li (and *max*) grade to be confidently considered as representative of the real potentiality of the deposit in question (see Houston et al., 2011). However, despite the time elapsed since the beginning of the Andean Li rush, in general, the hydrochemistry of only a limited number of samples is

available for each of Andean salt pans in the scientific literature, even today. In fact, a relatively restricted number of data is also a typical situation in the initial phases of most mining projects. This clearly represents a major drawback when estimating the mean Li grades (and *max*) of mining prospects. In this context, the formulation (1) proposed for predicting average Li values can provide a useful approach. It is important to note that the *mean* Li value obtained through equation (1) is valid from a statistic and regional perspective. Obviously, it does not replace the specific average value of a deposit obtained from a large dataset, but provides a useful order-of-magnitude indication which can be quite valuable (see for example the case of Salar de Olaroz in Fig. 10 c and in Table 4, where *max* Li measured is of $1,213 \text{ mg L}^{-1}$ whereas the average Li value that result from mining operations is of 841 mg L^{-1} ; Garcia et al., 2019).

The usefulness of the formulation proposed above lies in the fact that at any point in the exploration of a Li brine-type deposit, the maximum measured Li concentration can be used to predict an indicative average value of its grade. The formulation (1) thus defines a dynamic approach to mean Li values, which implies that the predicted *mean* Li will change and evolve as the dataset increases during prospection.

5.4. Li grade as function of salt pan / basin geomorphology

As seen in previous sections, a regional assessment has made it possible to define a relationship between mean and maximum Li concentrations for Andean salars, and to identify a proportionality between the surfaces of the salt pans and basins. In order to test these proportionalities, the concentrations of Li, mean and maximum, have been addressed with respect to the area of the salt pan or its basin catchments (Fig. 11). Despite the fact that the link between Li concentrations and surfaces does not follow a definite proportionality, there is some degree of relationship between Li grade and salt pan size. Larger salt pans do host, by

and large, higher Li-grade brines than smaller pans (Fig. 11 a). This proportionality seems to change according to grade-size scales: i) a relationship of increasing Li with salt pan size is evident for the larger salt pans, i.e., more than 300 km^2 ($R = 0.83$, $n = 7$; Fig. 11 a); ii) this Li-grade/pan-surface relationship is also observed for salt pans having surfaces between 200 and 300 km^2 ($R = 0.87$, $n = 4$; Fig. 11, inset of panel a); and iii) a Li-grade/pan-surface relationship is also observed in those less than $\sim 150 \text{ km}^2$ ($R = 0.63$, $n = 23$, Fig. 11 a, see also details in panels b and c). These three proportionality ranges comprise most (i.e., 34) of the Andean salt pans, with 15 salt pans not fitting any relationship (Fig. 11 b).

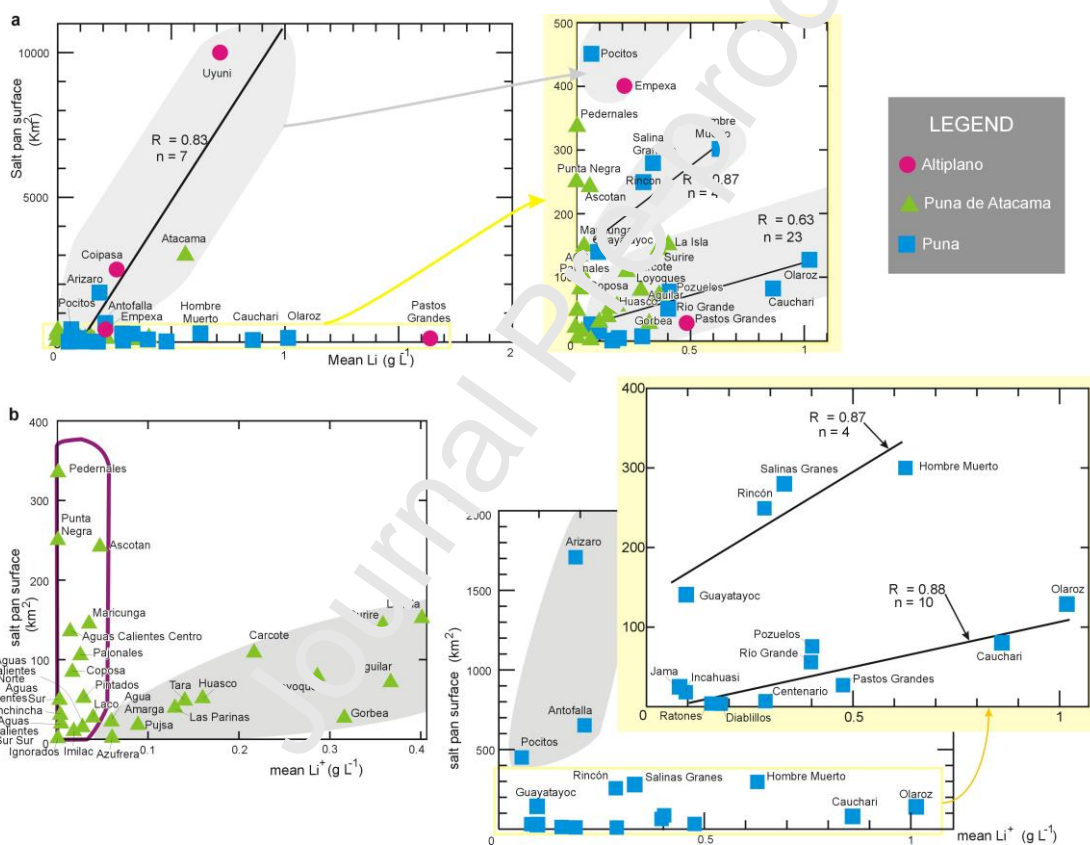


Figure 11. Scatter diagrams showing the relations between mean Li concentrations and pan surfaces for a) the 49 salt pans in the Andean plateau, b) salt pans from the Puna de Atacama, and c) salt pans from the Puna. Insets offer detailed views of the data displayed in the yellow boxes of panels a) and c). Gray areas group salt pans where there is some degree of proportionality between the mean Li values and the salt pans surfaces. In panel b, the purple thick line contours the 13 salt pans lacking a relationship between Li grade and salt pans surface. R is the correlation coefficient (continuous lines), n is the number of salt pans.

Arguably, the dependence of Li concentration on processes occurring at the basin scale is not the most widespread concept, particularly in the Andean and Tibetan literature. In most studies, the rate of supply of Li-bearing waters from hydrothermal springs is deemed as being the essential parameter in controlling Li grades (e.g., Davis et al., 1986; Ide and Kunasz, 1989; Kesler et al., 2012; Godfrey et al., 2013). However, as discussed in section 5.1, thanks to recent investigations on isotopic systematics, it is now apparent that the primary sources of Li in the Andes, including what is supplied by hydrothermal springs, are restricted varieties of lithologies of the Paleozoic basement that underlies the plateau (Egenhoff and Lucassen, 2003; Peralta Arnold et al., 2017; García et al., 2019; Meixner et al., 2019).

Likewise, not to be confused are the concepts of Li grades and Li reserves. Larger salt pans (i.e., of greater areal extent) do not necessarily contain greater Li reserves. This is because the total Li of a brine-type deposit (i.e., its reserves) is provided by the physical parameters of the aquifer (real size – i.e., horizontal areal extent plus thickness of the aquifer –, hydraulic conductivity, transmissivity, etc.), in addition to the actual Li grade in the brine.

Up to now, and contrarily to reserves, the sizes of salt pans or basins have not been related to Li levels, in the Andes or elsewhere, nor have they ever been considered as an integral condition for higher Li graded brines. However, regional data from the Andes show some degree of proportionality between Li concentrations and the surface area of basins and pans. This might imply that, under otherwise comparable conditions (i.e., substrate and surface lithology, characteristics and density of structures, number, density and hydrochemistry of hydrothermal sources, climate, etc.), large salt pans in endorheic basins would generally contain brines with a higher lithium content than smaller ones.

5.5. Lithium Crescent: when basin size matters

The most relevant factors governing Li grades in salt pans are the existence of input sources of Li, hydrological isolation, and aridity (Munk et al., 2016). Based on the general tendency of increasing Li concentrations with salt pan/basin sizes (Fig. 11), it follows that Li grades should be also (at least partially, in addition to the factors mentioned above) dependent on a geomorphological feature: the salt pan area (or its catchment area; Fig. 12). As discussed above, under analogous conditions (i.e., substrate and surface lithology, characteristic and density of displaying structures, number, density, and hydrochemical characteristics of springs, climate, etc.), larger salt pans should be expected to contain higher Li-graded brines than smaller ones, which would be a very useful criterion for surveying brine-type deposits. A correspondence between Li grades and salar sizes may reflect the importance of basin scale processes such as rock weathering, isolation, evaporation, and time (López Steinmetz et al., 2020b). This would be consistent with the model proposed for the formation of the Atacama's and Olaroz's brines, which took place in a near-surface setting through geochemical processes such as low-temperature weathering, evaporation, formation of transition-zone brines, and ultimately crystallization of halite to increase the concentration of Li in the brines (Munk et al., 2018; Franco et al., 2020). As already mentioned in section 5.1., other studies have reported Li isotopic data showing that volcanic and Paleozoic basement rocks represent the primary source for Li in the Andean plateau (Egenhoff and Lucassen, 2003; Peralta Arnold et al., 2017; García et al., 2019; Meixner et al., 2019). These models are consistent with the absence of a clear geographical distribution of Li in salars across the plateau, because Li is sourced from a lithological unit that is widespread the Paleozoic basement that underlies the salars across the plateau. On the other hand, the fact that Li levels increase with increasing salar size suggests that other processes are acting at the scale of the basin, and these are likely tied to geomorphology, and, presumably, the age of the basin. The implication of the latter would be that older basins had more time than younger ones to accumulate the products of

weathering and evaporation. Time dependence of Li grades implies a significant role of the age of endorheism onset, of the history of Li supply and of the persistence of arid conditions.

In summary, the integrity of the available regional data evidences some degree of correspondence between Li grades and salar sizes. This thus implies that not only the largest but also the oldest salars would be the ones expected to contain the largest Li resources. The fact that Li grade could be a function of salt pan/basin geomorphology may provide an insight on new approaches toward understanding the formation of Andean salars, and, more generally, brine-type deposits worldwide.

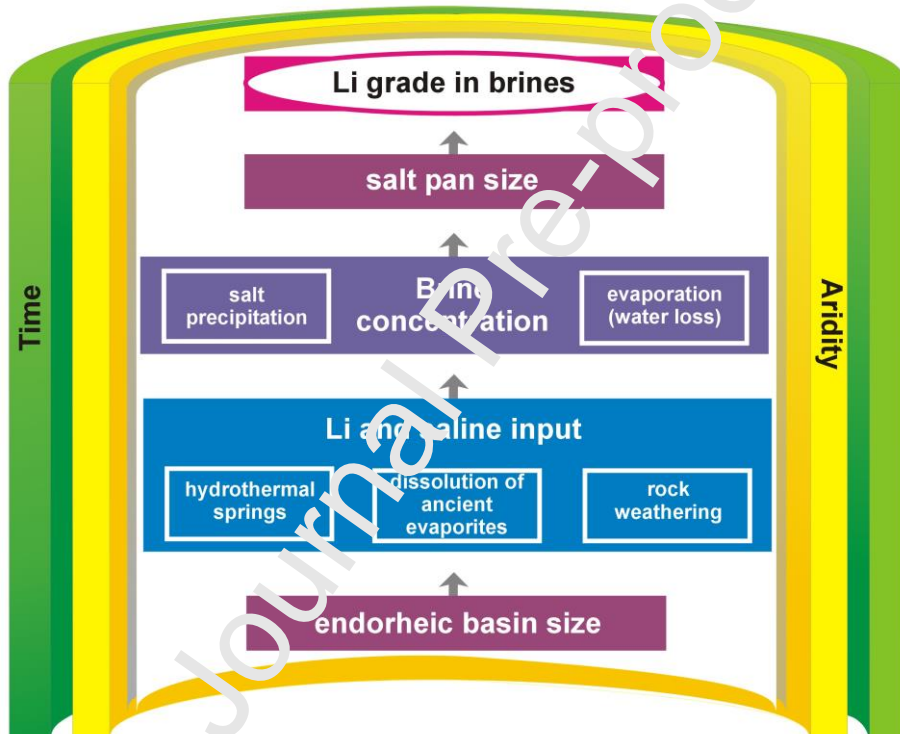


Figure 12. A schematic flow diagram illustrating Li -related processes from basin to salt pan (upwards). It illustrates the interplay between hydrological processes, climate and time, leading to Li accumulation (grade) in Andean brine-type deposits.

6. Conclusions

- The area involving all of the Andean Li-bearing salt pans extends beyond the Lithium Triangle and corresponds in fact to a curved crescent shape. We propose it be referred to as the Lithium Crescent.
- Andean brines are of the $\text{Cl}^- - \text{SO}_4^{2-}$ type, and the compositional variability is marked by major cations: $\text{Na}^+ - \text{Mg}^{2+}$ signatures largely predominate, with the exceptions of the $\text{Mg}^{2+} > \text{Na}^+$ signature of Uyuni, and the $\text{Na}^+ - \text{K}^+$ signature in the Northern Puna salars (Argentina). High Mg^{2+} concentrations occur in the Altiplano (Bolivia), and Ca^{2+} has highest values in the Puna de Atacama (Chile).
- Li lacks of a clear geographical distribution pattern across the Lithium Crescent, other than the fact that maximum Li^+ values occur in the central area of the Andean plateau, between $66^\circ 30' - 68^\circ 30'$ W and $20^\circ - 24^\circ$ S. Such an absence of a geographical distribution in the Li pattern is likely a consequence of the fact that the primary source of Li is the Paleozoic basement, which underlies all salt pans across the Andean plateau.
- Li-bearing Andean salt pans are exclusively hosted in endorheic basins. Across the Lithium Crescent, sizes of salt pans are proportionally related to the extent of their endorheic basin surface. The size ratio for the Qaidam Basin in the Tibetan Plateau is close to the proportions found at Uyuni. The salt pan/basin surface proportionality should thus be checked in detail in other regions of internal drainage, in order to confirm the application of this relationship to other parts of the globe.
- In the Andes, measured maximum Li values (max Li) are twice the mean Li concentrations: the equation $\text{mean Li} \approx \frac{1}{2} \text{max Li}$ can be employed to predict indicative mean grades during brine-type deposit surveying in the Lithium Crescent.
- The concentrations of Li (mean or maximum) can be addressed indistinctly with respect to the area of the salt pan or its basin catchments. Larger salt pans host, in general, higher-grade Li brines than smaller ones. This proportionality changes according to grade-size scales of

three groups: the largest salt pans of more than 300 km²; those having surfaces between 200 and 300 km², and salt pans of less than ~150 km².

- Li levels depend on basin-scale processes, on geomorphology and, presumably, also on the age of the basin: therefore, it is likely the largest and oldest salars that are expected to hold the greatest Li concentrations.

ACKNOWLEDGMENTS

This research did not receive any specific grant from funding agencies in the public, commercial, or not-for-profit sectors. We wish to thank to C. Helvaci and five anonymous reviewers for their helpful comments that greatly improved this manuscript, as well as J.-A. Sanchez-Cabeza for editorial handling. The authors declare no conflict of competing financial nor non-financial interests in relation to the work herein.

Declaration of competing interests

The authors declare that they have no known competing financial interests or personal relationships that could have appeared to influence the work reported in this paper.

REFERENCES

- Adad, M.J., López Steinmetz, R.L., Dávila, F.M., 2020. Seismic interpretation and Cenozoic tectonic evolution of the Pozuelos Basin, Andean Plateau, Argentina. Journal of South American Earth Sciences. doi:10.1016/j.jsames.2020.102938.
- Allmendinger, R.W., Ramos, V.A., Jordan, T.E., Palma, M., Isacks, B.L., 1983. Paleogeography and Andean structural geometry, northwest Argentina. Tectonics. 2 (1), 1-16.

- Allmendinger, R.W., Gubbels, T., 1996. Pure and simple shear plateau uplift, Altiplano-Puna, Argentina and Bolivia. *Tectonophysics*. 259 (1-3), 1-13.
- Allmendinger, R., Jordan, T., Kay, S., Isacks, B., 1997. The evolution of the Altiplano–Puna plateau of the Central Andes. *Annual Reviews on Earth and Planetary Sciences*. 25, 139-174.
- Alonso, H., Risacher, F., 1996. Geoquímica del Salar de Atacama, parte 1: origen de los componentes y balance salino. *Revista Geológica de Chile*. 23 (2), 113-122.
- Alonso, R.N., Helvaci, C., Sureda, R.J., and Viramonte, J.G., 1988. A new Tertiary borax deposit in the Andes. *Mineralium Deposita*. 23, 299-305.
- Alonso, R.N., Jordan, T.E., Tabbutt, K.T., Vandervoort, D.S., 1991. Giant evaporite belts of the Neogene Central Andes. *Geology*. 19, 401-404. doi:10.1130/0091-7613(1991)019<0401:GEBOTN>2.3.CO;2
- Alonso, R.N., Bookhagen, B., Carrasco, B., Coutand, I., Haschke, M., Hilley, G.E., Schoenbohm, L., Sobel, E.R., Strecker, M.R., Trauth, M.H., Villanueva, A., 2006. Tectonics, climate, and landscape evolution of the southern central Andes: the Argentine Puna Plateau and adjacent regions between 22 and 30° S, in: Oncken, Chong, O., Franz, G., Giese, P., Götze, H.-J., Ramos, V.A., Strecker, M.R., Wigger, P. (Eds.), *The Andes Active Subduction Orogeny*. Springer, Berlin, pp. 265-284.
- An, J.W., Kang, D.J., Tran, K.T., Kim, M.J., Lim, T., Tran, T., 2012. Recovery of lithium from Uyuni salar brine. *Hydrometallurgy*. 64-70, 117-118.
- Babeyko, Y.A., Sobolev, S.V., Trumbull, R.B., Oncken, O., Lavie, L.L., 2002. Numerical models of crustal scale convection and partial melting beneath the Altiplano-Puna plateau. *Earth and Planetary Science Letters*. 199, 373-388.
- Baby, P., Rochat, P., Mascle, G., Herail, G., 1997. Neogene shortening contribution to crustal thickening in the back arc of the Central Andes. *Geology*. 25 (10), 883-886.

- Belmonte, A., 2002. Krustale Seismizit7t, Struktur und Rheologie der Oberplatte zwischen der Pr7kordillere und dem magmatischen Bogen in Nordchile (228–248S). PhD thesis, Freie Universität Berlin, Germany.
- Banks, D., Markland, H., Smith, P.V., Mendez, C., Rodriguez, J., Huerta, A., Saether, O.M., 2004. Distribution, salinity and pH dependence of elements in surface waters of the catchment areas of the Salars of Coipasa and Uyuni, Bolivian Altiplano. *J. of Geochem. Explor.* 84, 141-166.
- Becker, A., Braun, P., 1999. Disaggregation, aggregation and spatial scaling in hydrological modelling. *Journal of Hydrology*. 217, 239-252.
- Bevacqua, P.S.J., 1992. Geomorfología del Salar de Atacama y estratigrafía de su núcleo y delta, Segunda Región de Antofagasta, Chile. Undergraduate thesis (unpublished). Universidad Católica del Norte, Antofagasta, 284 p.
- Borda, L.G., Franco, M.G., Córdoba, F., García, M.G., 2016. Geoquímica del Li y As en el salar de Olaroz, Puna de Jujuy. Resultados preliminares. 4th Reunión Argentina de Geoquímica de la Superficie (IV RAGSU). Actas de Resúmenes, 159.
- Boschetti, T., Cortecci, G., Bascieri, M., Mussi, M., 2007. New and past geochemical data on fresh to brine waters of the Salar de Atacama and Andean Altiplano, northern Chile. *Geofluids*. 7, 33-50.
- Bouttt, D.F., Hynek, S.A., Munk, L.A., Corenthal, L.G., 2016. Rapid recharge of fresh water to the halite-hosted brined aquifer of Salar de Atacama, Chile. *Hydrological Processes*. doi:10.1002/hyp.10994.
- Brackebusch, L., 1883. Estudios sobre la Formación Petrolífera de Jujuy. Boletín de la Academia Nacional de Ciencias de Córdoba. 5, 137-252.
- Brackebusch, L., 1891. Mapa geológico del interior de la República Argentina, escala 1:1.000.000. Gotha.

- Canavan, R.R., Carrapa, B., Clementz, M.T., Quade, J., DeCelles, P., Schoenbohm, L.M., 2014. Early Cenozoic uplift of the Puna Plateau, Central Andes, based on stable isotope paleoaltimetry of hydrated volcanic glass. *Geology*. 42 (5), 447-450. doi:10.1130/G35239.1.
- Catalano, L.R., 1964. Boro-Berilio-Litio (una nueva fuente natural de energía). Servicio Nacional Geológico Minero. Ministerio De Economía de la Nación Argentina, Buenos Aires, 99 p.
- Carmona, V., Pueyo, J.J., Taberner, C., Chong, G., Thirlwall M., 2000. Solute inputs in the Salar de Atacama (N. Chile). *J. of Geochem. Explor.* 69 (1), 449-452.
- Clark, F.W., 1924. The data of geochemistry, fifth ed. U.S. Geol. Survey Bull. 770, 841 p.
- COCHILCO, 2013. Compilación de informes sobre Mercado internacional del litio y potencial del litio en salares del norte de Chile. Comisión Chilena del Cobre y SerNaGeoMin, Secretaría de Minería, Santiago de Chile, 319 p.
http://www.cochilco.cl/estudios/info_litio.asp.
- Coira, B., Kay, S.M., Viramonte J. 1993. Upper Cenozoic magmatic evolution of the Argentine Puna - A model for changing subduction geometry. *International Geology Review*. 35 (8), 677-720.
- Corenthal, L.G., Boutt, D.R., Hynek, S.A., Munk, L.A., 2016. Regional groundwater flow and accumulation of a massive evaporate deposit at the margin of the Chilean Altiplano. *Geophysical Research Letters*. 43 (15), 8017-8025.
- Crespo, P., Palma, H., Quintanilla, J., Quispe, L., 1987. Tratamiento químico de salmueras del Salar de Uyuni, Potosí. UMSa-ORSTOM, Informe 7.
- Davis, J., Friedman, I., Gleason, J., 1986. Origin of the lithium-rich brine, Clayton Valley, Nevada. *U.S. Geol. Surv. Bull.* 1622, 131-138.

- Dingman, R.J., 1967. Geology and ground-water resources of the northern part of the Salar de Atacama, Antofagasta Province, Chile. U.S. Geological Survey Bulletin. 1219.
- Durán Iriza, R.J., 2012. Modelación numérica y su contribución al estudio del comportamiento hidrogeológico del sector SW del acuífero del Salar de Atacama, II Región de Antofagasta, Chile. Msc Thesis. Universidad de Chile, Facultad de Ciencias Físicas y Matemáticas, 201 p.
- Egenhoff, S.O., Lucassen, F., 2003. Chemical and isotopic composition of lower to upper Ordovician sedimentary rocks (Central Andes /South Bolivia): implications for their source. Journal of Geology. 111, 487-497.
- Erickson, G.E., 1961. Rhyolite tuff, a source of the salts of northern Chile. Geol. Survey Research. U.S. Geological Survey Professional Paper. 424, C224-C225.
- Erickson, G.E., 1963. Geology of the salt deposits and the salt industry of northern Chile. U.S. Geological Survey. Open-File Report, 16/ p.
- Erickson, G.E., Chong, G., Vila, T., 1976a. Lithium resources of salars in the central Andes. U.S. Geological Survey Professional Paper. 1005, 66-74.
- Erickson, G., Chong, G., Vila, T., 1976b. Lithium resources of salars in the central Andes, in: Vine, J.D., (Ed.), Lithium Resources and Requirements by the Year 2000. U.S. Geological Survey Professional Paper. 1005, 66-74.
- Erickson, G.E., Vine, J.D., Ballon, R., 1977. Lithium-rich brines at Salar de Uyuni and nearby salars in southwestern Bolivia. U.S. Geological Survey. Open-File Repository. 77-615, 52 p.
- Erickson, G.E., Salas, R., 1977. Geology and resources of salars in the central Andes. U.S. Geological Survey. Open File Repository. 88-210, 51 p.

- Ericksen, G.E., Vine, J.D., Ballon, R.A., 1978. Chemical composition and distribution of lithium-rich brines in salar de Uyuni and nearby salars in southwestern Bolivia. *Energy*. 3 (3), 355-363.
- Ericksen, G.E., Salas, R., 1987. Geology and resources of salars in the central Andes. U.S. Geological Survey. Open File Repository. 88-210, 51 p.
- Eugster, H.P., 1980. Geochemistry of evaporitic lacustrine deposits. *Ann. Rev. Earth Planet Sciences*. 8, 35-63.
- Franco, M.G., Borda, L., García, M.G., López Steinmetz, R.L., Flores, P., Córdoba, F., 2016. Geochemical and sedimentological characterization of the Salar de Olaroz, northern Argentinean Puna, Central Andes. 3rd International Workshop on Lithium, Industrial Minerals and Energy, Jujuy, Argentina.
- Franco, M.G., Peralta Arnold, Y.J., Santamaría, C.D., López Steinmetz, R.L., Tassi, F., Venturi, S., Jofré, C.B., Caffe, P.J., Córdoba, F.E., 2020. Chemical and isotopic features of Li-rich brines from the Salar de Olaroz, Central Andes of NW Argentina, 2020. *Journal of South American Earth Sciences* 103 10742. doi:10.1016/j.jsames.2020.102742.
- Garcés, I., López, P.L., Atagué, L.F., Chong, G., Vallès, V., Gimeno, M.J., 1996. Características geoquímicas generales del sistema salino del Salar de Llamara (Chile). *Estudios Geológicos*. 52, 23-35.
- García, M.G., Borda, L.G., Godfrey, L.V., López Steinmetz, R.L., Losada Calderón, A., 2019. Characterization of lithium cycling in the Salar de Olaroz, Central Andes, using a geochemical and isotopic approach. *Chemical Geology*. 531, 119340. doi:10.1016/j.chemgeo.2019.119340.
- García-Castellanos, D., 2006. Long-term evolution of tectonic lakes: Climatic controls on the development of internally drained basins, in: Willett, S.D., Hovius, N., Brandon, M.T., Fisher, D.M., (Eds.), *Tectonics, Climate, and Landscape Evolution*. Geological Society of

America Special Paper, 398. Penrose Conference Series, 283-294.

doi:10.1130/2006.2398(17).

Garzione, C.N., Hoke, G.D., Libarkin, J.C., Withers, S., MacFadden, B., Eiler, J., Ghosh, P.,

Mulch, A., 2008. Rise of the Andes. Sciences. 320 (5881), 1304-1307.

doi:10.1126/science.1148615.

Garzione, C.N., McQuarrie, N., Perez, N.D., Ehlers, T.A., Beck, S.L., Kar, N., Eichelberger,

Chapman, A.D., Ward, K.M., Ducea, M.N., Lease, R.O., Poulsen, C.J., Wagner, L.S.,

Saylor, J.E., Zandt, G., Horton, B.K., 2017. Tectonic Evolution of the Central Andean

Plateau and Implications for the Growthof Plateaus. Annual Review of Earth and Planetary

Sciences. 45, 29-59.

Garreaud, R.D., 2009. The Andes climate and weather. Adv. in Geosci. 22, 3-11.

Garrett, D.E., 2004. Handbook of lithium and natural calcium chloride: their deposits,

processing, uses and properties, first ed. Elsevier Academic Press.

Gianni, G.M., Dávila, F., Echaurren, A., Fennell, L., Tobal, J., Navarrete, C.R., Quezada, P.,

Folguera, A., Giménez, M., 2018. A geodynamic model linking Cretaceous orogeny, arc

migration, foreland basin subsidence and marine ingressions in southern South America.

Earth-Science Reviews. 185, 437-462. doi:10.1016/j.earscirev.2018.06.016.

Godfrey, L.V., Chan, L. H., Alonso, R.N., Lowenstein, T.K., McDonough, W.F., Houston, J.,

Li, J., Bobst, A., Jordan, T.E., 2013. The role of climate in the accumulation of lithium-rich

brine in the Central Andes. Applied Geochemistry. 38, 92-102.

Godfrey, L., Alvarez-Amado, F., 2020. Volcanic and saline lithium input to the Salar de

Atacama. Minerals. 10, 201. doi:10.3390/min10020201.

Götze, H.-J., Krause, S., 2002. The Central Andean gravity high, a relic of an old subduction

complex? Journal of South American Earth Sciences. 14, 799-811.

- Gruber, P., Medina, P., 2010. Global lithium availability: a constraint for electric vehicles? Master thesis, University of Michigan, 76 p.
- Hardie, L., Eugster, H., 1970. The evolution of closed-basin brines. Fiftieth Anniversary Symposia, Mineralogy and Geochemistry of Non-Marine Evaporites. Mineralogical Society of America Special Publication. 273-290.
- Helvacı, C., Mordogan, H., Çolak, M., Gündogan, I., 2004, Presence and distribution of lithium in borate deposits and some recent lake waters of west-central Turkey. International Geology Review. 46, 177-190. doi:10.2747/0020-13814.46.2.177.
- Herail, G., Oller, J., Baby, P., Bonhomme, M., Soler, P., 1995. Strike-slip faulting, thrusting and related basins in the Cenozoic evolution of the southern branch of the Bolivian Orocline. Tectonophysics. 259, 201-212.
- Hilley, G.E., Strecker, M.R., 2005. Processes of oscillatory basin filling and excavation in a tectonically active orogen: Quebrada del Toro basin, NW Argentina. Geological Society of America Bulletin. 117, 887-901. doi:10.1130/B25602.1.
- Hongn, F.D., Del Papa, C., Powell, I., Petrinovic, I., Mon, R., Deraco, V., 2007. Middle Eocene deformation and sedimentation in the Puna-Eastern Cordillera transition (23°-26°S): control by preexisting heterogeneities on the pattern of initial Andean shortening. Geology. 35, 271-274. doi:10.1130/G23189A.1.
- Houston, J., Butcher, A., Ehren, P., Evans, K., Godfrey, L., 2011. The evaluation of brine prospects and the requirement for modifications to filing standards. Economic Geology. 106, 1225-1239.
- Ide, F., Kunasz, I.A., 1989. Origin of lithium in Salar de Atacama, northern Chile, in: Ericken, G.E., Cañas Pinochet, M.T., Reinemund, J.A. (Eds.), Geology of the Andes and its relation to hydrocarbon and mineral resources. Circum-Pacific Council for Energy and Mineral Resources Earth Science Series, 11, pp. 165-172.

- Isacks, B., 1988. Uplift of the Central Andean Plateau and bending of the Bolivian orocline. Journal of Geophysical Research: Solid Earth. 93, 3211-3231. doi:10.1029/JB093iB04p03211.
- Jordan, T.E., Nester, P.L., Blanco, N., Hoke, G.D., Dávila, F., Tomlinson, A.J., 2010. Uplift of the Altiplano-Puna plateau: A view from the west. Tectonics. 29, TC5007. doi:10.1029/2010TC002661.
- Kaseman, S.A., Meixner, A., Erzinger, J., Viramonte, J.G., Alonso, R.N., Franz, G., 2004. Boron isotope composition of the geothermal fluids and borate minerals from salar deposits (central Andes/NW Argentina). Journal of South American Earth Sciences. 16 (8), 685-697. doi:10.1016/j.jsames.2003.12.004.
- Kay, S.M., Coira, B., Viramonte, J., 1994. Young magmatic back arc volcanic rocks as indicators of continental lithospheric delamination beneath the Argentine Puna plateau, central Andes. Journal of Geophysical Research: Solid Earth. 99 (B12), 24323-24339.
- Kesler, S.E., Gruber, P.W., Medina, R.A., Keoleian, G.A., Everson, M.P., Wallington, T.J., 2012. Global lithium resources: relative importance of pegmatites, brine and other deposits. Ore Geology Review. 48, 55-69.
- Kistler, R.B., Helvacı, C., 1994. Boron and Borates. In: Carr DD (Ed.) Industrial Minerals and Rocks. Society of Mining, Metallurgy and Exploration. 6th Edition, 171-186.
- Kunasz, I.A., 1976. Lithium resources - prospects for the future. In: Vine JD (Ed.) Lithium Resources and Requirements by the Year 2000. U.S. Geological Survey Professional Paper. 1005, 26-30.
- Kunasz, I.A., 2006. Lithium resources, in: Kogel, J.E., Trivedi, N.C., Barker, J.M., Krukowski, S.T. (Eds.), Industrial minerals and rocks, commodities, markets and uses. Society for Mining, Metallurgy, and Exploration.

- Langbein, W.B., 1961. Salinity and hydrology of closed lakes. U.S. Geological Survey Professional Paper. 412, 20 p.
- Li, X., Mo, Y., Qing, W., Shao, S., Tang, C.Y., Li, J., 2019a. Membrane-based technologies for lithium recovery from water lithium resources: A review. *Journal of Membrane Science*. 591. doi:10.1016/j.memsci.2019.117317.
- Li, Q., Fan, Q., Wang, J., Qin, J., Zhang, X., Wei, H., Du, Y., Shan, F., 2019b. Hydrochemistry, distribution and formation of lithium-rich brines in salt lakes on the Qinghai-Tibetan Plateau. *Minerals*. 9, 528. doi:10.3390/min9050528.
- López, P.L., Auqué, L.F., Garcés, I., Chong, G., Vallès, V., Gimeno, M.J., 1996. Aplicaciones de la modelización geoquímica al estudio de pautas evolutivas en las salmueras del Salar de Llamara (Chile). Aproximación de método inverso. *Estudios Geológicos*. 52, 197-209.
- López Julián, P.L., Garcés Millás, I.M., 2001. Relaciones geoquímicas entre los distintos tipos de aguas superficiales del salar de Curipe (Chile). Departamento Ciencias de la Tierra, Universidad de Zaragoza, 10 p.
- López Steinmetz, R.L., 2017. Lithium- and boron-bearing brines in the Central Andes: exploring hydrofacies on the eastern Puna plateau between 23° and 23°30'S. *Mineralium Deposita*. 52, 35-50.
- López Steinmetz, R.L., Galli, C.I., 2015. Hydrological change during the Pleistocene-Holocene transition associated with the Last Glacial Maximum-Altithermal in the eastern border of northern Puna. *Andean Geology*. 42 (1), 1-19.
- López Steinmetz, R.L., Fong, S.B., 2019. Water legislation in the context of lithium mining in Argentina. *Resources Policy*, 64, 101510. doi:10.1016/j.resourpol.2019.101510.
- López Steinmetz, R.L., Montero-López, C., 2019. Stratigraphy and sedimentary environments of the Villa María and Peña Colorada formations (Paleogene), westernmost Argentine plateau. *Latin American Journal of Sedimentology and Basin Analysis*. 26 (1), 39-56.

- López Steinmetz, R.L., Salvi, S., García, M.G., Béziat, D., Franco, G., Constantini, O., Córdoba, F., Caffe, P.J., 2018. Northern Puna plateau-scale survey of Li brine-type deposits in the Andes of NW Argentina. *Journal of Geochemical Exploration*. 190, 26-38.
- López Steinmetz, R.L., Salvi, S., Sarchi, C., Santamans, C., López Steinmetz, L.C., 2020a. Lithium and brine geochemistry in the salars of the Southern Puna, Andean plateau of Argentina. *Economic Geology*. 115 (5), 1079-1096. doi:10.5382/econgeo.4754.
- López Steinmetz, R.L., Avila, P., Dávila, F., 2020b. Landscape and drainage evolution during the Cenozoic in the Salinas Grandes Basin, Andean Plateau of NW Argentina. *Geomorphology*. 353, 107032. doi:10.1016/j.geomorph.2020.107032.
- López Steinmetz, R.L., Avila, P., Dávila, F., 2020c. Landscape and drainage evolution during the Cenozoic in the Salinas Grandes Basin Andean Plateau of NW Argentina. *Geomorphology*. 353, 107032. doi:10.1016/j.geomorph.2020.107032.
- Lowenstein, T., Risacher, F., 2009. Closed basin brine evolution and the influence of Ca–Cl inflow waters. Death Valley and Bristol Dry Lake, California, Qaidam Basin, China, and Salar de Atacama, Chile. *Aquat Geochim*. 15, 71-94.
- Mardones, L., 1986. Características geológicas e hidrogeológicas del Salar de Atacama. In Lagos, G. (Ed.), *El litio: Un nuevo recurso para Chile*. Universidad de Chile, Santiago, Chile, pp. 181-216.
- Mardones, L., Chong, G., 1991. Consecuencias hidrológicas de la explotación del Salar de Atacama, Norte de Chile. 6th Congreso Geológico Chileno. Resúmenes expandidos, 719-722.
- Maro, G., Caffe, P.J., Báez, W., 2017. Volcanismo monogenético máfico cenozoico de la Puna. 20th Congreso Geológico Argentino, Relatorio, 548-577.
- McQuarrie, N., 2002. The kinematic history of the Central Andean fold-thrust belt, Bolivia: implications for building a high plateau. *GSA Bulletin*. 114 (8), 950-963.

- Meixner, A., Sarchi, C., Lucassen, F., Becchio, R., Caffe, P.J., Lindsay, J., Rosner, M., Kasemann, S.A., 2019. Lithium concentrations and isotope signatures of Palaeozoic basement rocks and Cenozoic volcanic rocks from the Central Andean arc and back-arc. *Mineralium Deposita*. doi:10.1007/s00126-019-00915-2.
- Melvin, J.L., 1991. Evaporites, Petroleum and Mineral Resources. Developments in Sedimentology, fiftieth ed. Elsevier, 556 p.
- Mohr, S., Mudd, G., Giurco, D., 2010. Lithium Resources and Production: a critical global assessment. Prepared for CSIRO Minerals Down Under Flagship, by the Institute for Sustainable Futures, University of Technology, Sydney, and Department of Civil Engineering, Monash University. Final Report, 107 p.
- Montero-López, C., Hongn, F., López Steinmetz, P.L., Aramayo, A., Pingel, H., Strecker, M.R., Cottle, J.M., Bianchi, C., 2020. Development of an incipient Paleogene topography between the present-day eastern andean plateau (Puna) and the Eastern Cordillera, southern Central Andes, NW Argentina. *Basin Research*. doi:10.1111/bre.12510.
- Moraga, B.A., Chong, D.G., Fortez, M. A., Henriquez, A.H., 1974. Estudio geológico del Salar de Atacama, Provincia de Antofagasta. Instituto de Investigaciones Geológicas Boliviano. 29, 56 p.
- Mpodozis, C., Ramos, V., 1989. The Andes of Chile and Argentina. In: Erickson, G., Cañas-Pinochet, M., Reinemund, J. (Eds.), *Geology of the Andes and its Relation to Hidrocarbon and Mineral Resources*, Circum-Apcific Council for Energy and Mineral Resources Earth Sciences Series. 11, 59-90.
- Munk, L.A., Hynek, S.A., Bradley, D., Boutt, D., Labay, K., Jochens, H., 2016. Lithium brines: A Global Perspective. *Reviews in Economic Geology*. 18, 339-365.

- Munk, L.A., Boutt, D.F., Hynek, S.A., Moran, B.J., 2018. Hydrogeochemical fluxes and processes contributing to the formation of lithium-enriched brines in a hyper-arid continental basin. *Chemical Geology.* 493, 37-57.
- Muñoz, N., Charrier, R., 1996. Uplift of the western border of the Altiplano on a west-vergent thrust system, northern Chile. *Journal of South American Earth Sciences.* 9, 171-181.
- Orberger, B., Rojas, W., Millot, R., Flehoc, C., 2015. Stable isotopes (Li, O, H) combined with chemistry: powerful tracers for Li origins in Salar deposits from the Puna region, Argentina. *Procedia Earth and Planetary Science.* 13, 307-311.
- Ovejero Toledo, A., Alonso, R.N., Ruiz, T., Quiroga, A.G., 2009. Evapofacies halítica en el Salar del Rincón, Departamento Los Andes, Salta. *Revista de la Asociación Geológica Argentina.* 64 (3), 493-500.
- Paola, C., Kyle, S., Mohrig, D., Reinhardt, L., 2009. The “unreasonable effectiveness” of stratigraphic and geomorphic experiments. *Earth-Science Reviews.* 97, 1-43. doi:10.1016/j.earscirev.2009.05.003.
- Peralta Arnold, Y.J., Cabassi, J., Tassi, F., Caffe, J.P., Vaselli, O., 2017. Fluid geochemistry of a deep-seated geothermal resource in the Puna plateau (Jujuy Province, Argentina). *Journal of Volcanology and Geothermal Research.* doi:10.1016/j.jvolgeores.2017.03.030.
- Ramos, V., Cristallini, E., Pérez, D., 2002. The Pampean flat-slab of the Central Andes. *Journal of South American Earth Sciences.* 15, 59-78.
- Rettig, S.L., Jones, B.F., Risacher, F., 1987. Geochemical evolution of brines in the Salar de Uyuni, Bolivia. *Chemical Geology.* 30, 57-79.
- Riley, J.P., Tongudai, M., 1964. The lithium content of sea water. *Deep Sea Research and Oceanographic Abstracts.* 11 (4), 563-568. doi:10.1016/0011-7471(64)90002-6.
- Risacher, F., Fritz, B., 1991. Quaternary geochemical evolution of the Salar of Uyuni and Coipasa, Central Altiplano, Bolivia. *Chemical Geology.* 90, 211-231.

- Risacher, F., Alonso, H., 1996. Geoquímica del Salar de Atacama, parte 2: evolución de las aguas. Revista Geológica de Chile. 23 (2), 123-134.
- Risacher, F., Alonso, H., Salazar, C., 1999. Geoquímica de aguas en cuencas cerradas: I, II y III Regiones – Chile. Convenio de Cooperación Dirección General de Aguas de Chile, Universidad Católica del Norte, Institut de Recherche pour le Developpement. Report 51, 781 p.
- Risacher, F., Fritz, B., 2000. Bromine geochemistry of Salar de Uyuni and deeper salt crusts, Central Altiplano, Bolivia. Chemical Geology. 167, 373-392
- Risacher, F., Alonso, H., Salazar, C., 2002. Hydrochemistry of two adjacent saline lakes in the Andes of northern Chile. Chemical Geology. 187, 53-57.
- Risacher, F., Alonso, H., Salazar, C., 2003. The origin of brines and salts in Chilean Salars: a hydrochemical review. Earth-Science Review. 63, 249-292.
- Risacher, F., Fritz, B., 2009. Origin of salt and brine evolution of Bolivian and Chilean Salars. Aquat. Geochemistry. 15, 123-157.
- Ruetenik, G.A., Hoke, G.D., Moucha, R., Val, P., 2018. Regional landscape response to thrust belt dynamics: The Iglesia basin, Argentina. Basin Research. 30. doi:10.1111/bre.12295.
- Salas, J., Aravena, R., Guzmán, E., Comellà, O., Guimerà, J., Tore, C., Von Igel, W., Fock, A., Henríquez, A., 2009. Modelo de evolución hidroquímica e isotópica en el sistema de recarga del Salar de Atacama a través de su margen E. 12th Congreso Geológico Chileno, 1-4.
- Scandiffio, G., Alvarez, M., 1990. Informe geoquímico sobre la zona geotérmica de Laguna Colorada, Bolivia. Geothermal investigations with isotope and geochemical techniques in Latin American. Proc. of a Final Res. Co-ordination Meeting, Organismo Internacional de Energía Atómica, Costa Rica, 77-113.

- Scandiffio, G., Rodríguez, J., 1990. Geochemical report on the Sajama geothermal area, Bolivia. Geothermal investigations with isotope and geochemical techniques in Latin American. Proc of a Final Res Co-ordination Meeting, Organismo Internacional de Energía Atómica, Costa Rica, 114-168.
- Schmidt, N., 2010. Hydrological and hydrochemical investigations at the Salar de Uyuni (Bolivia) with regard to the extraction of lithium. FOG. 26.
- Schurr, B., Asch, G., Rietbrock, A., Kind, R., Pardo, M., Heit, B., Monfret, T., 1999. Seismicity and average velocities beneath the argentine Puna plateau. Geophysical Research Letters. 26 (19), 3025-3028.
- Scott, E.M., Allen, M.B., Macpherson, C.G., McCaffrey, K.J.W., Davidson, J.P., Saville, C., Ducea, M.N., 2018. Andean surface uplift constrained by radiogenic isotopes of arc lavas. Nature Communications. 9, 969. doi:10.1038/s41467-018-03173-4.
- Sempere, T., Butler, R.F., Richards, D.L., Marshall, L.G., Sharp, W. y Swisher, C.C. 1997. Stratigraphy and chronology of Upper Cretaceous-lower Paleogene strata in Bolivia and northwest Argentina. Bulletin of Geological Society of America. 109 (6), 709-727.
- Sobel, E.R., Hilley, G.E., Strecker, M.R., 2003. Formation of internally drained contractional basins by aridity-limited bedrock incision. Journal of Geophysical Research. 108. doi:10.1029/2002JB001083.
- Stoertz, G.E., Erickson, G.E., 1974. Geology of salars in northern chile. U.S. Geological Survey Professional Paper. 811, 65 p.
- Tassara, A., 2005. Interaction between the Nazca and South American plates and formation of the Altiplano-Puna plateau: Review of a flexural analysis along the Andean margin (15°-34°S). Tectonophysics. 399, 39-57. doi:10.1016/j.tecto.2004.12.014.
- Teng, F.-Z., McDonough, W.F., Rudnick, R.L., Dalpé, C., Tomascak, P.B., Chapell, B.W., Gao, S., 2004. Lithium isotopic composition and concentration of the upper continental

crust. *Geochimica et Cosmochimica Acta.* 68 (20), 4167-4178. doi: 10.1016/j.gca.2004.03.031.

Tremblay, M.M., Fox, M., Schmidt, J.L., Tripathy-Lang, A., Wielicki, M.M., Harrison, T.M., Zeitler, P.K., Shuster, D.L., 2015. Erosion in southern Tibet shut down at ~10 Ma due to enhanced rock uplift within the Himalaya. *Proceedings of the National Academy of Sciences of the United States of America.* 112. doi: 10.1073/pnas.1515652112.

Turner, J.C., 1959. Estratigrafía del cordón de Escaya y de la Sierra de Rinconada (Jujuy). *Revista de la Asociación Geológica Argentina.* 13 (1-2), 15-39.

Vandervoort, D., Jordan, T., Zeitler, P., Alonso, R.N., 1995. Chronology of internal drainage development and uplift, southern Puna plateau, Argentina Central Andes. *Geology.* 23, 145-148. doi:10.1130/0091-7613(1995)023<0145:CUDDA>2.3.CO;2.

Vásquez, C., Ortíz, C., Suárez, F., Muñoz, J.F., 2013. Modeling flow and reactive transport to explain mineral zoning in the Atacama salt flat aquifer, Chile. *Journal of Hydrology.* 490, 114-125.

Vila, T., 1975. Geología de los depósitos salinos andinos, Provincia de Antofagasta, Chile. *Revista Geológica de Chile.* 2, 41-55.

Vinante, D., Alonso, R.N., 2006. Evapofacies del Salar del Hombre Muerto, Puna Argentina: distribución y génesis. *Revista de la Asociación Geológica Argentina.* 61 (2), 286-297.

Vine, J.D., 1976. Lithium Resources and Requirements by the Year 2000. U.S. Geological Survey Professional Paper. 1005, 169 p.

Warren, J.K., 2010. Evaporites through time: Tectonic, climatic and eustatic controls in marine and non-marine deposits. *Earth-Science Reviews.* 98, 217-268. doi:10.1016/j.earscirev.2009.11.004.

Weissman, G.S., Hartley, A.J., Scuderi, L.A., Nichols, G.J., Owen, A., Wright, S., Felicia, A.L., Holland, F., Anaya, F.M.L., 2015. Fluvial geomorphic elements in modern

- sedimentary basins and their potential preservation in the rock record: A review. *Geomorphology*. 250, 187-219. doi:10.1016/j.geomorph.2015.09.005.
- Whitman, D., Isacks, B.L., Kay, S.M., 1996. Lithospheric structure and along-strike segmentation of the Central Andean Plateau: seismic Q, magmatism, flexure, topography and tectonics. *Tectonophysics*. 259 (1-3), 29-40. doi:10.1016/0040-1951(95)00130-1.
- Yu, J.Q., Gao, C.L., Cheng, A.Y., Liu, Y., Zhang, Y., He, X.H., 2013. Geomorphic, hydroclimatic and hydrothermal controls on the formation of lithium brine deposits in the Qaidam Basin, northern Tibetan Plateau, China. *Ore Geology Reviews*. 50, 171-183. doi:10.1016/j.oregeorev.2012.11.001.
- Zheng, M., Liu, X., 2009. Hydrochemistry of Salt Lakes of the Qinghai-Tibet Plateau, China. *Aquatic Geochemistry*. 15, 293-320. doi:10.1007/s10498-008-9055-y.

Table 1. Altitude and comparative areas of Andean salt pans and of their endorheic basin catchments.

| N° (Fig. 1) | Salt pan | Altitude (m asl) | Salt pan surface (km ²) | Basin surface (km ²) |
|----------------|----------------------------|---------------------|--|-------------------------------------|
| 1 | Surire | 4,260 | 144 | 574 |
| 2 | Coipasa | 3,656 | 1,650 | 29,817 |
| 3 | Uyuni | 3,633 | 10,000 | 45,239 |
| 4 | Empexa | 3,725 | 402 | 2,111 |
| 5 | Huasco | 3,778 | 51 | 1,572 |
| 6 | Coposa | 3,730 | 85 | 1,116 |
| 7 | Michincha | 4,130 | 25 | 282 |
| 8 | Alconcha | 4,250 | 4 | 128 |
| 9 | Carcote | 3,690 | 108 | 561 |
| 10 | Ascotan | 3,716 | 243 | 1,757 |
| 11 | Pastos Grandes (Altiplano) | 4,437 | 124 | 660 |
| 12 | Atacama | 2,300 | 3,000 | 18,100 |
| 13 | El Tara | 4,330 | 48 | 2,035 |

| | | | | |
|----|-----------------------------|-------|-------|-------|
| 14 | Aguas Calientes Norte o 1 | 4,280 | 15 | 281 |
| 15 | Pujsa | 4,500 | 18 | 634 |
| 16 | Loyoques o Quisquiro | 4,150 | 80 | 676 |
| 17 | Aguas Calientes Centro o 2 | 4,200 | 134 | 1,168 |
| 18 | El Laco | 4,250 | 16 | 306 |
| 19 | Aguas Calientes Sur o 3 | 3,950 | 46 | 476 |
| 20 | Capur | 3,950 | 27 | 137 |
| 21 | Imilac | 2,949 | 10 | 189 |
| 22 | Punta Negra | 2,945 | 250 | 4,253 |
| 23 | Aguas Calientes Sur Sur o 4 | 3,665 | 20 | 656 |
| 24 | Pajanoles | 3,537 | 104 | 1,984 |
| 25 | La Azufrera | 3,580 | 3 | 214 |
| 26 | Gorbea | 3,950 | 27 | 324 |
| 27 | Ignorados | 4,250 | 1 | 38 |
| 28 | Agua Amarga | 3,550 | 23 | 863 |
| 29 | Aguilar | 3,220 | 71 | 589 |
| 30 | La Isla | 3,900 | 152 | 858 |
| 31 | Los Infieles | 3,520 | 7 | 293 |
| 32 | Las Parinas | 3,987 | 40 | 676 |
| 33 | Salar Grande | 3,950 | 29 | 867 |
| 34 | Pedernales | 3,370 | 335 | 3,620 |
| 35 | Salar de la Laguna | 3,494 | 1 | 400 |
| 36 | La Piedra Parada | 4,150 | 28 | 388 |
| 37 | Wheelwright | 4,220 | 6 | 466 |
| 38 | Maricunga | 3,760 | 145 | 3,045 |
| 39 | Incahuasi | 3,269 | 18 | 1,620 |
| 40 | Antofalla-Botijuelas | 3,330 | 655 | 9,259 |
| 41 | Río Grande | 3,668 | 56 | 1,155 |
| 42 | Arizaro | 3,474 | 1,708 | 7,508 |
| 43 | Hombre Muerto | 3,970 | 300 | 3,881 |
| 44 | Diablillos | 4,032 | 4 | 481 |
| 45 | Ratones | 3,822 | 3 | 605 |
| 46 | Centenario | 3,816 | 7 | 1,044 |
| 47 | Pocitos-Quirón | 3,663 | 450 | 2,969 |
| 48 | Pozuelos | 3,663 | 75 | 367 |
| 49 | Pastos Grandes (Puna) | 3,780 | 27 | 1,752 |

| | | | | |
|----|----------------|-------|-----|--------|
| 50 | Rincón | 3,725 | 250 | 3,017 |
| 51 | Cauchari | 3,903 | 80 | 2,557 |
| 52 | Olaroz | 3,903 | 130 | 2,519 |
| 53 | Jama | 4,080 | 25 | 1,500 |
| 54 | Salinas Granes | 3,410 | 280 | 5,529 |
| 55 | Guayatayoc | 3,400 | 140 | 11,805 |

Table 2. Chemical composition of brines from Andean salt pans. Hydrochemical data of the Altiplano salars correspond to values reported by Risacher and Fritz (1991), excepting for samples Uyu0, C0, EMP, and PGB that are from Erickson and Salas (1987). Summarized data for the Puna de Atacama salars follow Risacher et al. (1992) summarized by COCHILCO, 2013), excepting for samples LAC0, SUR0, HCO0, ALC0, ATA0, ATAd0, and AZU0 that are from Erickson and Salas (1987). Brine chemistry of the Puna salt pans follows data reported by López Steinmetz (2017), López Steinmetz et al. (2018), and López Steinmetz et al. (2020a), excepting for samples CE0, HMO, F30, AR0, PC0, RI0, and RG0 that are from Erickson and Salas (1987). TDS in g L⁻¹, remaining concentrations in mg L⁻¹.

| | g L ⁻¹ | mg L ⁻¹ | | | | | | | | | |
|--------------|-------------------|--------------------|------------|-------------|------------|-----------|-------------|------------|-----------------|-------------------|-----------|
| sample | TDS | Ca | Mg | Na | K | Li | Cl | SO4 | CO ₃ | HC O ₃ | B |
| UYUNI | | | | | | | | | | | |
| uyu0 | 351 | 161 | 11,8 00 | 94,90 0 | 13,50 0 | 700 | 191,8 00 | 13,20 0 | - | 592 | 1,13 6 |
| UA15 | 121 | 545 | 7,78 0 | 107,0 00 | 9,380 | 412 | 190,0 00 | 9,550 | - | - | 302 |
| UA80 | 122 | 310 | 16,1 00 | 91,80 0 | 17,60 0 | 770 | 190,0 00 | 23,00 0 | - | - | 669 |
| UA200 | 123 | 316 | 16,6 00 | 90,30 0 | 17,30 0 | 812 | 191,0 00 | 22,40 0 | - | - | 655 |
| UA400 | 123 | 327 | 16,8 00 | 94,90 0 | 17,40 0 | 812 | 196,0 00 | 22,50 0 | - | - | 657 |
| UA600 | 123 | 315 | 17,3 00 | 91,40 0 | 17,60 0 | 826 | 192,0 00 | 24,40 0 | - | - | 668 |
| UB10 | 125 | 137 | 38,4 00 | 57,00 0 | 29,70 0 | 1,78 0 | 200,0 00 | 43,90 0 | - | - | 1,71 0 |
| UB100 | 224 | 149 | 51,0 00 | 36,10 0 | 19,40 0 | 2,56 0 | 210,0 00 | 32,80 0 | - | - | 2,02 0 |
| UB250 | 125 | 50 | 55,4 00 | 28,80 0 | 19,40 0 | 2,79 0 | 214,0 00 | 34,30 0 | - | - | 2,16 0 |
| UB400 | 125 | 50 | 55,9 00 | 29,20 0 | 19,70 0 | 2,83 0 | 215,0 00 | 34,60 0 | - | - | 2,19 0 |

| | | | | | | | | | | | |
|--------|-----|-----|------------|--------------|------------|-----------|-------------|------------|---|---|-----------|
| UC5 | 123 | 233 | 32,3 00 | 68,30 0 | 20,10 0 | 1,46 0 | 194,0 00 | 30,70 0 | - | - | 1,23 0 |
| UC100 | 122 | 268 | 19,2 00 | 88,60 0 | 19,00 0 | 888 | 190,0 00 | 25,60 0 | - | - | 843 |
| UC250 | 122 | 269 | 19,3 00 | 88,60 0 | 18,60 0 | 868 | 192,0 00 | 26,20 0 | - | - | 871 |
| UC400 | 122 | 269 | 19,2 00 | 89,20 0 | 18,80 0 | 881 | 191,0 00 | 26,70 0 | - | - | 970 |
| UD10 | 122 | 208 | 30,6 00 | 66,20 0 | 26,70 0 | 1,31 0 | 197,0 00 | 30,80 0 | - | - | 1,24 0 |
| UD100 | 122 | 317 | 19,9 00 | 85,10 0 | 21,60 0 | 888 | 194,0 00 | 22,60 0 | - | - | 864 |
| UD250 | 122 | 293 | 19,2 00 | 87,60 0 | 20,30 0 | 819 | 193,0 00 | 25,30 0 | - | - | 864 |
| UD400 | 122 | 294 | 19,3 00 | 88,10 0 | 20,30 0 | 819 | 191,0 00 | 25,40 0 | - | - | 871 |
| UE5 | 123 | 294 | 24,5 00 | 78,70 0 | 22,60 0 | 708 | 195,0 00 | 27,70 0 | - | - | 987 |
| UE100 | 122 | 269 | 17,6 00 | 92,00 0 | 19,30 0 | 708 | 190,0 00 | 29,40 0 | - | - | 871 |
| UE250 | 122 | 269 | 17,4 00 | 92,20 0 | 19,20 0 | 708 | 190,0 00 | 28,60 0 | - | - | 859 |
| UE400 | 122 | 269 | 17,3 00 | 92,00 0 | 19,30 0 | 708 | 189,0 00 | 28,10 0 | - | - | 860 |
| UF30 | 121 | 654 | 7,39 0 | 109,0 0 | 7,430 | 339 | 190,0 00 | 10,30 0 | - | - | 239 |
| UF110 | 121 | 618 | 7,62 0 | 1' 8,0 00 | 7,510 | 339 | 190,0 00 | 10,70 0 | - | - | 232 |
| UG15 | 121 | 834 | 5,78 0 | 112,0 00 | 5,790 | 254 | 190,0 00 | 8,200 | - | - | 171 |
| UG95 | 121 | 738 | 6,39 0 | 110,0 00 | 6,180 | 266 | 191,0 00 | 9,140 | - | - | 199 |
| UG270 | 121 | 666 | 6,97 0 | 109,0 00 | 6,800 | 303 | 190,0 00 | 9,790 | - | - | 233 |
| UH10 | 121 | 750 | 6,93 0 | 109,0 00 | 7,190 | 315 | 191,0 00 | 8,960 | - | - | 236 |
| UH100 | 121 | 666 | 7,85 0 | 107,0 00 | 7,940 | 351 | 190,0 00 | 10,10 0 | - | - | 266 |
| UH300 | 122 | 437 | 11,5 00 | 100,0 00 | 10,30 0 | 463 | 189,0 00 | 18,70 0 | - | - | 372 |
| UH500 | 122 | 401 | 12,1 00 | 98,20 0 | 10,50 0 | 488 | 189,0 00 | 20,30 0 | - | - | 397 |
| UH700 | 122 | 391 | 12,1 00 | 99,40 0 | 10,80 0 | 489 | 190,0 00 | 20,70 0 | - | - | 405 |
| UH900 | 122 | 367 | 12,6 00 | 100,0 00 | 11,20 0 | 513 | 188,0 00 | 22,20 0 | - | - | 423 |
| UI15 | 121 | 714 | 6,66 0 | 109,0 00 | 7,120 | 303 | 190,0 00 | 9,370 | - | - | 226 |
| UI100 | 121 | 702 | 6,63 0 | 106,0 00 | 6,760 | 303 | 189,0 00 | 9,360 | - | - | 214 |
| UI1000 | 121 | 569 | 7,29 0 | 106,0 00 | 7,590 | 303 | 189,0 00 | 14,10 0 | - | - | 261 |
| UJ15 | 121 | 786 | 7,00 0 | 107,0 00 | 7,590 | 339 | 190,0 00 | 8,930 | - | - | 254 |
| UJ100 | 122 | 521 | 11,1 | 100,0 | 11,00 | 584 | 191,0 | 14,20 | - | - | 399 |

| | | | | | | | | | | |
|-------|-----|-----|------------|-------------|------------|-----|-------------|------------|---|-------|
| | | | 00 | 00 | 0 | | 00 | 0 | | |
| UJ300 | 122 | 437 | 12,8 00 | 95,90 0 | 12,00 0 | 560 | 189,0 00 | 18,10 0 | - | - 437 |
| UJ700 | 122 | 391 | 14,1 00 | 94,80 0 | 12,40 0 | 575 | 187,0 00 | 24,10 0 | - | - 525 |
| UK10 | 122 | 622 | 8,82 0 | 103,0 00 | 8,880 | 413 | 191,0 00 | 11,00 0 | - | - 288 |
| UK100 | 122 | 417 | 14,7 00 | 94,30 0 | 14,60 0 | 685 | 192,0 00 | 18,70 0 | - | - 457 |
| UK200 | 123 | 319 | 15,6 00 | 93,80 0 | 14,40 0 | 688 | 190,0 00 | 25,10 0 | - | - 453 |
| UK400 | 123 | 295 | 15,9 00 | 93,80 0 | 24,00 0 | 688 | 187,0 00 | 28,50 0 | - | - 441 |
| UL20 | 122 | 401 | 17,5 00 | 87,60 0 | 19,50 0 | 805 | 194,0 00 | 16,00 0 | - | - 452 |
| UL100 | 122 | 390 | 17,1 00 | 87,90 0 | 17,80 0 | 805 | 195,0 00 | 16,30 0 | - | - 557 |
| UL250 | 122 | 340 | 18,9 00 | 82,80 0 | 17,40 0 | 846 | 190,0 00 | 18,10 0 | - | - 590 |
| UM17 | 121 | 638 | 6,42 0 | 109,0 00 | 7,160 | 277 | 189,0 00 | 7,870 | - | - 669 |
| UM100 | 122 | 425 | 13,5 00 | 91,00 0 | 12,30 0 | 559 | 191,0 00 | 15,10 0 | - | - 319 |
| UM400 | 122 | 269 | 16,3 00 | 92,50 0 | 13,90 0 | 672 | 187,0 00 | 26,00 0 | - | - 461 |
| UN16 | 122 | 354 | 19,1 00 | 85,60 0 | 18,00 0 | 868 | 194,0 00 | 19,10 0 | - | - 563 |
| UN100 | 122 | 354 | 19,4 00 | 85,10 0 | 19,40 0 | 916 | 193,0 00 | 19,30 0 | - | - 591 |
| UN300 | 123 | 245 | 21,7 00 | 80,50 0 | 19,40 0 | 979 | 192,0 00 | 24,80 0 | - | - 718 |
| UO9 | 121 | 523 | 10,5 00 | 103,0 00 | 10,80 0 | 471 | 191,0 00 | 11,60 0 | - | - 250 |
| UO100 | 122 | 342 | 17,8 00 | 89,20 0 | 16,60 0 | 784 | 190,0 00 | 20,00 0 | - | - 533 |
| UO500 | 123 | 234 | 21,8 00 | 88,60 0 | 18,30 0 | 937 | 190,0 00 | 36,00 0 | - | - 892 |
| UP17 | 122 | 378 | 16,7 00 | 82,60 0 | 16,30 0 | 756 | 192,0 00 | 17,10 0 | - | - 486 |
| UP100 | 122 | 305 | 20,6 00 | 78,20 0 | 19,40 0 | 930 | 193,0 00 | 21,00 0 | - | - 662 |
| UP500 | 123 | 282 | 21,3 00 | 77,30 0 | 19,00 0 | 944 | 193,0 00 | 24,00 0 | - | - 770 |
| UQ17 | 120 | 577 | 7,29 0 | 111,0 00 | 7,510 | 313 | 190,0 00 | 9,020 | - | - 141 |
| UQ100 | 121 | 533 | 9,40 0 | 104,0 00 | 9,460 | 399 | 190,0 00 | 10,90 0 | - | - 232 |
| UQ450 | 121 | 545 | 9,96 0 | 101,0 00 | 9,660 | 411 | 192,0 00 | 11,70 0 | - | - 241 |
| UQ800 | 121 | 509 | 10,4 00 | 98,20 0 | 10,00 0 | 424 | 190,0 00 | 12,80 0 | - | - 202 |
| UR15 | 121 | 457 | 5,69 0 | 112,0 00 | 5,470 | 217 | 190,0 00 | 8,090 | - | - 639 |
| UR100 | 121 | 565 | 8,09 0 | 107,0 00 | 7,980 | 314 | 190,0 00 | 10,80 0 | - | - 101 |

| | | | | | | | | | | | |
|-------|-----|-----|------------|-------------|------------|------|-------------|------------|---|---|------|
| UR450 | 121 | 577 | 8,31 0 | 106,0 00 | 8,330 | 338 | 188,0 00 | 11,20 0 | - | - | 134 |
| UR800 | 122 | 413 | 12,5 00 | 102,0 00 | 11,30 0 | 413 | 187,0 00 | 19,70 0 | - | - | 482 |
| US9 | 120 | 577 | 6,34 0 | 108,0 00 | 6,650 | 276 | 190,0 00 | 8,870 | - | - | 164 |
| US100 | 121 | 606 | 7,63 0 | 106,0 00 | 7,980 | 314 | 192,0 00 | 10,50 0 | - | - | 195 |
| US450 | 122 | 401 | 11,2 00 | 99,40 0 | 12,00 0 | 389 | 187,0 00 | 21,60 0 | - | - | 494 |
| US00 | 122 | 294 | 13,5 00 | 101,0 00 | 14,00 0 | 465 | 186,0 00 | 30,30 0 | - | - | 785 |
| UT15 | 121 | 642 | 6,83 0 | 109,0 00 | 7,470 | 278 | 190,0 00 | 10,10 0 | - | - | 198 |
| UT100 | 120 | 626 | 6,97 0 | 107,0 00 | 7,350 | 277 | 189,0 00 | 10,20 0 | - | - | 197 |
| UT450 | 121 | 630 | 6,90 0 | 106,0 00 | 7,230 | 266 | 190,0 00 | 10,20 0 | - | - | 195 |
| UT800 | 121 | 533 | 8,31 0 | 106,0 00 | 8,800 | 227 | 189,0 00 | 13,00 0 | - | - | 244 |
| UU20 | 121 | 565 | 10,3 00 | 106,0 00 | 6,650 | 350 | 188,0 00 | 12,30 0 | - | - | 273 |
| UU350 | 120 | 533 | 8,97 0 | 103,0 00 | 7,590 | 291 | 191,0 00 | 11,80 0 | - | - | 275 |
| UU700 | 121 | 388 | 10,8 00 | 107,0 00 | 7,580 | 316 | 188,0 00 | 19,20 0 | - | - | 328 |
| UV10 | 121 | 630 | 8,14 0 | 100,0 00 | 6,450 | 242 | 191,0 00 | 10,10 0 | - | - | 235 |
| UV100 | 121 | 618 | 8,92 0 | 110,0 00 | 6,490 | 242 | 190,0 00 | 10,60 0 | - | - | 244 |
| UV500 | 121 | 618 | 8,92 0 | 108,0 00 | 6,370 | 242 | 191,0 00 | 10,70 0 | - | - | 226 |
| UW22 | 123 | 180 | 27,7 00 | 69,90 0 | 22,80 0 | 1,03 | 200,0 00 | 18,80 0 | - | - | 1,08 |
| UW100 | 123 | 43 | 20,9 00 | 86,30 0 | 16,20 0 | 784 | 196,0 00 | 14,20 0 | - | - | 878 |
| UX90 | 123 | 294 | 28,9 00 | 72,00 0 | 17,70 0 | 1,13 | 195,0 00 | 22,60 0 | - | - | 1,06 |
| UX300 | 123 | 307 | 28,9 00 | 72,00 0 | 17,90 0 | 1,18 | 195,0 00 | 23,00 0 | - | - | 1,05 |
| UY16 | 121 | 726 | 7,19 0 | 111,0 00 | 6,330 | 254 | 191,0 00 | 8,690 | - | - | 238 |
| UY100 | 121 | 581 | 9,55 0 | 105,0 00 | 8,130 | 340 | 190,0 00 | 11,10 0 | - | - | 315 |
| UY300 | 122 | 354 | 14,5 00 | 97,80 0 | 12,60 0 | 500 | 189,0 00 | 22,20 0 | - | - | 650 |
| UY600 | 122 | 316 | 15,3 00 | 96,40 0 | 13,10 0 | 511 | 188,0 00 | 24,80 0 | - | - | 712 |
| UZ12 | 121 | 557 | 8,89 0 | 101,0 00 | 9,190 | 484 | 191,0 00 | 9,890 | - | - | 303 |
| UZ100 | 122 | 413 | 15,1 00 | 95,70 0 | 12,40 0 | 536 | 191,0 00 | 16,30 0 | - | - | 557 |
| UZ450 | 122 | 354 | 17,1 00 | 92,90 0 | 13,40 0 | 599 | 192,0 00 | 19,30 0 | - | - | 608 |
| UZ800 | 122 | 342 | 17,0 | 91,10 | 13,30 | 598 | 190,0 | 19,50 | - | - | 665 |

| | | | | | | | | | | |
|-------|-----|------|------------|-------------|------------|-----|-------------|------------|---|-------------|
| | | | 00 | 0 | 0 | 00 | 0 | | | |
| U112 | 122 | 425 | 16,6 00 | 92,00 0 | 15,80 0 | 701 | 196,0 00 | 17,00 0 | - | - 578 |
| U1400 | 123 | 264 | 21,3 00 | 86,50 0 | 19,20 0 | 895 | 197,0 00 | 29,50 0 | - | - 987 |
| U1800 | 123 | 247 | 21,6 00 | 83,70 0 | 19,50 0 | 930 | 193,0 00 | 31,70 0 | - | - 1,04 0 |
| U213 | 121 | 433 | 14,5 00 | 92,90 0 | 14,30 0 | 640 | 195,0 00 | 15,90 0 | - | - 480 |
| U2100 | 122 | 331 | 17,3 00 | 92,00 0 | 16,60 0 | 750 | 196,0 00 | 23,00 0 | - | - 618 |
| U2200 | 122 | 307 | 17,7 00 | 88,30 0 | 17,40 0 | 791 | 193,0 00 | 25,20 0 | - | - 700 |
| U2300 | 122 | 284 | 18,7 00 | 86,50 0 | 17,90 0 | 826 | 190,0 00 | 27,40 0 | - | - 766 |
| U2400 | 123 | 234 | 20,4 00 | 85,60 0 | 18,60 0 | 909 | 187,0 00 | 33,10 0 | - | - 976 |
| U2500 | 123 | 223 | 20,5 00 | 85,60 0 | 18,60 0 | 916 | 189,0 00 | 34,10 0 | - | - 1,01 0 |
| U2600 | 123 | 223 | 20,7 00 | 85,60 0 | 18,40 0 | 895 | 187,0 00 | 34,10 0 | - | - 1,02 0 |
| YA17 | 121 | 577 | 9,53 0 | 102,0 00 | 12,20 0 | 435 | 192,0 00 | 10,10 0 | - | - 360 |
| YA100 | 121 | 449 | 12,2 00 | 95,90 0 | 13,60 0 | 557 | 191,0 00 | 13,70 0 | - | - 483 |
| YB11 | 120 | 758 | 4,37 0 | 111,0 00 | 4,690 | 144 | 190,0 00 | 5,830 | - | - 155 |
| YB100 | 121 | 581 | 8,65 0 | 123,0 00 | 8,910 | 338 | 190,0 00 | 10,20 0 | - | - 299 |
| YB500 | 121 | 364 | 11,1 00 | 93,20 0 | 12,90 0 | 534 | 189,0 00 | 19,80 0 | - | - 488 |
| YC12 | 120 | 662 | 3,84 0 | 112,0 00 | 3,860 | 120 | 191,0 00 | 5,070 | - | - 103 |
| YC100 | 120 | 630 | 6,66 0 | 107,0 00 | 6,450 | 229 | 189,0 00 | 8,540 | - | - 219 |
| YD9 | 120 | 758 | 6,03 0 | 107,0 00 | 6,450 | 229 | 191,0 00 | 7,470 | - | - 216 |
| YD100 | 121 | 421 | 12,2 00 | 94,80 0 | 12,50 0 | 496 | 192,0 00 | 14,40 0 | - | - 427 |
| YD450 | 120 | 341 | 15,5 00 | 90,20 0 | 14,50 0 | 621 | 191,0 00 | 20,20 0 | - | - 615 |
| YD800 | 122 | 329 | 16,5 00 | 90,20 0 | 15,40 0 | 670 | 192,0 00 | 22,70 0 | - | - 692 |
| YE8 | 121 | 662 | 5,30 0 | 110,0 00 | 5,750 | 193 | 192,0 00 | 6,300 | - | - 204 |
| YE100 | 121 | 400 | 12,4 00 | 95,90 0 | 12,60 0 | 509 | 192,0 00 | 15,20 0 | - | - 438 |
| YE450 | 125 | 274 | 17,2 00 | 91,50 0 | 16,10 0 | 673 | 195,0 00 | 28,10 0 | - | - 790 |
| YE800 | 123 | 269 | 16,9 00 | 89,50 0 | 15,80 0 | 661 | 191,0 00 | 27,40 0 | - | - 791 |
| YF23 | 120 | 1,03 | 2,96 0 | 113,0 00 | 3,090 | 72 | 192,0 00 | 4,690 | - | - 88 |
| YF200 | 120 | 854 | 4,50 0 | 109,0 00 | 4,650 | 144 | 190,0 00 | 6,240 | - | - 143 |

| | | | | | | | | | | | |
|-------|-----|-----------|------------|-------------|------------|-----------|-------------|------------|---|---|-----------|
| YG15 | 121 | 473 | 11,0 00 | 100,0 00 | 10,60 0 | 521 | 191,0 00 | 12,00 0 | - | - | 301 |
| YG100 | 120 | 806 | 4,52 0 | 112,0 00 | 5,160 | 228 | 191,0 00 | 6,020 | - | - | 164 |
| YH1 | 126 | 100 | 51,0 00 | 37,30 0 | 26,80 0 | 2,46 0 | 207,0 00 | 44,40 0 | - | - | 2,03 0 |
| YH100 | 125 | 137 | 53,2 00 | 34,00 0 | 19,90 0 | 2,59 0 | 212,0 00 | 29,20 0 | - | - | 1,95 0 |
| YH250 | 125 | 87 | 53,9 00 | 32,40 0 | 19,90 0 | 2,59 0 | 213,0 00 | 29,50 0 | - | - | 2,04 0 |
| YI8 | 121 | 517 | 8,41 0 | 105,0 00 | 8,800 | 362 | 192,0 00 | 9,030 | - | - | 273 |
| YI100 | 121 | 533 | 9,33 0 | 101,0 00 | 9,310 | 399 | 192,0 00 | 9,590 | - | - | 305 |
| YI450 | 121 | 509 | 9,84 0 | 100,0 00 | 9,930 | 411 | 191,0 00 | 10,10 0 | - | - | 321 |
| YI800 | 121 | 437 | 11,0 00 | 95,40 0 | 11,00 0 | 484 | 191,0 00 | 11,50 0 | - | - | 351 |
| YJ17 | 120 | 698 | 6,66 0 | 110,0 00 | 8,640 | 201 | 193,0 00 | 8,110 | - | - | 271 |
| YJ100 | 121 | 461 | 11,8 00 | 94,10 0 | 12,70 0 | 545 | 194,0 00 | 12,80 0 | - | - | 428 |
| YJ400 | 122 | 257 | 16,9 00 | 88,80 0 | 16,10 0 | 743 | 189,0 00 | 27,20 0 | - | - | 620 |
| YK1 | 120 | 710 | 7,78 0 | 105,0 00 | 3,210 | 325 | 191,0 00 | 10,40 0 | - | - | 277 |
| YK100 | 121 | 529 | 9,87 0 | 101,0 00 | 10,20 0 | 410 | 192,0 00 | 11,70 0 | - | - | 320 |
| YK400 | 122 | 304 | 15,1 00 | 93,60 0 | 13,90 0 | 584 | 190,0 00 | 24,00 0 | - | - | 522 |
| YK700 | 122 | 281 | 15,4 00 | 97,50 0 | 15,30 0 | 634 | 189,0 00 | 27,00 0 | - | - | 576 |
| YL22 | 120 | 794 | 4,37 0 | 112,0 00 | 4,930 | 156 | 192,0 00 | 6,250 | - | - | 141 |
| YL100 | 121 | 455 | 9,38 0 | 102,0 00 | 9,580 | 375 | 193,0 00 | 12,80 0 | - | - | 324 |
| YL400 | 121 | 421 | 10,4 00 | 100,0 00 | 10,50 0 | 423 | 191,0 00 | 14,80 0 | - | - | 360 |
| RA130 | 101 | 429 | 197 | 1,550 | 80 | 10 | 3,380 | 600 | - | - | 21 |
| RB180 | 102 | 1,20 0 | 566 | 6,650 | 300 | 27 | 12,50 0 | 2,400 | - | - | 31 |
| RC120 | 105 | 846 | 3,40 0 | 19,60 0 | 1,800 | 14 | 40,10 0 | 5,700 | - | - | 116 |
| RD160 | 109 | 1,95 0 | 4,67 0 | 39,80 0 | 3,200 | 217 | 79,50 0 | 5,120 | - | - | 250 |
| RE100 | 114 | 2,67 0 | 8,65 0 | 61,60 0 | 6,140 | 575 | 129,0 00 | 3,600 | - | - | 481 |
| RF90 | 115 | 1,66 0 | 9,43 0 | 65,10 0 | 7,310 | 631 | 135,0 00 | 5,700 | - | - | 837 |
| RG30 | 116 | 1,25 0 | 11,4 00 | 69,20 0 | 7,900 | 674 | 147,0 00 | 7,650 | - | - | 546 |
| RH10 | 121 | 565 | 10,2 00 | 97,50 0 | 10,50 0 | 538 | 190,0 00 | 11,10 0 | - | - | 368 |
| RI15 | 120 | 457 | 13,5 00 | 81,90 0 | 12,40 0 | 736 | 171,0 00 | 15,60 0 | - | - | 507 |

| | | | | | | | | | | | |
|-------|-----|-----------|------------|-------------|------------|-----------|-------------|------------|---|---|-----------|
| RJ10 | 122 | 390 | 11,4 00 | 95,70 0 | 11,00 0 | 633 | 190,0 00 | 12,80 0 | - | - | 626 |
| RK90 | 115 | 1,93 0 | 10,5 00 | 62,60 0 | 7,820 | 701 | 137,0 00 | 5,100 | - | - | 1,02 0 |
| RL110 | 111 | 2,53 0 | 6,44 00 | 45,50 0 | 5,000 | 417 | 96,60 0 | 4,830 | - | - | 971 |
| RM100 | 109 | 2,13 0 | 5,78 00 | 37,00 0 | 4,500 | 347 | 80,20 0 | 5,100 | - | - | 318 |
| RN75 | 115 | 2,02 0 | 3,89 00 | 79,10 0 | 4,500 | 359 | 132,0 00 | 5,000 | - | - | 491 |
| RO80 | 114 | 1,59 0 | 6,73 00 | 62,60 0 | 5,400 | 483 | 122,0 00 | 7,200 | - | - | 965 |
| RP50 | 110 | 1,96 0 | 2,33 00 | 45,50 0 | 2,800 | 182 | 82,00 0 | 6,990 | - | - | 137 |
| RQ70 | 113 | 1,32 0 | 5,27 00 | 62,60 0 | 4,500 | 272 | 110,0 00 | 9,700 | - | - | 507 |
| RR60 | 116 | 1,24 0 | 4,13 00 | 88,10 0 | 4,500 | 239 | 115,0 00 | 7,250 | - | - | 419 |
| RS15 | 127 | 52 | 69,0 00 | 12,50 0 | 17,60 0 | 1,23 0 | 231,0 00 | 31,40 0 | - | - | 3,70 0 |
| RT15 | 127 | 60 | 68,8 00 | 14,00 0 | 17,60 0 | 4,03 0 | 229,0 00 | 29,50 0 | - | - | 3,52 0 |
| RU1 | 124 | 238 | 27,2 00 | 66,20 0 | 26,40 0 | 1,60 0 | 198,0 00 | 30,90 0 | - | - | 1,42 0 |
| RV20 | 122 | 413 | 13,4 00 | 101,0 0 | 11,70 0 | 563 | 189,0 00 | 13,90 0 | - | - | 507 |
| RW10 | 122 | 338 | 15,1 00 | 9,50 0 | 15,70 0 | 763 | 191,0 00 | 19,80 0 | - | - | 623 |
| RX10 | 127 | 69 | 6,0 00 | 21,30 0 | 19,10 0 | 3,55 0 | 223,0 00 | 32,00 0 | - | - | 3,45 0 |
| RY95 | 116 | 1,84 5 | 1,1 00 | 63,00 0 | 6,840 | 763 | 138,0 00 | 6,100 | - | - | 766 |
| RZ1 | 128 | 02 | 75,3 00 | 10,70 0 | 15,10 0 | 4,72 0 | 253,0 00 | 26,50 0 | - | - | 4,33 0 |
| CA0 | 124 | 315 | 10,9 00 | 105,0 00 | 9,230 | 237 | 185,0 00 | 28,10 0 | - | - | 720 |

COIPASA

| sample | Ti / S | Ca | Mg | Na | K | Li | Cl | SO4 | CO3 | HC O3 | B |
|--------|--------|-----|------------|-------------|------------|-----|-------------|-------------|-----|-------|-----------|
| C0 | 368 | 253 | 12,1 20 | 100,4 00 | 9,080 | 338 | 186,0 00 | 25,30 0 | - | 785 | 2,20 8 |
| CA150 | 124 | 194 | 14,1 00 | 104,0 00 | 10,00 0 | 275 | 172,0 00 | 54,00 0 | - | - | 870 |
| CA250 | 126 | 164 | 10,5 00 | 111,0 00 | 8,330 | 212 | 132,0 00 | 104,0 00 | - | - | 644 |
| CB0 | 123 | 301 | 10,7 00 | 108,0 00 | 9,190 | 237 | 187,0 00 | 29,30 0 | - | - | 690 |
| CB150 | 126 | 102 | 23,0 00 | 94,70 0 | 14,30 0 | 416 | 168,0 00 | 80,10 0 | - | - | 1,35 0 |
| C10 | 121 | 541 | 10,2 00 | 104,0 00 | 7,120 | 198 | 189,0 00 | 14,70 0 | - | - | 601 |
| C20 | 122 | 521 | 15,1 00 | 99,10 0 | 11,60 0 | 333 | 188,0 00 | 17,60 0 | - | - | 952 |
| C3 | 122 | 319 | 10,1 | 109,0 | 7,310 | 205 | 179,0 | 25,90 | - | - | 614 |

| | | | | | | | | | | | |
|---------------------------------------|-----|-----------|------------|-------------|------------|-----------|-------------|-------------|---------|-----------|----------|
| | | | 00 | 00 | | | 00 | 0 | | | |
| C40 | 122 | 509 | 10,8 00 | 107,0 00 | 8,560 | 230 | 187,0 00 | 18,00 00 | - | - | 640 |
| C50 | 121 | 738 | 6,80 0 | 111,0 00 | 5,980 | 154 | 186,0 00 | 13,90 00 | - | - | 428 |
| EMPEXA | | | | | | | | | | | |
| sample | TDS | Ca | Mg | Na | K | Li | Cl | SO4 | CO 3 | HC O3 | B |
| EMP | 239 | 259 | 8,48 0 | 67,20 0 | 3,400 | 213 | 120,0 00 | 34,10 0 | - | 430 | 702 |
| PASTOS GRANDES (ALTIPLANO) | | | | | | | | | | | |
| sample | TDS | Ca | Mg | Na | K | Li | Cl | SO4 | CO 3 | HC O3 | B |
| PGB | 321 | 3,10 0 | 3,48 0 | 101,0 00 | 14,20 0 | 1,64 0 | 104,0 00 | 2,460 | - | - | 304 1 |
| EL TARA | | | | | | | | | | | |
| sample | TDS | Ca | Mg | Na | K | Li | Cl | SO4 | CO 3 | HC O3 | B |
| TAR-RT-001 | 1 | 108 | 12 | 340 | 7 | 4 | 596 | 46 | 19 | 83 | 18 |
| TAR-RT-002 | 1 | 96 | 10 | 350 | 7 | 4 | 612 | 47 | 0 | 135 | 19 |
| TAR-RT-003 | 1 | 88 | 8 | 275 | 6 | 3 | 478 | 35 | 6 | 91 | 15 |
| TAR-RT-004 | 2 | 92 | 14 | 525 | 18 | 6 | 846 | 68 | 0 | 157 | 17 |
| TAR-RT-005 | 1 | 80 | 20 | 440 | 8 | 4 | 688 | 66 | 0 | 141 | 11 |
| TAR-RT-006 | 1 | 80 | 20 | 415 | 12 | 4 | 680 | 64 | 0 | 137 | 11 |
| TAR-RT-007 | 90 | 300 | 135 | 500 | 580 | 420 | 87,40 0 | 6,060 | 0 | 2,35 0 | 710 |
| TAR-RT-008 | 79 | 275 | 350 | 48,00 0 | 420 | 340 | 69,80 0 | 7,480 | 0 | 1,98 1 | 570 |
| TAR-RT-009 | 16 | 102 | 208 | 7,100 | 480 | 34 | 10,74 0 | 1,036 | 52 | 1,68 9 | 119 |
| TAR-RT-010 | 2 | 84 | 32 | 600 | 40 | 6 | 836 | 159 | 62 | 333 | 16 |
| TAR-RT-011 | 112 | 1,15 0 | 430 | 80,00 0 | 700 | 440 | 127,0 00 | 11,24 0 | 0 | 1,10 2 | 486 |
| TAR-RT-012 | 102 | 1,40 0 | 440 | 76,00 0 | 640 | 420 | 123,2 00 | 10,70 0 | 0 | 1,06 0 | 415 |
| AGUAS CALIENTES NORTE | | | | | | | | | | | |
| sample | TDS | Ca | Mg | Na | K | Li | Cl | SO4 | CO 3 | HC O3 | B |
| ACN-RT-001 | 1 | 94 | 24 | 340 | 8 | 4 | 602 | 58 | 0 | 154 | 8 |
| ACN-RT-002 | 1 | 94 | 26 | 225 | 7 | 3 | 480 | 55 | 0 | 160 | 6 |
| ACN-RT-003 | 1 | 86 | 22 | 330 | 12 | 4 | 578 | 62 | 8 | 98 | 5 |
| ACN-RT-004 | 3 | 240 | 12 | 1,100 | 18 | 6 | 2,100 | 101 | 0 | 50 | 9 |
| ACN-RT-005 | 12 | 800 | 50 | 4,300 | 56 | 20 | 8,260 | 270 | 0 | 209 | 28 |
| ACN-RT-006 | 5 | 320 | 100 | 1,600 | 34 | 10 | 2,930 | 229 | 0 | 452 | 16 |
| ACN-RT-007 | 50 | 2,80 0 | 820 | 23,00 0 | 1,020 | 130 | 40,80 0 | 3,010 | 0 | 842 | 392 |
| PUJSA | | | | | | | | | | | |
| sample | TDS | Ca | Mg | Na | K | Li | Cl | SO4 | CO 3 | HC O3 | B |

| | | | | | | | | | | | |
|------------|---|-----------|-----------|------------|-------|-----|------------|------------|-----------|-----------|-----|
| PUJ-RT-001 | - | 125 | 35 | 280 | 28 | 2 | 338 | 384 | 0 | 173 | 0 |
| PUJ-RT-002 | - | 180 | 790 | 26,00 0 | 2,825 | 175 | 37,00 0 | 15,00 0 | 834 | 1,32 4 | 450 |
| PUJ-RT-003 | - | 180 | 835 | 32,00 0 | 3,175 | 200 | 39,80 0 | 22,60 0 | 1,01 0 | 1,47 6 | 529 |
| PUJ-RT-004 | - | 70 | 28 | 260 | 26 | 1 | 286 | 264 | 0 | 225 | 0 |
| PUJ-RT-005 | - | 50 | 12 | 220 | 16 | 1 | 232 | 208 | 0 | 128 | 0 |
| PUJ-RT-006 | - | 175 | 250 | 23,00 0 | 975 | 60 | 12,88 0 | 32,20 0 | 586 | 0 | 177 |
| PUJ-RT-007 | - | 300 | 98 | 9,500 | 300 | 20 | 3,520 | 15,44 0 | 457 | 0 | 184 |
| PUJ-RT-008 | - | 80 | 16 | 1,050 | 32 | 2 | 441 | 1,600 | 52 | 186 | 0 |
| PUJ-RT-009 | - | 1,00 0 | 1,51 5 | 52,00 0 | 3,400 | 400 | 87,20 0 | 14,34 0 | 0 | 1,54 2 | 317 |
| PUJ-RT-010 | - | 525 | 183 | 13,00 0 | 525 | 27 | 5,300 | 21,96 0 | 548 | 568 | 230 |

LOYOQUES

| sample | TDS | Ca | Mg | Na | K | Li | Cl | SO4 | CO ₃ | HC O ₃ | B |
|------------|-----|------------|-----------|-------------|-------|-----|-------------|-------|-----------------|-------------------|-----|
| LOY-RT-001 | 3 | 220 | 34 | 890 | 22 | 6 | 1,765 | 97 | 40 | 0 | 4 |
| LOY-RT-002 | 123 | 18,0 00 | 2,30 0 | 9,600 | 123 | 350 | 202,0 00 | 1,820 | 0 | 655 | 430 |
| LOY-RT-003 | 123 | 15,8 50 | 2,47 5 | 100,0 00 | 23 | 375 | 196,8 00 | 1,720 | 0 | 779 | 681 |
| LOY-RT-004 | 122 | 17,6 00 | 2,85 5 | >5,00 0 | 128 | 425 | 194,8 00 | 1,840 | 0 | 827 | 756 |
| LOY-RT-005 | 102 | 5600 | 2,13 5 | 0,00 0 | 1,650 | 275 | 114,2 00 | 2,600 | 0 | 733 | 527 |

AGUAS CALIENTES CENTRO

| sample | TDS | Ca | Mg | Na | K | Li | Cl | SO4 | CO ₃ | HC O ₃ | B |
|------------|-----|-----------|-----------|------------|-------|----|------------|-------|-----------------|-------------------|----|
| ACC-RT-001 | 15 | 2,42 5 | 415 | 3,750 | 325 | 10 | 10,74 0 | 1,302 | 0 | 143 | 0 |
| ACC-RT-002 | 7 | 600 | 413 | 2,150 | 228 | 5 | 4,660 | 752 | 0 | 448 | 0 |
| ACC-RT-003 | 11 | 1,65 0 | 273 | 2,600 | 240 | 8 | 7,260 | 882 | 0 | 142 | 0 |
| ACC-RT-004 | 44 | 875 | 3,33 8 | 19,00 0 | 1,025 | 45 | 33,80 0 | 5,530 | 0 | 819 | 33 |
| ACC-RT-005 | 9 | 575 | 293 | 2,800 | 150 | 8 | 5,840 | 236 | 0 | 144 | 0 |

EL LACO

| sample | TDS | Ca | Mg | Na | K | Li | Cl | SO4 | CO ₃ | HC O ₃ | B |
|------------|-----|-----------|-----------|------------|-------|-----|-------------|------------|-----------------|-------------------|-----------|
| LAC0 | 210 | 820 | 6,25 1 | 62,20 0 | 4,800 | 101 | 109,6 30 | 15,36 0 | - | 620 | 1,07 8 |
| LAC-RT-001 | 44 | 1,30 0 | 2,03 5 | 19,00 0 | 1,525 | 40 | 34,20 0 | 5,370 | 0 | 400 | 0 |
| LAC-RT-002 | 47 | 1,22 5 | 2,64 5 | 21,00 0 | 1,850 | 33 | 36,30 0 | 7,280 | 0 | 428 | 0 |
| LAC-RT-003 | 43 | 800 | 2,16 5 | 19,00 0 | 1,550 | 28 | 32,20 0 | 5,930 | 0 | 370 | 0 |
| LAC-RT-004 | 26 | 775 | 1,10 | 12,00 | 900 | 20 | 18,08 | 3,768 | 0 | 367 | 0 |

| | | | | | | | | | | | |
|----------------------------|-----|-----------|-----------|------------|-------|----|------------|-------|-----------------|-------------------|-----|
| LAC-RT-005 | 2 | 190 | 2 | 0 | 95 | 2 | 0 | 340 | 0 | 175 | 0 |
| AGUAS CALIENTES SUR | | | | | | | | | | | |
| sample | TDS | Ca | Mg | Na | K | Li | Cl | SO4 | CO ₃ | HC O ₃ | B |
| ACT-RT-001 | 33 | 1,62 5 | 1,37 0 | 13,00 0 | 900 | 18 | 24,36 0 | 4,160 | 0 | 225 | 0 |
| ACT-RT-002 | 6 | 275 | 170 | 2,100 | 182 | 3 | 3,590 | 642 | 0 | 81 | 0 |
| ACT-RT-003 | 2 | 180 | 62 | 500 | 60 | 1 | 980 | 447 | 0 | 109 | 0 |
| ACT-RT-004 | 2 | 170 | 60 | 550 | 60 | 1 | 935 | 424 | 0 | 104 | 0 |
| ACT-RT-005 | 7 | 425 | 193 | 2,400 | 155 | 3 | 4,170 | 606 | 0 | 353 | 0 |
| ACT-RT-006 | 1 | 410 | 33 | 250 | 27 | 1 | 256 | 1,186 | 0 | 57 | 0 |
| ACT-RT-007 | 4 | 230 | 150 | 1,100 | 85 | 5 | 1,850 | 689 | 0 | 243 | 0 |
| ACT-RT-008 | 2 | 140 | 85 | 650 | 46 | 3 | 135 | 343 | 0 | 164 | 0 |
| AGUAS CALIENTES SUR | | | | | | | | | | | |
| SUR | | | | | | | | | | | |
| sample | TDS | Ca | Mg | Na | K | Li | Cl | SO4 | CO ₃ | HC O ₃ | B |
| ACS-RT-001 | 1 | 85 | 43 | 400 | ~ | 1 | 590 | 332 | 0 | 92 | 1 |
| ACS-RT-002 | 1 | 85 | 43 | 375 | ~ | 1 | 594 | 334 | 0 | 93 | 1 |
| ACS-RT-003 | 1 | 85 | 43 | 400 | 40 | 2 | 590 | 330 | 0 | 96 | 2 |
| ACS-RT-004 | 25 | 750 | 850 | 10,30 | 1,050 | 35 | 18,40 0 | 4,060 | 66 | 349 | 131 |
| ACS-RT-005 | 1 | 100 | 16 | 175 | 4 | <1 | 194 | 334 | 0 | 42 | 0 |
| ACS-RT-006 | 1 | 100 | 16 | 175 | 3 | <1 | 193 | 344 | 0 | 42 | 0 |
| ACS-RT-007 | 1 | 83 | 16 | 175 | 3 | <1 | 197 | 342 | 0 | 41 | 0 |
| ACS-RT-008 | 3 | 190 | 100 | 875 | 100 | 3 | 1,380 | 1,010 | 0 | 111 | 9 |
| ACS-RT-009 | 3 | 170 | 86 | 750 | 80 | 2 | 1,115 | 895 | 0 | 99 | 7 |
| ACS-RT-010 | 7 | 37 | 98 | 3,050 | 270 | 9 | 3,930 | 2,160 | 0 | 117 | 40 |
| PAJONALES | | | | | | | | | | | |
| sample | TDS | Ca | Mg | Na | K | Li | Cl | SO4 | CO ₃ | HC O ₃ | B |
| PAJ-RT-001 | 16 | 775 | 500 | 6,500 | 325 | 6 | 11,58 0 | 1,084 | 0 | 76 | 36 |
| PAJ-RT-002 | 15 | 775 | 475 | 5,800 | 305 | 6 | 10,74 0 | 894 | 0 | 74 | 31 |
| PAJ-RT-003 | 1 | 625 | 250 | 5,000 | 285 | 5 | 8,940 | 1,042 | 0 | 75 | 27 |
| PAJ-RT-004 | 36 | 2,12 5 | 1,17 5 | 1,360 | 925 | 16 | 28,45 0 | 2,850 | 0 | 190 | 85 |
| PAJ-RT-005 | 35 | 1,90 0 | 1,15 0 | 15,00 0 | 900 | 16 | 27,50 0 | 2,685 | 0 | 182 | 91 |
| PAJ-RT-006 | 39 | 2,37 5 | 1,27 5 | 13,80 0 | 1,025 | 18 | 29,30 0 | 3,100 | 0 | 208 | 102 |
| PAJ-RT-007 | 67 | 2,52 5 | 1,97 5 | 33,40 0 | 1,725 | 58 | 62,00 0 | 2,550 | 0 | 314 | 177 |
| PAJ-RT-008 | 71 | 2,62 5 | 2,17 5 | 33,80 0 | 1,825 | 62 | 67,40 0 | 2,820 | 0 | 448 | 190 |
| PAJ-RT-009 | 48 | 1,30 0 | 1,52 5 | 2,050 | 1,275 | 40 | 40,40 0 | 1,650 | 0 | 334 | 125 |
| PAJ-RT-010 | 78 | 5,70 0 | 2,30 0 | 33,80 0 | 1,675 | 31 | 76,80 0 | 590 | 0 | 193 | 86 |

| | | | | | | | | | | | |
|------------|-----|-----------|-----------|------------|-------|----|-------------|-------|---|-----|-----|
| PAJ-RT-011 | 54 | 4,94 5 | 2,27 5 | 20,10 0 | 1,208 | 18 | 47,60 0 | 780 | 0 | 134 | 54 |
| PAJ-RT-012 | 47 | 4,63 5 | 2,02 5 | 16,60 0 | 1,135 | 18 | 39,30 0 | 0 | 0 | 135 | 46 |
| PAJ-RT-013 | 68 | 5,01 8 | 1,75 0 | 30,80 0 | 1,803 | 35 | 61,30 0 | 3,700 | 0 | 511 | 329 |
| PAJ-RT-014 | 69 | 5,01 8 | 1,80 0 | 32,00 0 | 1,828 | 35 | 62,20 0 | 3,730 | 0 | 523 | 349 |
| PAJ-RT-015 | 69 | 5,01 8 | 1,77 5 | 31,70 0 | 1,810 | 35 | 63,40 0 | 3,720 | 0 | 516 | 334 |
| PAJ-RT-016 | 96 | 5,01 8 | 3,05 0 | 52,80 0 | 2,800 | 45 | 104,0 00 | 200 | 0 | 864 | 524 |
| PAJ-RT-017 | 96 | 5,01 5 | 3,27 5 | 53,40 0 | 2,825 | 44 | 102,4 00 | 2,820 | 0 | 854 | 457 |
| PAJ-RT-018 | 84 | 5,01 8 | 2,40 0 | 4,120 | 2,315 | 41 | 82,40 0 | 3,380 | 0 | 704 | 402 |
| PAJ-RT-019 | 19 | 1,54 0 | 375 | 6,100 | 353 | 8 | 17,90 0 | 725 | 0 | 46 | 54 |
| PAJ-RT-020 | 19 | 1,54 2 | 375 | 6,300 | 345 | 8 | 13,35 0 | 705 | 0 | 46 | 54 |
| PAJ-RT-021 | 23 | 2,06 5 | 475 | 7,500 | 405 | 9 | 17,10 0 | 865 | 0 | 52 | 58 |
| PAJ-RT-022 | 23 | 1,91 5 | 450 | 7,600 | 410 | 9 | 16,40 0 | 1,055 | 0 | 60 | 59 |
| PAJ-RT-023 | 24 | 1,98 0 | 500 | 7,800 | 430 | 10 | 17,45 0 | 1,155 | 0 | 64 | 64 |
| PAJ-RT-024 | 23 | 1,90 0 | 475 | 7,800 | 405 | 10 | 17,00 0 | 1,085 | 0 | 63 | 62 |
| PAJ-RT-025 | 103 | 9,50 0 | 520 0 | 50,80 0 | 2,200 | 36 | 118,8 00 | 2,060 | 0 | 399 | 195 |

GORBEA

| sample | TDS | C | Mg | Na | K | Li | Cl | SO4 | CO 3 | HC O3 | B |
|------------|-----|-----|------------|------------|-------|-----|-------------|-------------|---------|----------|-----------|
| GOR-RT-001 | 66 | 163 | 39,5 00 | 66,00 0 | 5,000 | 475 | 162,8 06 | 107,3 67 | 0 | 0 | 2,08 4 |
| GOR-RT-002 | 66 | 165 | 38,5 00 | 64,00 0 | 4,600 | 500 | 156,5 95 | 102,3 55 | 0 | 0 | 1,98 6 |
| GOR-RT-003 | 66 | 410 | 27,5 00 | 52,00 0 | 5,000 | 300 | 124,7 11 | 74,82 5 | 0 | 0 | 1,50 9 |
| GOR-RT-004 | 76 | 275 | 28,0 00 | 52,00 0 | 5,000 | 300 | 123,7 53 | 74,29 0 | 0 | 0 | 1,45 8 |
| GOR-RT-005 | 5 | 425 | 550 | 1,300 | 25 | 5 | 2,486 | 3,107 | 0 | 0 | 4,55 9 |

AGUA AMARGA

| sample | TDS | Ca | Mg | Na | K | Li | Cl | SO4 | CO 3 | HC O3 | B |
|------------|-----|------------|-----------|------------|-------|----|-------------|-------|---------|----------|-----|
| AAM-RT-001 | 15 | 2363 | 325 | 3,600 | 185 | 14 | 10,54 0 | 1,308 | 0 | 112 | 69 |
| AAM-RT-002 | 15 | 2448 | 300 | 3,700 | 198 | 14 | 10,65 0 | 1,150 | 0 | 113 | 69 |
| AAM-RT-003 | 109 | 23,0 00 | 3,52 5 | 51,20 0 | 1,980 | 58 | 136,0 00 | 1,120 | 0 | 166 | 397 |
| AAM-RT-004 | 113 | 25,0 00 | 4,22 5 | 59,40 0 | 2,035 | 61 | 150,0 00 | 1,200 | 0 | 162 | 426 |

| | | | | | | | | | | | |
|------------|-----|------------|-----------|------------|-------|-----|-------------|-------|---|-----|-----|
| AAM-RT-005 | 105 | 23,0 00 | 3,00 0 | 47,60 0 | 1,683 | 56 | 124,4 00 | 1,120 | 0 | 170 | 392 |
| AMA-04 | 93 | 24,1 00 | 3,09 0 | 43,20 0 | 2,490 | 157 | 121,0 00 | 674 | 0 | 0 | 515 |

LA ISLA

| sample | TDS | Ca | Mg | Na | K | Li | Cl | SO4 | CO 3 | HC O3 | B |
|------------|-----|-----|-----------|-------------|-------------|-----------|-------------|------------|---------|-----------|-----|
| LIS-RT-001 | 5 | 150 | 78 | 2,000 | 42 | 13 | 3,167 | 666 | 0 | 32 | 0 |
| LIS-RT-002 | 30 | 350 | 450 | 13,00 0 | 880 | 98 | 22,66 1 | 2,118 | 0 | 73 | 10 |
| LIS-RT-003 | 8 | 165 | 125 | 3,000 | 75 | 23 | 4,839 | 857 | 0 | 41 | 0 |
| LIS-RT-004 | 13 | 475 | 183 | 5,200 | 275 | 30 | 8,650 | 1,201 | 0 | 35 | 0 |
| LIS-RT-005 | 15 | 375 | 250 | 6,200 | 375 | 35 | 9,928 | 1,273 | 0 | 42 | 0 |
| LIS-RT-006 | 23 | 425 | 25 | 9,600 | 750 | 73 | 16,20 0 | 1,624 | 0 | 50 | 0 |
| LIS-RT-007 | 123 | 525 | 5,30 0 | 12,00 0 | 8,600 | 850 | 109,3 88 | 14,29 2 | 0 | 188 | 272 |
| LIS-RT-008 | 123 | 500 | 5,00 0 | 130,0 00 | 800 | 200 | 196,7 01 | 13,68 7 | 0 | 152 | 268 |
| LIS-RT-009 | 123 | 475 | 4,90 0 | 126,0 00 | 800 | 800 | 180,0 54 | 13,36 2 | 0 | 152 | 262 |
| LIS-RT-010 | 122 | 525 | 5,40 0 | 122,0 00 | 8,500 | 875 | 191,3 38 | 14,86 4 | 0 | 190 | 297 |
| LIS-RT-011 | 120 | 525 | 8,30 0 | 110,0 00 | 108,0 00 | 1,15 0 | 189,0 57 | 17,88 4 | 0 | 1,17 3 | 284 |
| LIS-RT-012 | 45 | 195 | 925 | 2,00 0 | 1,575 | 78 | 35,35 1 | 2,346 | 44 | 132 | 26 |

AGUILAR

| sample | TDS | Ca | Mg | Na | K | Li | Cl | SO4 | CO 3 | HC O3 | B |
|------------|-----|------------|-----------|------------|-------|-----|-------------|-------|---------|-----------|-----|
| AGU-RT-001 | 113 | 55,0 00 | 5,80 0 | 60,00 0 | 2,600 | 375 | 212,1 26 | 1,382 | 0 | 860 | 692 |
| AGU-RT-002 | 113 | 55,0 00 | 6,90 0 | 60,00 0 | 2,600 | 375 | 206,7 50 | 0 | 0 | 862 | 697 |
| AGU-RT-003 | 115 | 45,0 00 | 6,10 0 | 62,00 0 | 2,600 | 350 | 191,1 25 | 0 | 0 | 1,02 9 | 829 |

LAS PARINAS

| sample | TDS | Ca | Mg | Na | K | Li | Cl | SO4 | CO 3 | HC O3 | B |
|------------|-----|-----|-----------|-------------|-------|-----|-------------|------------|---------|----------|-----|
| LPA-RT-001 | 9 | 105 | 95 | 4,100 | 54 | 10 | 6,058 | 498 | 0 | 211 | 14 |
| LPA-RT-002 | 7 | 100 | 65 | 2,600 | 41 | 7 | 4,431 | 341 | 0 | 209 | 6 |
| LPA-RT-003 | 7 | 113 | 75 | 3,300 | 44 | 8 | 4,786 | 368 | 0 | 217 | 0 |
| LPA-RT-004 | 7 | 130 | 73 | 2,900 | 45 | 7 | 4,672 | 480 | 0 | 87 | 0 |
| LPA-RT-005 | 122 | 725 | 3,20 0 | 100,0 00 | 500 | 350 | 170,1 11 | 12,79 6 | 0 | 580 | 423 |
| LPA-RT-006 | 123 | 625 | 3,60 0 | 105,0 00 | 6,000 | 400 | 167,5 84 | 12,52 2 | 0 | 651 | 447 |

SURIRE

| sample | TDS | Ca | Mg | Na | K | Li | Cl | SO4 | CO 3 | HC O3 | B |
|--------|-----|-----|-----------|------------|------------|-----|-------------|------------|---------|----------|-----------|
| SUR0 | 236 | 890 | 3,83 0 | 73,20 0 | 13,20 0 | 540 | 131,3 80 | 11,43 0 | - | - | 3,70 0 |

| | | | | | | | | | | | |
|-------------------|-----|-----------|-----------|------------|------------|-----|-------------|------------|---------|----------|-----------|
| SUR-22 | 12 | 1,16 0 | 84 | 1,710 | 310 | 8 | 1,800 | 4,060 | 26 | 297 | 544 |
| SUR-23 | 285 | 850 | 2,96 0 | 93,40 0 | 14,10 0 | 530 | 155,0 00 | 11,50 0 | 0 | 0 | 1,30 0 |
| PEDERNALES | | | | | | | | | | | |
| sample | TDS | Ca | Mg | Na | K | Li | Cl | SO4 | CO 3 | HC O3 | B |
| PED-26 | 1 | 135 | 43 | 711 | 50 | 3 | 1,250 | 305 | 1 | 127 | 9 |
| PED-27 | 1 | 125 | 42 | 711 | 48 | 3 | 1,180 | 341 | 8 | 126 | 9 |
| PED-28 | 2 | 166 | 58 | 817 | 61 | 3 | 1,450 | 387 | 1 | 92 | 10 |
| PED-29 | 1 | 145 | 46 | 699 | 51 | 3 | 1,260 | 334 | 0 | 103 | 10 |
| MARICUNGA | | | | | | | | | | | |
| sample | TDS | Ca | Mg | Na | K | Li | Cl | SO4 | CO 3 | HC O3 | B |
| MAR-16 | 4 | 165 | 58 | 1,220 | 161 | 11 | 2,200 | 169 | 0 | 273 | 18 |
| MAR-17 | 2 | 147 | 17 | 543 | 63 | 5 | 927 | 175 | 0 | 227 | 11 |
| MAR-19 | 51 | 1,24 0 | 680 | 16,20 0 | 1,230 | 92 | 30,80 0 | 171 | 0 | 0 | 50 |
| PINTADOS | | | | | | | | | | | |
| sample | TDS | Ca | Mg | Na | K | Li | Cl | SO4 | CO 3 | HC O3 | B |
| PIN-07 | 68 | 4,53 0 | 0 | 19,30 0 | 2,10 | 69 | 39,80 0 | 1,900 | 0 | 0 | 21 |
| PIN-16 | 1 | 43 | 9 | 135 | 49 | 1 | 689 | 121 | 1 | 9 | 10 |
| PIN-41 | 23 | 529 | 179 | 7,080 | 696 | 15 | 5,890 | 58 | 11 | 124 | 60 |
| HUASCO | | | | | | | | | | | |
| sample | TDS | Ca | Mg | Na | K | Li | Cl | SO4 | CO 3 | HC O3 | B |
| HCO0 | 277 | 6,10 | 5,88 0 | 65,00 | 13,50 0 | 480 | 112,9 | 26,70 0 | - | - | 2,33 3 |
| HCO-6 | 0 | 11 | 8 | 122 | 13 | <1 | 82 | 74 | 1 | 2 | 2 |
| HCO-9 | 0 | 13 | 5 | 45 | 11 | <1 | 20 | 156 | 0 | 59 | 1 |
| COPOSA | | | | | | | | | | | |
| sample | TDS | Ca | Mg | Na | K | Li | Cl | SO4 | CO 3 | HC O3 | B |
| COP-03 | 0 | 7 | 4 | 14 | 3 | <1 | 10 | 38 | 0 | 9 | 1 |
| COP-07 | 3 | 214 | 163 | 573 | 45 | 2 | 1,010 | 488 | 2 | 79 | 4 |
| COP-08 | 0 | 32 | 18 | 29 | 6 | <1 | 28 | 67 | 0 | 146 | 1 |
| COP-09 | 3 | 362 | 53 | 483 | 50 | 1 | 753 | 1,030 | 1 | 111 | 3 |
| COP-11 | 112 | 742 | 4,93 0 | 31,10 0 | 3,080 | 90 | 50,80 0 | 20,40 0 | 16 | 465 | 101 |
| COP-16 | 2 | 119 | 44 | 382 | 18 | 1 | 742 | 235 | 1 | 63 | 2 |
| MICHINCHA | | | | | | | | | | | |
| sample | TDS | Ca | Mg | Na | K | Li | Cl | SO4 | CO 3 | HC O3 | B |
| MIC-08 | 0 | 25 | 19 | 35 | 18 | <1 | 18 | - | 0 | 90 | <1 |
| MIC-09 | 0 | 32 | 8 | 41 | 16 | <1 | 25 | - | 2 | 46 | <1 |
| MIC-10 | 1 | 69 | 25 | 33 | 12 | <1 | 24 | - | 0 | 25 | <1 |
| MIC-11 | 0 | 10 | 3 | 15 | 7 | <1 | 10 | - | 0 | 31 | <1 |

| sample | TDS | Ca | Mg | Na | K | Li | Cl | SO4 | CO ₃ | HC O ₃ | B |
|--------------------|-----|-----|------|-------|-------|-----|-------|-------|-----------------|-------------------|------|
| IMI-01 | 1 | 39 | 3 | 132 | 11 | <1 | 96 | 233 | 1 | 28 | 2 |
| IMI-03 | 6 | 593 | 52 | 1,460 | 73 | 73 | 1,970 | 1,900 | 0 | 68 | 6 |
| IMI-04 | 2 | 11 | 7 | 30,40 | 0 | 19 | 1 | 1,000 | 60 | 13 | 73 |
| IMI-8D | 12 | 642 | 66 | 3,800 | 94 | 2 | 6,430 | 1,010 | 0 | 66 | 8 |
| PUNTA NEGRA | | | | | | | | | | | |
| sample | TDS | Ca | Mg | Na | K | Li | Cl | SO4 | CO ₃ | HC O ₃ | B |
| PUN-08 | 7 | 78 | 24 | 2,420 | 140 | 3 | 3,980 | 101 | 1 | 70 | 2 |
| PUN-16 | 3 | 9 | 53 | 653 | 89 | 3 | 1,560 | 420 | 0 | 40 | 20 |
| PUN-18 | 3 | 158 | 24 | 791 | 104 | 2 | 1,440 | 240 | 0 | 6 | 10 |
| PUN-19 | 1 | 19 | 3 | 127 | 15 | <1 | 172 | 30 | 5 | 79 | 1 |
| PUN-20 | 1 | 3 | 0 | 175 | 8 | <1 | 152 | 37 | 30 | 129 | 0 |
| PUN-24 | 0 | 31 | 2 | 139 | 9 | <1 | 244 | 37 | 1 | 13 | 0 |
| IGNORADOS | | | | | | | | | | | |
| sample | TDS | Ca | Mg | Na | K | Li | Cl | SO4 | CO ₃ | HC O ₃ | B |
| IGN-04 | 10 | 485 | 445 | 342 | 342 | 1 | 444 | 6,490 | 0 | 0 | 18 |
| IGN-05 | 13 | 505 | 707 | 637 | 637 | 2 | 1,410 | 7,300 | 0 | 0 | 29 |
| LA AZUFRERA | | | | | | | | | | | |
| sample | TDS | Ca | Mg | Na | K | Li | Cl | SO4 | CO ₃ | HC O ₃ | B |
| AZU0 | 400 | 88 | 48,6 | 100 | 14,96 | 86 | 172,1 | 87,99 | - | 0 | 740 |
| AZU-07 | 1 | 117 | 9 | 34 | 11 | <1 | 157 | 148 | 0 | 29 | 0 |
| JAMA | | | | | | | | | | | |
| sample | TDS | Ca | Mg | Na | K | Li | Cl | SO4 | CO ₃ | HC O ₃ | B |
| JA1 | 7 | 178 | 402 | 2,004 | 201 | 6 | 2,560 | 7,009 | 0 | 349 | 539 |
| JA2 | 7 | 991 | 243 | 2,860 | 343 | 11 | 2,627 | 4,587 | 0 | 387 | 3,07 |
| JA3 | 6 | 131 | 17 | 3,523 | 210 | 10 | 6,170 | 2,051 | 0 | 332 | 236 |
| JA4 | 6 | 122 | 48 | 3,422 | 344 | 2 | 4,927 | 2,537 | 0 | 234 | 493 |
| JA5 | 6 | 65 | 47 | 4,183 | 297 | 2 | 5,868 | 1,219 | 0 | 263 | 239 |
| JA6 | 91 | 647 | 469 | 60,43 | 4,591 | 262 | 97,01 | 14,61 | 0 | 286 | 1,42 |
| JA7 | 6 | 122 | 48 | 3,475 | 344 | 2 | 4,929 | 2,535 | 0 | 341 | 493 |
| JA8 | 6 | 122 | 47 | 3,482 | 344 | 2 | 4,930 | 2,541 | 0 | 344 | 494 |
| JA9 | 90 | 647 | 467 | 60,42 | 3,356 | 262 | 97,01 | 14,61 | 0 | 282 | 1,42 |
| JA10 | 92 | 646 | 492 | 60,43 | 4,658 | 261 | 97,01 | 14,61 | 0 | 272 | 1,42 |
| OLAROZ | | | | | | | | | | | |
| sample | TDS | Ca | Mg | Na | K | Li | Cl | SO4 | CO ₃ | HC O ₃ | B |
| OL1 | 157 | 584 | 1,53 | 112,1 | 5,051 | 771 | 181,7 | 9,678 | 0 | 421 | 2,09 |
| | | | 9 | 91 | | | 49 | | | | 0 |

| | | | | | | | | | | | |
|------|-----|-----|------|-------|-------|------|-------|-------|---|-----|------|
| OL2 | 158 | 529 | 1,98 | 112,1 | 5,504 | 968 | 181,0 | 10,22 | 0 | 419 | 2,09 |
| OL3 | 155 | 526 | 1,97 | 107,6 | 6,019 | 1,00 | 179,6 | 10,19 | 0 | 435 | 2,30 |
| OL4 | 157 | 481 | 2,30 | 107,9 | 7,984 | 1,20 | 180,8 | 8,982 | 0 | 328 | 3,17 |
| OL5 | 137 | 448 | 2,18 | 69,85 | 6,563 | 1,09 | 175,6 | 10,58 | 0 | 343 | 2,51 |
| OL6 | 153 | 496 | 2,27 | 79,67 | 7,870 | 1,21 | 187,0 | 10,01 | 0 | 366 | 2,25 |
| OL7 | 158 | 513 | 1,98 | 107,7 | 5,179 | 868 | 176,3 | 9,856 | 0 | 331 | 2,42 |
| OL8 | 160 | 537 | 2,18 | 107,0 | 5,501 | 1,09 | 184,9 | 10,20 | 0 | 280 | 3,03 |
| OL9 | 159 | 447 | 1,62 | 112,3 | 6,003 | 1,06 | 179,0 | 10,65 | 0 | 247 | 2,80 |
| OL10 | 145 | 598 | 1,97 | 71,78 | 6,569 | 861 | 181,6 | 10,37 | 0 | 266 | 2,65 |

CAUCHARI

| sample | TDS | Ca | Mg | Na | K | Li | Cl | SO4 | CO ₃ | HC O ₃ | B |
|--------|-----|-----|------|-------|-------|------|-------|-------|-----------------|-------------------|------|
| CA1 | 97 | 556 | 1,85 | 69,82 | 2,76 | 535 | 108,0 | 9,060 | 0 | 279 | 1,33 |
| CA2 | 92 | 764 | 1,50 | 58,03 | 2,14 | 442 | 102,2 | 14,47 | 0 | 355 | 2,19 |
| CA3 | 124 | 603 | 1,67 | 8,76 | 8,594 | 1,74 | 130,4 | 11,95 | 0 | 490 | 2,83 |
| CA4 | 139 | 477 | 1,59 | 10,13 | 4,769 | 713 | 149,8 | 16,35 | 0 | 461 | 2,30 |
| CA5 | 144 | 599 | 2,20 | 104,5 | 4,733 | 873 | 163,8 | 9,685 | 0 | 623 | 2,12 |

SALINAS GRANDES

| sample | TDS | Ca | Mg | Na | K | Li | Cl | SO4 | CO ₃ | HC O ₃ | B |
|--------|-----|------|------|-------|-------|------|-------|-------|-----------------|-------------------|-----|
| SG1 | 12 | 877 | 115 | 6,413 | 694 | 25 | 10,20 | 3,982 | 0 | 375 | 527 |
| SG2 | 120 | 1,30 | 803 | 86,37 | 3,325 | 218 | 140,6 | 1,746 | 0 | 342 | 509 |
| SG3 | 119 | 1,46 | 1,01 | 84,71 | 3,498 | 244 | 141,3 | 1,573 | 0 | 344 | 542 |
| SG4 | 121 | 1,44 | 1,13 | 86,81 | 3,762 | 270 | 140,2 | 2,174 | 0 | 339 | 444 |
| SG5 | 116 | 1,90 | 1,30 | 77,46 | 4,521 | 382 | 140,4 | 1,908 | 0 | 256 | 452 |
| SG6 | 116 | 1,47 | 843 | 79,32 | 3,651 | 241 | 139,3 | 2,388 | 0 | 278 | 342 |
| SG7 | 116 | 2,11 | 2,28 | 67,95 | 8,149 | 1,01 | 139,0 | 1,441 | 0 | 230 | 361 |
| SG8 | 119 | 1,43 | 924 | 80,24 | 3,890 | 247 | 139,7 | 1,959 | 0 | 351 | 309 |
| SG9 | 118 | 1,39 | 1,02 | 85,69 | 4,668 | 325 | 137,8 | 1,900 | 0 | 368 | 512 |
| SG10 | 116 | 1,78 | 1,23 | 77,53 | 5,196 | 352 | 137,6 | 1,751 | 0 | 260 | 469 |

| GUAYATAYOC | | | | | | | | | | | | |
|---------------|-----|-----------|-----------|-------------|------------|-----------|-------------|------------|-----------------|-------------------|-----------|--|
| sample | TDS | Ca | Mg | Na | K | Li | Cl | SO4 | CO ₃ | HC O ₃ | B | |
| GG3 | 48 | 2,08 4 | 292 | 20,00 0 | 8070 | 45 | 58,50 0 | 7,560 | 0 | 384 | 310 | |
| GQ0 | 86 | 1,38 2 | 134 | 32,40 0 | 21,00 0 | 125 | 252,8 00 | 13,00 0 | 0 | 286 | 450 | |
| GG4 | 81 | 1,27 0 | 123 | 31,70 0 | 20,87 0 | 117 | 245,0 90 | 13,50 0 | 0 | 276 | 321 | |
| CENTENARIO | | | | | | | | | | | | |
| sample | TDS | Ca | Mg | Na | K | Li | Cl | SO4 | CO ₃ | HC O ₃ | B | |
| CE0 | 343 | 320 | 7,55 0 | 112,3 00 | 8,170 | 1,02 0 | 192,7 00 | 19,98 0 | - | - | 3,76 5 | |
| CE1 | 26 | 831 | 916 | 6,752 | 966 | 65 | 1,159 5 | 2,960 | 0 | 498 | 365 | |
| CE2 | 26 | 508 | 604 | 7,134 | 843 | 25 | 1,27 6 | 3,056 | 0 | 496 | 277 | |
| CE3 | 41 | 395 | 1,19 6 | 10,61 3 | 2,860 | 106 | 17,13 3 | 12,46 1 | 0 | 322 | 434 | |
| CE4 | 45 | 842 | 1,21 7 | 11,76 7 | 2,91 | 133 | 18,46 6 | 12,66 3 | 0 | 343 | 581 | |
| CE5 | 49 | 619 | 2,27 7 | 10,45 0 | 3,25 | 377 | 21,49 3 | 12,18 4 | 0 | 494 | 402 | |
| DIABLILLOS | | | | | | | | | | | | |
| sample | TDS | Ca | Mg | Na | K | Li | Cl | SO4 | CO ₃ | HC O ₃ | B | |
| DI1 | 38 | 791 | 1,82 4 | 9,533 | 746 | 47 | 21,89 7 | 3,541 | 0 | 230 | 360 | |
| DI2 | 26 | 791 | 1,12 1 | 6,943 | 687 | 81 | 15,04 1 | 2,715 | 0 | 376 | 584 | |
| DI3 | 78 | 1,40 2 | 933 | 21,53 5 | 7,876 | 235 | 38,27 0 | 9,587 | 0 | 351 | 808 | |
| DI4 | 81 | 1,18 6 | 964 | 21,78 4 | 6,370 | 357 | 37,73 1 | 11,61 8 | 0 | 334 | 614 | |
| HOMBRE MUERTO | | | | | | | | | | | | |
| sample | TDS | Ca | Mg | Na | K | Li | Cl | SO4 | CO ₃ | HC O ₃ | B | |
| MH0 | 341 | 1,00 0 | 268 | 121,9 00 | 9,340 | 914 | 194,8 00 | 11,10 0 | - | - | 1,45 5 | |
| HM1 | 31 | 792 | 916 | 8,197 | 2,984 | 114 | 18,76 6 | 1,017 | 0 | 133 | 377 | |
| HM2 | 33 | 410 | 678 | 8,871 | 4,310 | 85 | 19,49 0 | 1,216 | 0 | 204 | 538 | |
| HM3 | 194 | 1,16 2 | 1,11 4 | 64,92 7 | 6,430 | 966 | 137,9 10 | 1,284 | 0 | 62 | 1,32 3 | |
| HM4 | 205 | 592 | 833 | 72,48 4 | 4,022 | 674 | 139,4 09 | 1,312 | 0 | 321 | 515 | |
| HM5 | 196 | 874 | 1,91 5 | 62,40 0 | 5,660 | 1,01 3 | 125,3 13 | 934 | 0 | 105 | 149 0 | |
| INCAHUASI | | | | | | | | | | | | |
| sample | TDS | Ca | Mg | Na | K | Li | Cl | SO4 | CO | HC | B | |

| | | | | | | | | | | 3 | O3 |
|------------------------------|-----|-----------|------------|-------------|-------|-----|-------------|------------|---------|----------|-----------|
| IN1 | 48 | 1,28 4 | 5283 | 7,360 | 2,754 | 22 | 32,63 1 | 362 | 0 | 315 | 114 |
| IN2 | 69 | 976 | 10,3 76 | 6,548 | 6,896 | 82 | 48,67 5 | 930 | 0 | 75 | 558 |
| IN3 | 100 | 1,19 4 | 15,8 94 | 12,34 4 | 4,012 | 132 | 72,91 3 | 678 | 0 | 15 | 510 |
| IN4 | 107 | 988 | 14,6 87 | 11,78 2 | 7,130 | 145 | 74,35 3 | 736 | 0 | 44 | 570 |
| IN5 | 86 | 1,07 4 | 9828 | 10,49 1 | 7,732 | 96 | 61,34 5 | 855 | 0 | 276 | 427 |
| PASTOS GRANDES (PUNA) | | | | | | | | | | | |
| sample | TDS | Ca | Mg | Na | K | Li | Cl | SO4 | CO 3 | HC O3 | B |
| PG0 | 333 | 740 | 2,98 0 | 118,2 00 | 4,730 | 440 | 178,7 00 | 26,08 0 | - | - | 2,22 0 |
| PG1 | 154 | 766 | 3,78 5 | 50,22 0 | 919 | 355 | 97,05 3 | 968 | 0 | 822 | 702 |
| PG2 | 227 | 745 | 2,43 1 | 80,73 2 | 652 | 510 | 161,3 90 | 970 | 0 | 896 | 784 |
| PG3 | 157 | 512 | 4,47 9 | 50,67 3 | 5,56 | 410 | 102,8 50 | 970 | 0 | 980 | 300 |
| PG4 | 158 | 580 | 5,64 6 | 49,77 2 | 3,590 | 305 | 101,0 60 | 943 | 0 | 955 | 455 |
| PG5 | 158 | 498 | 5,61 1 | 41,45 4 | 5,914 | 857 | 91,50 5 | 14,90 3 | 0 | 865 | 812 |
| POZUELOS | | | | | | | | | | | |
| sample | TDS | Ca | Mg | Na | K | Li | Cl | SO4 | CO 3 | HC O3 | B |
| PZ1 | 237 | 447 | 1,13 3 | 89,66 1 | 1,011 | 96 | 154,5 21 | 8,864 | 0 | 213 | 650 |
| PZ2 | 291 | 358 | 1,85 4 | 107,7 72 | 2,976 | 207 | 176,2 83 | 9,060 | 0 | 278 | 1,36 6 |
| PZ3 | 290 | 2,13 | 2,58 7 | 102,7 15 | 6,314 | 712 | 178,2 50 | 10,78 5 | 0 | 12 | 398 |
| PZ4 | 220 | 604 | 1,81 6 | 115,9 75 | 4,044 | 260 | 198,9 70 | 2,974 | 0 | 0 | 1,65 5 |
| PZ5 | 254 | 1,60 | 1,71 5 | 87,01 2 | 5,213 | 940 | 150,6 70 | 13,11 5 | 0 | 0 | 2,10 2 |
| PZ6 | 295 | 1,61 | 2,09 9 | 102,1 52 | 4,728 | 835 | 190,9 56 | 9,685 | 0 | 0 | 202 |
| PZ7 | 256 | 444 | 1,18 0 | 91,67 4 | 1,024 | 86 | 171,3 60 | 8,812 | 0 | 240 | 415 |
| PZ8 | 205 | 672 | 741 | 76,59 1 | 816 | 75 | 122,0 34 | 9,005 | 0 | 266 | 396 |
| RATONES | | | | | | | | | | | |
| sample | TDS | Ca | Mg | Na | K | Li | Cl | SO4 | CO 3 | HC O3 | B |
| RA1 | 28 | 1,21 3 | 135 | 9,780 | 852 | 88 | 17,26 0 | 2,731 | 0 | 647 | 312 |
| RA2 | 83 | 1,54 0 | 323 | 30,53 3 | 3,205 | 260 | 54,45 7 | 5,125 | 0 | 415 | 433 |
| RA3 | 72 | 1408 | 210 | 27,31 | 3,024 | 125 | 53,19 | 3,580 | 0 | 348 | 509 |

2 2

| ANTOFALLA | | | | | | | | | | | | |
|-----------|-----|-----------|-----------|-------------|------------|-----|-------------|------------|-----------------|-------------------|-----------|--|
| sample | TDS | Ca | Mg | Na | K | Li | Cl | SO4 | CO ₃ | HC O ₃ | B | |
| AN1 | 55 | 2,96 4 | 705 | 15,97 5 | 2,490 | 164 | 29,05 8 | 8,714 | 0 | 77 | 530 | |
| AN2 | 185 | 662 | 725 | 63,71 3 | 3,518 | 615 | 113,9 85 | 7,725 | 0 | 358 | 815 | |
| AN3 | 148 | 535 | 816 | 55,77 0 | 807 | 311 | 88,20 1 | 7,815 | 0 | 241 | 878 | |
| AN4 | 25 | 1,31 0 | 365 | 6,889 | 365 | 95 | 14,10 0 | 1,830 | 0 | 710 | 814 | |
| AN5 | 19 | 692 | 644 | 5,271 | 476 | 46 | 9,460 | 1,005 | 0 | 865 | 807 | |
| AN6 | 9 | 286 | 206 | 2,580 | 166 | 25 | 4,873 | 356 | 0 | 492 | 415 | |
| ARIZARO | | | | | | | | | | | | |
| sample | TDS | Ca | Mg | Na | K | Li | Cl | SO4 | CO ₃ | HC O ₃ | B | |
| AR0 | 321 | 760 | 1,84 0 | 119,5 00 | 160 | 100 | 190,7 00 | 9,260 | - | - | 138 | |
| AR1 | 274 | 415 | 484 | 100,5 81 | 4,112 | 106 | 182,2 13 | 12,48 3 | 0 | 81 | 1,10 9 | |
| AR2 | 155 | 473 | 545 | 53,10 7 | 2,061 | 83 | 98,09 0 | 5,521 | 0 | 122 | 2,06 6 | |
| AR3 | 92 | 512 | 1,61 6 | 23,45 0 | 5,686 | 375 | 42,61 1 | 17,62 0 | 0 | 74 | 1,21 6 | |
| AR4 | 130 | 517 | 7,73 5 | 25,56 5 | 7,543 | 318 | 58,84 7 | 30,24 6 | 0 | 119 | 3,30 6 | |
| AR5 | 308 | 429 | 4,14 4 | 99,47 8 | 10,07 1 | 180 | 184,2 34 | 30,39 0 | 0 | 225 | 3,22 5 | |
| AR6 | 80 | 515 | 5,13 4 | 24,94 4 | 1,098 | 112 | 39,24 3 | 13,92 3 | 0 | 96 | 1,23 2 | |
| AR7 | 105 | 494 | 4,09 2 | 24,99 0 | 10,01 1 | 465 | 56,89 7 | 17,62 0 | 0 | 60 | 1,31 3 | |
| AR8 | 48 | 515 | 1,07 0 | 15,56 4 | 1,480 | 52 | 23,46 8 | 7,922 | 0 | 93 | 2,36 6 | |
| AR9 | 50 | 432 | 376 | 10,80 5 | 1,315 | 97 | 16,66 2 | 2,497 | 0 | 75 | 3,38 2 | |
| AR10 | 64 | 410 | 484 | 22,53 0 | 1,180 | 122 | 38,53 4 | 7,682 | 0 | 74 | 380 | |
| POCITOS | | | | | | | | | | | | |
| sample | TDS | Ca | Mg | Na | K | Li | Cl | SO4 | CO ₃ | HC O ₃ | B | |
| PC0 | 327 | 600 | 1,29 0 | 123,1 00 | 3,400 | 97 | 190,6 00 | 7,440 | - | - | 708 | |
| PC1 | 32 | 1,23 5 | 246 | 9,584 | 421 | 27 | 18,02 0 | 2,690 | 0 | 74 | 70 | |
| PC2 | 34 | 1,44 3 | 285 | 9,667 | 105 | 30 | 17,85 9 | 6,240 | 0 | 56 | 85 | |
| PC3 | 278 | 795 | 1,22 5 | 102,5 97 | 610 | 101 | 182,2 35 | 9,050 | 0 | 0 | 208 | |
| PC4 | 299 | 815 | 1,38 4 | 110,8 62 | 1,197 | 86 | 190,7 50 | 4,300 | 0 | 0 | 194 | |
| PC5 | 38 | 1,54 | 260 | 11,44 | 1,488 | 46 | 18,34 | 6,955 | 0 | 37 | 88 | |

| | 0 | 0 | 5 | | | | | | | | | |
|------|----|-----|-----|------------|-------|----|------------|-------|---|----|-----|--|
| PC6 | 41 | 412 | 568 | 12,54 4 | 1,670 | 65 | 23,95 0 | 5,272 | 0 | 37 | 170 | |
| PC7 | 36 | 645 | 633 | 10,38 0 | 1,771 | 68 | 16,05 5 | 7,925 | 0 | 0 | 162 | |
| PC8 | 29 | 408 | 596 | 10,30 1 | 1,612 | 53 | 15,25 2 | 3,897 | 0 | 15 | 60 | |
| PC9 | 30 | 944 | 578 | 10,29 8 | 1,644 | 22 | 18,09 5 | 2,102 | 0 | 22 | 63 | |
| PC10 | 45 | 365 | 135 | 12,86 3 | 1,702 | 68 | 20,33 3 | 9,970 | 0 | 13 | 63 | |

RINCON

| sample | TDS | Ca | Mg | Na | K | Li | Cl | SO4 | CO 3 | HC O3 | B |
|--------|-----|-----------|-----------|-------------|-------|-----------|-------------|------------|---------|----------|-----------|
| RI0 | 339 | 280 | 2,12 0 | 122,2 00 | 6,570 | 350 | 190,5 0 | 15,99 0 | - | - | 1,60 9 |
| RI1 | 281 | 1,05 0 | 1,81 5 | 95,23 5 | 7,130 | 211 36 | 16,9 4 | 17,48 4 | 0 | 150 | 1,90 4 |
| RI2 | 285 | 813 | 2,29 7 | 99,19 9 | 6,543 | 270 57 | 172,5 3 | 25,23 3 | 0 | 134 | 2,09 8 |
| RI3 | 152 | 805 | 2,21 0 | 47,03 00 | 5,612 | 112 | 84,82 3 | 13,31 4 | 0 | 163 | 1,61 2 |
| RI4 | 145 | 833 | 2,28 4 | 47,76 4 | 6,341 | 122 | 83,63 5 | 14,58 4 | 0 | 177 | 1,40 5 |
| RI5 | 140 | 1,10 2 | 1,78 8 | 41,14 0 | 6,974 | 360 | 73,81 4 | 15,41 5 | 0 | 210 | 1,81 2 |
| RI6 | 141 | 910 | 2,04 4 | 18,94 5 | 6,530 | 268 | 74,72 2 | 16,11 2 | 0 | 147 | 2,04 1 |
| RI7 | 152 | 930 | 1,83 3 | 50,16 3 | 6,812 | 195 | 96,23 1 | 10,34 1 | 0 | 207 | 1,90 4 |
| RI8 | 183 | 652 | 2,03 0 | 61,24 0 | 7,315 | 651 | 108,3 78 | 11,01 2 | 0 | 215 | 1,41 2 |
| RI9 | 187 | 8,14 | 1,91 8 | 59,15 2 | 7,015 | 337 | 107,5 00 | 10,40 4 | 0 | 219 | 1,78 7 |
| RI10 | 190 | 330 | 2,01 6 | 60,48 8 | 4,916 | 150 | 102,3 34 | 10,48 2 | 0 | 112 | 1,47 0 |

RIO GRANDE

| sample | TDS | Ca | Mg | Na | K | Li | Cl | SO4 | CO 3 | HC O3 | B |
|--------|-----|-----------|-----------|------------|-------|-----|-------------|------------|---------|----------|-----------|
| RG0 | 260 | 800 | 2,60 0 | 92,40 0 | 3,710 | 420 | 148,9 00 | 10,61 0 | - | - | 1,67 3 |
| RG1 | 285 | 1,86 2 | 2,21 5 | 96,48 5 | 3,012 | 336 | 162,8 40 | 18,68 0 | 0 | 416 | 414 |
| RG2 | 280 | 1,96 6 | 2,19 0 | 98,18 7 | 3,305 | 274 | 163,7 73 | 19,99 0 | 0 | 297 | 302 |
| RG3 | 257 | 1,98 7 | 2,13 6 | 89,37 3 | 3,315 | 468 | 169,0 85 | 8,654 | 0 | 25 | 415 |
| RG4 | 207 | 2,10 4 | 2,23 0 | 77,91 0 | 3,588 | 502 | 131,5 28 | 6,940 | 0 | 76 | 545 |
| RG5 | 260 | 1,97 0 | 1,39 0 | 87,76 1 | 2,469 | 139 | 166,2 35 | 4,974 | 0 | 72 | 348 |
| RG6 | 259 | 2,10 3 | 1,50 5 | 99,82 8 | 2,645 | 152 | 164,6 15 | 5,134 | 0 | 98 | 366 |

| | | | | | | | | | | | |
|------|-----|-----------|-----------|-------------|-------|-----|-------------|-------|---|-----|-----|
| RG7 | 252 | 2,10 0 | 2,23 4 | 103,4 66 | 3,316 | 480 | 162,2 00 | 4,909 | 0 | 44 | 423 |
| RG8 | 199 | 1,28 3 | 2,97 4 | 74,57 2 | 2,890 | 692 | 131,6 65 | 2,022 | 0 | 366 | 315 |
| RG 9 | 234 | 2,33 0 | 2,21 2 | 78,28 8 | 3,325 | 475 | 150,7 55 | 3,080 | 0 | 381 | 442 |
| RG10 | 226 | 2,04 9 | 2,08 4 | 75,34 2 | 3,191 | 443 | 147,7 65 | 2,315 | 0 | 337 | 404 |

- not reported

Table 3. Mean values for hydrochemical compositions of brines from Andean salt pans. Values correspond to averages computed on data presented in Table 2. n: number of samples. TDS in g L⁻¹, the remaining concentrations in mg L⁻¹.

| N° | Salt pan | n | Mean | | | | | | | | | | |
|----|-----------|---------|----------|-----------|------------|------------|------------|-------------|-------------|-----------------|---------------------|----------------------|-------------|
| | | | TDS | Ca | Mg | Na | K | Li | Cl | SO ₄ | C O ₃ | HC O ₃ | |
| 1 | Surire | 3 | 17 8 | 96, 1 | 2,22 1 | 56,10 3 | 9,20 3 | 359 | 96,06 0 | 8,99 7 | 13 - | 99 785 | 1,84 883 |
| 2 | Coipasa | 11 | 14 5 | 350 11 | 12,2 36 | 104,8 5 | 9,15 5 | 258 | 178,0 91 | 37,3 55 | - | - | 785 883 |
| 3 | Uyuni | 16 5 | 12 3 | 550 33 | 15,5 0 | 87,67 0 | 12,3 89 | 715 | 183,8 85 | 17,1 49 | - | 4 - | 646 |
| 4 | Empexa | 23 9 | 259 0 | 8,48 0 | 67,20 0 | 3,40 0 | 213 | 120,0 00 | 34,1 00 | - | 430 | 702 | |
| 5 | Huasco | 3 | 93 | 221 | 1,96 4 | 21,72 2 | 4,50 8 | 160 | 37,69 4 | 8,97 7 | <1 - | 20 | 779 |
| 6 | Coposa | 6 | 20 | 246 | 869 | 5,430 | 534 | 16 | 8,890 | 3,71 0 | 3 | 146 | 19 |
| 7 | Michinchá | 5 | <1 | 31 | 13 | 28 | 12 | <1 | 18 | - | <1 | 46 | <1 |
| 8 | Alconcha | 1 | 1 | 150 | 2 | 97 | 13 | <1 | 90 | - | 0 | 87 | 3 |
| 9 | Carcote | 4 | 23 4 | 7,03 9 | 4,15 1 | 70,56 7 | 7,26 8 | 217 | 61,81 2 | 3,03 8 | 5 | 169 | 224 |
| 10 | Ascotán | 10 | 29 | 280 | 786 | 8,497 | 899 | 47 | 13,58 1 | 3,88 5 | 14 | 593 | 374 |

| | | | | | | | | | | | | | |
|---|---------------------|----|----|------|------|-------|------|------|-------|------|----|-----|------|
| 1 | Pastos Grandes | | 32 | 3,10 | 3,48 | 101,0 | 14,2 | 1,64 | 194,0 | 2,46 | - | - | 3,04 |
| 1 | (Altiplano) | 1 | 1 | 0 | 0 | 00 | 00 | 0 | 00 | 0 | - | - | 1 |
| 1 | Atacama | 10 | 18 | 606 | 4,06 | 46,79 | 8,70 | 562 | 90,04 | 9,85 | <1 | 273 | 482 |
| 2 | | 1 | | | 4 | 3 | 6 | | 7 | 6 | | | |
| 1 | El Tara | 12 | 35 | 346 | 165 | 22,50 | 243 | 140 | 35,24 | 3,08 | 12 | 772 | 201 |
| 3 | | | | | 4 | | | | 0 | 3 | | | |
| 1 | Aguas Calientes | 7 | 10 | 633 | 151 | 4,414 | 165 | 25 | 7,964 | 541 | 1 | 281 | 66 |
| 4 | Norte | | | | | | | | | | | | |
| 1 | Pujsa | 10 | - | 269 | 376 | 15,73 | 1,13 | 89 | 18,67 | 12,4 | 34 | 562 | 189 |
| 5 | | | | | | 1 | 0 | | 0 | 00 | 9 | | |
| 1 | Loyoques o | 5 | 94 | 11,4 | 1,96 | 53,69 | 409 | 700 | 141,9 | 1,61 | 8 | 599 | 480 |
| 6 | Quisquiro | | | 54 | 0 | 8 | | | 13 | 5 | | | |
| 1 | Aguas Calientes | 5 | 17 | 1,22 | 946 | 6,060 | 394 | 15 | 12,46 | 1,74 | 0 | 339 | 7 |
| 7 | Centro | | | 5 | | | | | 0 | 0 | | | |
| 1 | El Laco | 6 | 62 | 852 | 2,37 | 22,30 | 1,78 | 37 | 38,58 | 6,34 | 0 | 393 | 180 |
| 8 | | | | | 2 | 8 | 7 | | 3 | 1 | | | |
| 1 | Aguas Calientes Sur | 8 | 7 | 432 | 265 | 2,569 | 189 | 4 | 4,660 | 1,06 | 0 | 167 | 0 |
| 9 | | | | | | | | | 2 | | | | |
| 2 | Imilac | 4 | 5 | 321 | 32 | 8,948 | 49 | 19 | 2,374 | 801 | 4 | 59 | 4 |
| 1 | | | | | | | | | | | | | |
| 2 | Punta Negra | 6 | 2 | 50 | 18 | 718 | 61 | 1 | 1,255 | 144 | 6 | 56 | 5 |
| 2 | Aguas Calientes Sur | 10 | 4 | 202 | 131 | 1,668 | 163 | 5 | 2,718 | 1,01 | 7 | 108 | 19 |
| 3 | Sur | | | | | | | | 4 | | | | |
| 2 | Pajanoles | 25 | 49 | 3,23 | 1,56 | 19,43 | 1,22 | 25 | 45,58 | 1,81 | 0 | 283 | 160 |
| 4 | | | | | 4 | 0 | 7 | 1 | 8 | 0 | | | |
| 2 | La Azufrera | 2 | 28 | 441 | 34,4 | 42,31 | 10,7 | 61 | 121,1 | 65,8 | 0 | 36 | 532 |
| 5 | | 7 | | | 00 | 7 | 73 | | 57 | 34 | | | |
| 2 | Gorbea | 5 | 58 | 288 | 26,8 | 47,06 | 3,92 | 316 | 114,0 | 72,3 | 0 | 0 | 2,31 |
| 6 | | | | | 10 | 0 | 5 | | 70 | 89 | 0 | 0 | 9 |
| 2 | Ignorados | 2 | 11 | 495 | 576 | 490 | 490 | 2 | 927 | 6,89 | 0 | 0 | 24 |
| 7 | | | | | | | | | 5 | | | | |
| 2 | Agua Amarga | 6 | 75 | 16,6 | 2,41 | 34,78 | 1,42 | 60 | 92,09 | 1,09 | 0 | 121 | 311 |
| 8 | | | | | 52 | 1 | 3 | 9 | 8 | 5 | | | |
| 2 | Aguilar | 3 | 11 | 51,6 | 6,60 | 60,66 | 2,60 | 367 | 203,3 | 461 | 0 | 917 | 739 |
| 9 | | 3 | | | 67 | 0 | 7 | 0 | 34 | | | | |

| | | | | | | | | | | | | | |
|--------|--------------------------|----|----|-----------|------------|------------|------------|-----------|-------------|------------|---|-----|-----------|
| 3 0 | La Isla | 12 | 62 | 390 | 2,57 8 | 46,66 7 | 10,8 98 | 402 | 87,27 8 | 7,01 5 | 4 | 188 | 118 |
| 3 2 | Las Parinas | 6 | 46 | 300 | 1,18 5 | 36,31 7 | 1,11 4 | 130 | 59,60 7 | 4,50 1 | 0 | 326 | 148 |
| 3 4 | Pedernales | 4 | 1 | 143 | 47 | 735 | 53 | 3 | 1,285 | 342 | 2 | 112 | 10 |
| 3 8 | Maricunga | 3 | 19 | 517 | 252 | 5,988 | 485 | 36 | 11,30 9 | 172 | 0 | 167 | 26 |
| 3 9 | Incahuasi | 5 | 82 | 1,10 3 | 11,2 14 | 9,705 | 5,70 5 | 95 | 57,98 3 | 712 | 0 | 145 | 436 |
| 4 0 | Antofalla-Botijuelas | 6 | 73 | 1,07 5 | 577 | 25,03 3 | 1,30 4 | 205 | 43,28 0 | 4,57 4 | 0 | 457 | 710 |
| 4 1 | Río Grande | 11 | 24 | 1,86 | 2,16 | 88,51 | 3,1 1 | 298 | 154,4 87 | 7,93 7 | 0 | 211 | 513 |
| 4 2 | Arizaro | 11 | 14 | 497 | 2,08 | 47,32 | 4,15 0 | 188 | 84,68 2 | 14,1 06 | 0 | 102 | 1,79 4 |
| 4 3 | Hombre Muerto | 6 | 16 | 805 | 954 | 5,46 3 | 5,45 8 | 628 | 105,9 48 | 2,81 1 | 0 | 165 | 950 |
| 4 4 | Diablillos | 4 | 56 | 1,11 9 | 1,22 6 | 14,94 9 | 3,92 0 | 180 | 28,23 5 | 6,86 5 | 0 | 323 | 592 |
| 4 5 | Ratones | 3 | 61 | 1,38 7 | 223 | 22,54 2 | 2,36 0 | 158 | 41,63 6 | 3,81 2 | 0 | 470 | 418 |
| 4 6 | Centenario | 6 | 28 | 586 | 2,29 3 | 26,50 3 | 3,13 0 | 288 | 46,44 4 | 10,5 51 | 0 | 431 | 971 |
| 4 7 | Pocitos-Quirón | 11 | 10 | 837 | 655 | 38,51 2 | 1,42 0 | 60 | 64,68 1 | 5,98 6 | 0 | 25 | 170 |
| 4 8 | Pozuelos | 8 | 26 | 1,07 | 1,64 | 96,69 | 3,26 | 401 | 167,8 80 | 9,03 8 | 0 | 126 | 898 |
| 4 9 | Pastos Grandes (Puna) | 6 | 19 | 640 | 4,15 5 | 65,17 7 | 3,55 2 | 476 | 122,0 93 | 7,47 2 | 0 | 904 | 879 |
| 5 0 | Rincón | 11 | 19 | 823 | 2,03 2 | 65,69 6 | 6,33 3 | 287 | 115,5 85 | 14,5 79 | 0 | 173 | 1,73 2 |
| 5 1 | Cauchari | 5 | 11 | 600 | 1,74 6 | 83,88 6 | 4,75 7 | 860 | 130,8 67 | 12,3 06 | 0 | 442 | 2,15 8 |
| 5 2 | Olaroz | 10 | 15 | 516 | 2,00 2 | 98,84 6 | 6,22 4 | 1,01 4 | 180,7 98 | 10,0 77 | 0 | 344 | 2,53 3 |

| | | | | | | | | | | | | | |
|---|----------------|----|----|------|------|-------|------|-----|-------|------|---|-----|-----|
| 5 | Jama | 10 | 32 | 527 | 228 | 20,42 | 1,46 | 82 | 32,30 | 6,63 | 0 | 309 | 983 |
| 3 | | | | | | 4 | 9 | | 6 | 3 | | | |
| 5 | Salinas Granes | 10 | 10 | 1,52 | 1,06 | 73,25 | 4,13 | 332 | 126,6 | 2,08 | 0 | 314 | 447 |
| 4 | | | 7 | 0 | 8 | 5 | 5 | | 63 | 2 | | | |
| 5 | Guayatayoc | 3 | 72 | 1,57 | 183 | 28,03 | 16,6 | 96 | 185,4 | 11,3 | 0 | 315 | 360 |
| 5 | | | | 9 | | 3 | 47 | | 63 | 53 | | | |

Table 4. Summary of mean, maximum (*max*), and concentration ratios of Li⁺ and Mg²⁺ in brines from Andean salt pans. The * values for the Atacama brines follow Moraga et al. (1974), Ide and Kunasz (1989), and Kunasz (2006). The * mean Li⁺ concentration for Olaroz is from García et al. (2019). Remaining values and ratios correspond to data presented in Table 3.

| N o | salt pan | mean Li ⁺ (mg L ⁻¹) | mean Mg ²⁺ (mg L ⁻¹) | max Li ⁺ (mg L ⁻¹) | max Mg ²⁺ (mg L ⁻¹) | Mg:Li mean ratio | max:mea n Li ratio |
|--------|----------------|---|---|--|---|------------------------|--------------------------|
| 1 | Surire | 359 | 2,291 | 540 | 3,830 | 6 | 2 |
| 2 | Coipasa | 253 | 12,211 | 416 | 23,000 | 47 | 2 |
| 3 | Uyuni | 715 | 15,533 | 4,720 | 75,300 | 22 | 7 |
| 4 | Empexa | 213 | 8,480 | 213 | 8,480 | 40 | 1 |
| 5 | Huasco | 160 | 1,964 | 480 | 5,880 | 12 | 3 |
| 6 | Coposa | 16 | 869 | 90 | 4,930 | 56 | 6 |
| 7 | Michinchá | <1 | 13 | <1 | 25 | 641 | 2 |
| 8 | Alconcha | <1 | 2 | <1 | 2 | 16 | 1 |
| 9 | Carcote | 217 | 4,151 | 339 | 6,850 | 19 | 2 |
| 1 | Ascotán | 47 | 786 | 245 | 5,125 | 17 | 5 |
| 0 | | | | | | | |
| 1 | Pastos Grandes | | | | | | |
| 1 | (Altiplano) | 1,640 | 3,480 | 1,640 | 3,480 | 2 | 1 |
| 1 | Atacama | 562 - | 4,064 | 1,570 - | 9,650 - | 7 | 3 - 5* |
| 2 | | 1,400* | | 6,400* | 80,000* | | |
| 1 | El Tara | 140 | 165 | 420 | 440 | 1 | 3 |

| | | | | | | | |
|---|-------------------------|-----|--------|-------|--------|-----|---|
| 3 | | | | | | | |
| 1 | Aguas Calientes Norte | 25 | 151 | 130 | 820 | 6 | 5 |
| 4 | | | | | | | |
| 1 | Pujsa | 89 | 376 | 400 | 3,762 | 4 | 5 |
| 5 | | | | | | | |
| 1 | Loyoques | 286 | 1,960 | 425 | 2,855 | 7 | 1 |
| 6 | | | | | | | |
| 1 | Aguas Calientes Centro | 15 | 946 | 45 | 7,981 | 63 | 3 |
| 7 | | | | | | | |
| 1 | El Laco | 37 | 2,372 | 101 | 6,250 | 64 | 3 |
| 8 | | | | | | | |
| 1 | Aguas Calientes Sur | 4 | 265 | 17 | 1,370 | 67 | 4 |
| 9 | | | | | | | |
| 2 | Imilac | 19 | 32 | 13 | 66 | 2 | 4 |
| 1 | | | | | | | |
| 2 | Punta Negra | 1 | 18 | 3 | 53 | 18 | 3 |
| 2 | | | | | | | |
| 2 | Aguas Calientes Sur Sur | 5 | 131 | 35 | 1,311 | 25 | 7 |
| 3 | | | | | | | |
| 2 | Pajonales | 25 | 1,560 | 62 | 5,200 | 63 | 3 |
| 4 | | | | | | | |
| 2 | La Azufrera | 51 | 34,400 | 86 | 48,640 | 562 | 1 |
| 5 | | | | | | | |
| 2 | Gorbea | 516 | 26,810 | 500 | 4,225 | 85 | 2 |
| 6 | | | | | | | |
| 2 | Ignorados | 2 | 576 | 2 | 707 | 339 | 1 |
| 7 | | | | | | | |
| 2 | Aguas Amarga | 60 | 2,411 | 157 | 39,500 | 40 | 3 |
| 8 | | | | | | | |
| 2 | Aguilar | 367 | 6,600 | 375 | 6,900 | 18 | 1 |
| 9 | | | | | | | |
| 3 | La Isla | 402 | 2,578 | 1,150 | 8,300 | 6 | 3 |
| 0 | | | | | | | |
| 3 | Las Parinas | 130 | 1,185 | 400 | 3,600 | 9 | 3 |
| 2 | | | | | | | |
| 3 | Pedernales | 3 | 47 | 3 | 58 | 15 | 1 |
| 3 | | | | | | | |

| | | | | | | | |
|---|-----------------------|-----------------|--------|-------|--------|-----|---|
| 4 | | | | | | | |
| 3 | Maricunga | 36 | 252 | 92 | 680 | 7 | 3 |
| 8 | | | | | | | |
| 3 | Incahuasi | 95 | 11,214 | 145 | 15,896 | 118 | 2 |
| 9 | | | | | | | |
| 4 | Antofalla-Botijuelas | 209 | 577 | 615 | 816 | 3 | 3 |
| 0 | | | | | | | |
| 4 | Rio Grande | 398 | 2,161 | 692 | 2,234 | 5 | 2 |
| 1 | | | | | | | |
| 4 | Arizaro | 188 | 2,082 | 465 | 7,736 | 11 | 2 |
| 2 | | | | | | | |
| 4 | Hombre Muerto | 628 | 954 | 1,013 | 1,915 | 2 | 2 |
| 3 | | | | | | | |
| 4 | Diablillos | 180 | 1,226 | 557 | 1,884 | 7 | 2 |
| 4 | | | | | | | |
| 4 | Ratones | 158 | 223 | 260 | 323 | 1 | 2 |
| 5 | | | | | | | |
| 4 | Centenario | 288 | 2,293 | 1,020 | 7,550 | 8 | 4 |
| 6 | | | | | | | |
| 4 | Pocitos-Quirón | 60 | 655 | 101 | 1,384 | 11 | 2 |
| 7 | | | | | | | |
| 4 | Pozuelos | 101 | 1,641 | 940 | 2,587 | 4 | 2 |
| 8 | | | | | | | |
| 4 | Pastos Grandes (Puna) | 476 | 4,155 | 857 | 5,647 | 9 | 2 |
| 9 | | | | | | | |
| 5 | Rincon | 287 | 2,032 | 651 | 2,297 | 7 | 2 |
| 0 | | | | | | | |
| 5 | Cacuhari | 860 | 1,746 | 1,740 | 2,104 | 2 | 2 |
| 1 | | | | | | | |
| 5 | Olaroz | 1,014 - 841* | 2,002 | 1,213 | 2,301 | 2 | 1 |
| 2 | | | | | | | |
| 5 | Jama | 82 | 228 | 262 | 492 | 3 | 3 |
| 3 | | | | | | | |
| 5 | Salinas Grandes | 332 | 1,068 | 1,018 | 2,289 | 3 | 3 |
| 4 | | | | | | | |
| 5 | Guayatayoc | 96 | 183 | 125 | 183 | 2 | 1 |

Highlights

- Sizes of Andean salt pans are proportional to the extent of their endorheic basin.
- The equation $mean\ Li \approx \frac{1}{2}\ max\ Li$ is a tool for surveying of brine-type deposits.
- The greatest Li levels are expected to be found in largest and oldest salt pans.